ELSEVIER

Biochimica et Biophysica Acta 1318 (1997) 322–373

BIOCHIMICA ET BIOPHYSICA ACTA
BBA

Review

Electron transfer and arrangement of the redox cofactors in photosystem I

Klaus Brettel *

Section de Bioénergétique and CNRS-URA 2096, Département de Biologie Cellulaire et Moléculaire, CEA Saclay, 91191 Gif-sur-Yvette Cedex, France

Received 9 July 1996; accepted 4 September 1996

Keywords: Photosystem I; Electron transfer; Photosynthesis

Contents

Abbreviations: Chl, chlorophyll; E_A, activation energy; E_m, redox midpoint potential; ENDOR, electron nuclear double resonance; EPR, electron paramagnetic resonance; (F.C.), Franck-Condon factor; LHC-I, light harvesting complex I; λ, reorganisation energy; λ_i and λ_o, inner and outer reorganisation energy, respectively; NMR, nuclear magnetic resonance; PhyQ, phylloquinone; PS I, photosystem I; PS II, photosystem II; r, center-to-center distance between two molecules; R, edge-to-edge distance between two molecules; SDS, sodium dodecyl sulphate; $t_{1/2}$, half-time; τ, lifetime ($\tau = t_{1/2}/\ln 2$ for a monoexponential decay).

* Corresponding author. Fax: +33 169088717; E-mail: brettel@dsvidf.cea.fr

PII S0005-2728(96)00112-0

1. Introduction

Photosystem I (PS I) is a pigment protein complex embedded in the photosynthetic membrane of oxygenic photosynthetic organisms (higher plants, algae and cyanobacteria). Under illumination with light at wavelengths shorter than approx. 700 nm (photon energy higher than approx. 1.77 eV), PS I performs a transmembrane electron transfer from its primary electron donor, a special chlorophyll pair named P700 (referring to the wavelength of maximal bleaching upon oxidation), through a chain of intermediate electron acceptors, to the terminal acceptor originally named P430 (now known to be one or both of two closely spaced [4Fe-4S] clusters called F_A and F_B). The reduced terminal acceptor $(F_AF_B)^-$ is a strong reductant (redox midpoint potential $E_m \approx -540$ mV). Under physiological conditions, it donates its excess electron to $NADP^+$ via water soluble ferredoxin (or in some cases flavodoxin) on the stromal side of the photosynthetic membrane, while the oxidant $P700^+$ ($E_m \approx 490$ mV) receives an electron from water oxidising photosystem II (PS II) via the cytochrome b_6f complex and water soluble plastocyanin (or in some cases cytochrome c_6) on the lumenal side. Thus, PS I acts in series with PS II as a driving force in linear electron transport from water to $NADP^+$. However, PS I alone may also drive a cyclic electron transport, the pathway of which is not yet well established [122].

When no suitable extrinsic donors and acceptors are available, the charge separated state $P700^+$ $(F_AF_B)^-$ decays by internal charge recombination, but this dissipative reaction is relatively slow ($t_{1/2} \approx$ 50 ms) so that it can hardly compete with electron transfer to and from the soluble electron carriers under physiological conditions. The standard free energy of the state $P700^+$ $(F_AF_B)^-$ is approx. 1.03 eV above that of the neutral ground state (estimated from the midpoint potentials). This corresponds to nearly 60% of the minimal photon energy (1.77 eV) required for charge separation in PS I.

Considering the different photosynthetic reaction centres discovered so far, it has been suggested to classify them in two groups, according to the chemical nature of the terminal electron acceptor: the iron-sulphur type (or type I) comprising PS I and the reaction centres of green sulphur bacteria and heliobacteria, and the quinone type (or type II) comprising PS II and the reaction centres of purple bacteria and certain green bacteria, such as *Chloroflexus* [80,184]. A breakthrough in the understanding of photosynthetic charge separation in a quinone type reaction centre was achieved through the crystallisation and X-ray structure determination of purple bacterial reaction centres at atomic resolution [50]; accounts of recent research on structure and function of purple bacterial reaction centres can be found in Refs. [19,165]. It is of particular interest to establish whether the charge separation mechanisms in other photosynthetic reaction centres are similar to those in purple bacteria or whether rather distinct mechanisms have evolved in different organisms. Possibly, the first two steps of charge separation (fast electron transfer from the excited primary donor chlorophyll via pheophytin or chlorophyll to a quinone) occur rather similarly in all photosynthetic reaction centres. The subsequent electron transport to the low potential iron sulphur

centres in the type I reaction centres, however, has no analogue in type II reaction centres. In PS I, this electron transport involves a phylloquinone and three distinct [4Fe-4S] clusters with presumably rather small free energy gaps for the individual electron transfer steps (see Section 6). The understanding of these steps may be relevant to other biological electron transfer reactions with small driving forces.

The recent crystallisation of the PS I complex from the cyanobacterium *Synechococcus* sp. (now reclassified as *Synechococcus elongatus* [69] and the X-ray structure analysis at a resolution of 4.5 Å [138,218,276,277] provided essential new information on the structure of the PS I complex. Although only some of the cofactors could so far be identified and located unambiguously in the electron density map, these structural data are highly relevant for the elucidation of the electron transfer pathway and for the interpretation of kinetic and spectroscopic data on electron transfer in PS I. On the other hand, kinetic and spectroscopic data may provide helpful constraints for the interpretation of the X-ray diffraction data. It is the purpose of the present review to confront structural data with kinetic and spectroscopic data in order to improve our understanding of electron transfer within the PS I complex. The main emphasis will be on recent publications which are relevant in this context. For more comprehensive reviews and coverage of earlier literature on PS I, the reader may consult, e.g., Refs. [77,78,82,144,158, 209,229].

2. Summary of some basic features of photosystem I

2.1. Composition and architecture of the PS I complex

The PS I complex is composed of more than 10 subunits, named PsaA to PsaN (for alternative nomenclatures, see Ref. [43]). The two largest subunits, PsaA (83.2 kDa) and PsaB (82.5 kDa) are homologous and form the heterodimeric core of PS I. They bind a large number of antenna pigments (see Section 2.2), as well as all known redox cofactors except iron-sulphur clusters F_A and F_B. The latter are bound to PsaC (8.9 kDa), a peripheral protein located on the stromal side of the PS I complex. PsaA, PsaB and PsaC are highly conserved between different organisms. The other subunits have molecular masses between 3 and 17 kDa and are mostly less well conserved. They are believed to play structural roles, e.g., for the docking of ferredoxin (PsaD and PsaE) and plastocyanin (PsaF), for the formation of PS I trimers in cyanobacteria (PsaL and PsaI), or for the correct assembly and stability of the PS I complex. Some of the subunits may be specific for certain organisms (PsaM was detected only in cyanobacteria, PsaG, PsaH and PsaN only in plants and algae). A model for the architecture of the PS I complex as proposed by Golbeck [78] is shown in Fig. 1. It includes only proteins which are common to both eukaryotic and cyanobacterial PS I. For references and details on the polypeptides of PS I, the reader is referred to recent reviews [43,81].

It is of note that the recent refinement of the

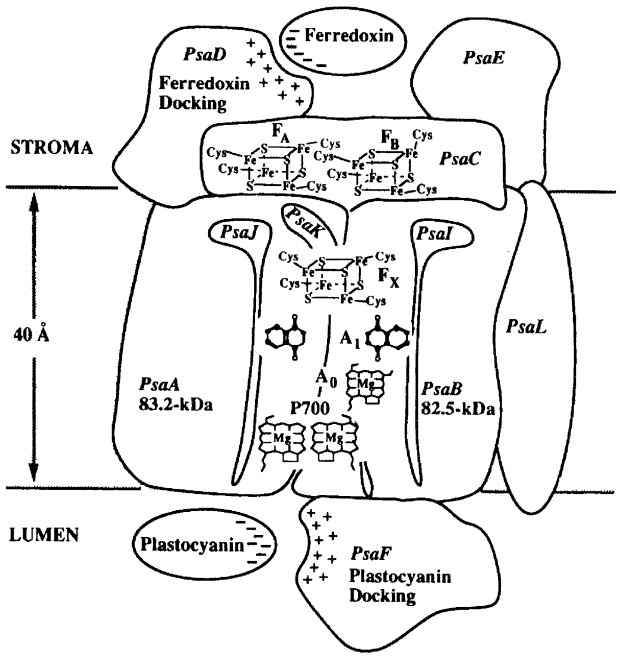

Fig. 1. Schematic presentation of the architecture of PS I as proposed by Golbeck [78] prior to the publication of the X-ray crystallography data. Only those proteins common to both eukaryotic and cyanobacterial PS I are illustrated. Reproduced, with permission, from the Annual Review of Plant Physiology and Plant Molecular Biology, Volume 43, ©1992, by Annual Reviews Inc.

crystal structure analysis of PS I allowed the observation of 29 transmembrane helices, from which twice 11 could be attributed to the subunits PsaA and PsaB, respectively, because of their symmetry relation [218], in line with the number of transmembrane helices predicted from hydrophobicity plots of PsaA and PsaB [66,132,179,180].

2.2. Antenna system and excitation energy transfer

The subunits PsaA and PsaB contain together approx. 100 Chl *a* molecules and 12–16 β-carotenes which absorb incident light and direct the excitation energy to the primary electron donor, P700. In higher plants and algae (but not in cyanobacteria), PS I is associated with another antenna system, the light-harvesting complex I (LHC-I) which consists of a number of proteins carrying together approx. 100 chlorophyll molecules (Chl *a* and Chl *b* at a ratio of approx. 3.5:1). The presence of a large number of antenna pigments on the two subunits carrying most of the redox cofactors of PS I is in contrast to type II reaction centres (see Section 1) where most antenna pigments are organised in separate antenna proteins. Thus, the study of excitation energy transfer in PS I may increase our knowledge about different ways of 'light-harvesting' realised in nature.

The antenna system of PS I contains several spectral forms of Chl *a* with absorption maxima between 666 and 693 nm, and a few 'long wavelength' chlorophylls absorbing beyond 700 nm (for different organisms the peaks vary between 708 and 730 nm), i.e., the excited state energies of the latter are below that of P700. Excitation energy transfer from the antenna pigments to P700 and trapping (presumably due to primary charge separation) occurs in about 20–40 ps in PS I lacking LHC-I, and 50–120 ps in the presence of LHC-I, as concluded from the decay kinetics of fluorescence. The short lifetime of the excited states explains the low fluorescence yield of PS I (below 1% in isolated PS I). With respect to the spatial and functional organisation of the antenna chlorophylls and especially of the 'long wavelength' chlorophylls, several rather crude models have been proposed which could simulate experimental data on excitation energy transfer. Refinement of the crystal structure of PS I from *Synechococcus elongatus* should help to put forward more realistic models. It is of note that the antenna chlorophylls observed in the most recent electron density map are located preferentially close to the periphery of subunits PsaA and PsaB [218]. Such a structure may be in favour of a 'transfer-to-the-trap limited' process as suggested recently by Valkunas et al. [258]. In their model, the typical distance between antenna chlorophylls and P700 is larger than the typical distance in between neighbouring antenna pigments, and the trapping rate is in fact limited by the relatively slow ($\tau \approx 30$ ps) energy transfer from the antenna chlorophylls to P700. For references and details on energy transfer in PS I, the reader is referred to a recent review [262].

2.3. The electron transport chain

It is widely accepted that the electron transport chain of PS I (see Figs. 1 and 2) comprises the primary electron donor P700 (dimer of Chl *a*) and 5 electron acceptors: the primary acceptor A_0 (Chl *a*), the secondary acceptor A_1, (phylloquinone, known also as vitamin K_1), the tertiary acceptor F_X (inter-polypeptide [4Fe-4S] cluster which bridges subunits PsaA and PsaB), and the terminal acceptors F_A and F_B (both [4Fe-4S] clusters bound to subunit PsaC). F_X, F_A and F_B, in their reduced forms, can be distinguished spectroscopically by low temperature EPR (see Sections 3.2.4 and 3.2.5). The arrangement of the redox cofactors as depicted in Fig. 1 (from Ref. [78]) is a very schematic one which was proposed prior to the publication of the X-ray crystallography data (see Section 3.1). Upon excitation of P700 to its lowest excited singlet state ($P700^*$), an electron is transferred from $P700^*$ to A_0 and further to A_1 on a picosecond time scale, then further to F_X on a nanosecond time scale and finally to F_B and/or F_A with not yet well established kinetics. A widely accepted scheme of charge separation in PS I, based on measured and estimated midpoint potentials, is shown in Fig. 2 (adapted from Ref. [82] and supplemented with kinetic data reviewed in Section 4.1; note that a modification of some of the indicated midpont potentials will be suggested in Section 6). Recent experimental results and ideas on electron transfer in PS I will be presented and discussed in detail below.

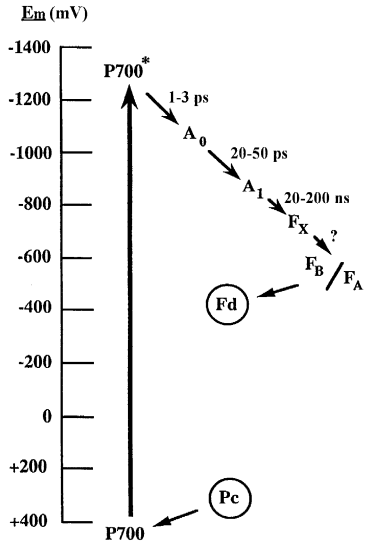

Fig. 2. Energetics of charge separation in PS I as proposed by Golbeck and Bryant (adapted from Fig. 1 in Ref. [82]). Time constants of electron transfer at room temperature (see Section 4.1) are also indicated.

2.4. Relationship with other type-I reaction centres

As was pointed out by Nitschke and Rutherford [184], the reaction centre of green sulphur bacteria, the reaction centre of heliobacteria and PS I show important similarities which distinguish them from type-II reaction centres (see Section 1), such as the presence of low potential [4Fe-4S] clusters which serve as terminal electron acceptors, the chemical nature of the primary acceptor (chlorophyll, instead of pheophytin in type-II reaction centres), and the presence of a large number of antenna pigments within the reaction centre core. There are also significant sequence homologies between the largest subunits of the type-I reaction centres, and it is believed that they share a common ancestor. Interestingly, both green sulphur bacteria and heliobacteria apparently contain a homodimeric protein core, consisting of two identical copies of a single polypeptide [36,149], in contrast to the PsaA/PsaB heterodimer in PS I. This may suggest that two symmetric electron transfer pathways are active in green sulphur bacteria and heliobacteria [36,149]. For references and details on the reaction centres of green sulphur bacteria and heliobacteria, the reader is referred to recent review articles [3,64,80].

3. Recent data on the nature and arrangement of the redox cofactors

3.1. X-ray crystallography data

Based on X-ray diffraction of PS I crystals from *Synechococcus elongatus* at a resolution of 4.5 Å, Schubert et al. [218] derived a model for the arrangement of the redox cofactors within the PS I complex (Fig. 3). The positions of the centres of the three iron-sulphur clusters (cubane-like structures in Fig. 3) were well resolved because of their high electron densities. The assignment of F_X was obvious because it is bound to the core subunits PsaA and PsaB, and should hence be deeper in the complex than F_A and F_B which are bound to the extrinsic subunit PsaC. It is not yet possible, however, to decide which of the two peripheral clusters is F_A and which F_B. Therefore, I use the term F_{AB1} for the cluster proximate to F_X, and F_{AB2} for the distal cluster. With respect to the chemical nature of F_X which was controversial for some time (see Refs. [77,144] for reviews), the comparable electron densities of the three iron-sulphur

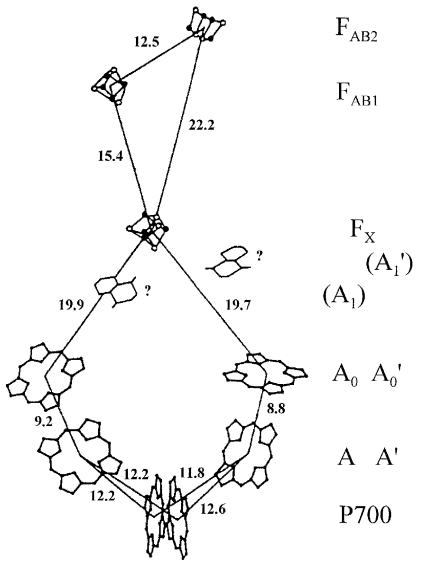

Fig. 3. Model for the arrangement of the redox cofactors of PS I from *Synechococcus elongatus* proposed by Schubert et al. [218] on the basis of X-ray diffraction data at a resolution of 4.5 Å. The membrane plane is perpendicular to the connection between the centres of P700 and F_X. Distances are given in Å. Redrawn from Ref. [218] with modification of the nomenclature.

clusters contradict the notion that F_X may be a [2Fe-2S] cluster and support that F_X has the same composition as F_A and F_B, i.e., is a [4Fe-4S] cluster [138]. The orientations of the [4Fe-4S] clusters could not be determined from the X-ray diffraction data at the present resolution, but for F_A and F_B a proposal based on EPR data on single crystals was put forward (see Section 3.2.5).

P700 was assigned to an electron density which – in agreement with spectroscopic data (see Section 3.2.1) – could be modeled by two chlorophylls having their planes parallel to each other and perpendicular to the membrane, with a distance of 4.5 Å between the planes and 7.5 Å between the centres of the chlorophylls (note that the distance of 9 Å quoted in Ref. [218] was an erratum) (Witt, H.T., personal communication). In search for the primary acceptor A_0, Schubert et al. [218] found two electron densities compatible with Chl *a* molecules at positions corresponding to those of the two bacteriopheophytins in purple bacterial reaction centres. One of them was assumed to represent A_0, while the other one (A'_0) would be a member of a symmetry-related but inactive electron transfer branch, in analogy to purple bacteria. Two further Chl *a* molecules (A and A′) at positions corresponding to the accessory bacteriochlorophylls in purple bacteria were also fitted into the electron density map. Thus, the arrangement of the redox centres involved in primary charge separation may be similar to that in purple bacteria, although it seems still possible that higher resolved data will reveal structural elements differing from those in purple bacteria. Fig. 3 also shows two positions where the electron density map could possibly accommodate phylloquinone molecules (A_1 and A'_1). However, they were not yet distinguishable from aromatic side chains of α-helices [218]. It is not yet clear along which of the two indicated branches electron transfer from P700 to F_X proceeds [218]. The possibility that both branches are active in PS I cannot be ruled out at present (see Section 4.1.2).

3.2. Biochemical and spectroscopic data

3.2.1. P700

It was disputed for long time whether P700 is a monomer or a dimer, and whether it is constituted of Chl *a* or of some Chl *a* derivative, but most evidence is now in favour of a dimer of regular Chl *a* (see Ref. [220] for a review). Arguments in favour of a monomeric nature of P700 were mainly based on the spectroscopic features of its oxidised state ($P700^+$) and its triplet state ($^3P700$) which appeared to be indicative of monomeric Chl *a*. These data are not in contradiction, however, with P700 being made of two chlorophylls which interact in the singlet excited state to yield optical properties of an excitonically coupled dimer (see Ref. [45] for a brief description of exciton coupling); nevertheless, the positive charge of $P700^+$ and the unpaired spins of $^3P700$ may be localised on one of these two chlorophylls, leaving the other one in the neutral ground state (at least on the time scale characteristic for the respective measurement; slow electron or triplet hopping between the two chlorophylls could still occur; see, e.g., Ref. [240]). In line with this idea, Schaffernicht and Junge [213] explained the main features of the optical $P700^+/P700$ difference spectrum between 670 and 720 nm as a superposition of three spectral components: (1) disappearance of a wide band around 695 nm attributed to the superposition of the two (overlapping) Q_y exciton bands of a Chl *a* dimer with weak or negligible exciton coupling (not resolved in the experiments), (2) appearance of a narrower band around 690 nm with approx. half the oscillator strength of component 1, attributed to the Q_y transition of the non-oxidised chlorophyll in $P700^+$, and (3) a bathochromic bandshift centred around 688 nm reflecting the local electrochromic response of nearby Chl *a* molecule(s) to the formation of $P700^+$. A variation of the amplitude of component 3 might account for the variability of the observed $P700^+/P700$ difference spectra between different samples and as a function of temperature [214]. It is generally accepted that the low energy exciton band of P700 is around 695 nm and accounts for the majority of the oscillator strength of P700 in the Q_y region. For the high energy exciton band, an alternative position around 650 nm (with weak intensity) has been proposed [52,267]; this implies a stronger excitonic coupling between the two chlorophylls than in the case of two overlapping bands close to 695 nm as assumed in Ref. [213], but would be consistent with what was expected for a dimer of Chl *a* with the same geometry as the primary donors in purple bacteria [267] (see also below).

Recent reports using magnetic resonance spectro-

scopies to study $P700^+$ at cryogenic temperatures [49,58,125–127,153,202] support earlier conclusions (reviewed in Ref. [220]) that the unpaired spin is either distributed asymmetrically over two chlorophylls (spin-density ratio $\geq 3:1$) or is even completely localised on one (possibly modified) chlorophyll with a spin-density distribution different from that in monomeric Chl a^+ in vitro. The g-tensor of $P700^+$ was measured with high resolution at room temperature using a 140 GHz EPR spectrometer [198]. Predominant localisation of the positive charge on one chlorophyll was also supported by a recent study of P700 oxidation by Fourier transform infrared difference spectroscopy at 5°C [90]; see Ref. [220] for a discussion of earlier data from vibrational spectroscopies.

Sieckmannn et al. [240] studied the spin-polarised EPR spectrum of ^{3}P700 as a function of temperature. It turned out that the non-axial zero field splitting parameter |E| decreased by 40–45% when increasing the temperature from 4 to 298 K; the axial parameter |D| was nearly constant throughout this temperature range. The values of |D| and |E| observed at below approx. 50 K were indicative of a triplet state localised on a single Chl *a*, in agreement with earlier observations (reviewed in Ref. [220]). The decrease of |E| at higher temperatures without change of |D|, was explained by a 'delocalisation' (presumably by rapid ($> 10^8$ s^{-1}) hopping) of the triplet excitation over two chlorophylls which have their magnetic *z*-axes (and hence their planes) parallel, and their magnetic *y*-axes at an angle of approx. 55°. Thus, these data provide new evidence for a dimeric nature of P700 and allow a prediction for the orientation of the two chlorophylls (see below).

New evidence in favour of a dimeric nature of P700 was also obtained from measurements of the Stark effect, yielding a 5-fold larger change in the permanent dipole moment, $\Delta\mu$, on excitation of P700 compared to monomeric Chl *a* [139,140]; the large value of $\Delta\mu$ was explained by a charge transfer contribution to the singlet excited state of P700 as observed in other chlorophyll dimers. Magnetic circular dichroism data were also interpreted as indication for a dimeric nature of P700 [186].

With respect to the orientation of the two chlorophylls relative to each other and relative to the membrane, predictions from spectroscopic data can now be compared with the electron density map obtained from X-ray diffraction of PS I crystals. EPR spectra of ^{3}P700 in PS I complexes oriented on mylar sheets indicated that the plane of the chlorophyll carrying the triplet excitation at low temperature is perpendicular to the membrane [210], and according to Ref. [240] (see above), the two chlorophylls, over which the triplet excitation is delocalised at room temperature, should have their planes parallel to each other. A chlorophyll dimer with this orientation could in fact be fitted into the electron density map at a position which is reasonable for P700 [218] (see above). The in-plane orientations of the two chlorophylls cannot yet be resolved by X-ray crystallography. In the following, I will put forward a suggestion based on spectroscopic results.

According to Ref. [240] (see above), the angle between the magnetic *y*-axes of the individual triplet states of the two chorophylls should be approx. 55°. Assuming a symmetric arrangement of the two chlorophylls with a C_2 axis perpendicular to the membrane (the transmembrane helices of PsaA and PsaB are approximately related by such a symmetry [218]), the magnetic *y*-axes of each of the two chlorophylls should be tilted out of the membrane by either 27.5° or 62.5°. Only the latter value is compatible with the reported tilt angle of 60–70° for the magnetic *y*-axis of the localised triplet state at low temperature [210]. It was recently reported [268] that the magnetic *y*-axis of ^{3}Chl *a* lies in the chlorophyll plane at an angle of 35–45° (depending on the solvent) from the optical Q_y transition moment (the latter coincides approx. with the molecular y-axis connecting the nitrogens of pyrrole rings I and III). This leads to Q_y transition moments of the constituents of P700 tilted by either approx. 22.5° or 77.5° from the membrane. Only the former value is compatible with the observation that the main optical bleaching due to the oxidation of P700 (around 700 nm) is polarised almost parallel to the membrane [25,26], since for tilt angles exceeding 45°, the stronger one of the two exciton bands of P700 would be polarised perpendicularly to the membrane. Fig. 4 shows an arrangement of the two chlorophylls which is consistent with these considerations (y_T denotes the magnetic *y*-axes of the localised triplet states). Other consistent orientations can be obtained by rotating both chlorophylls by 180° around their Q_y-axes

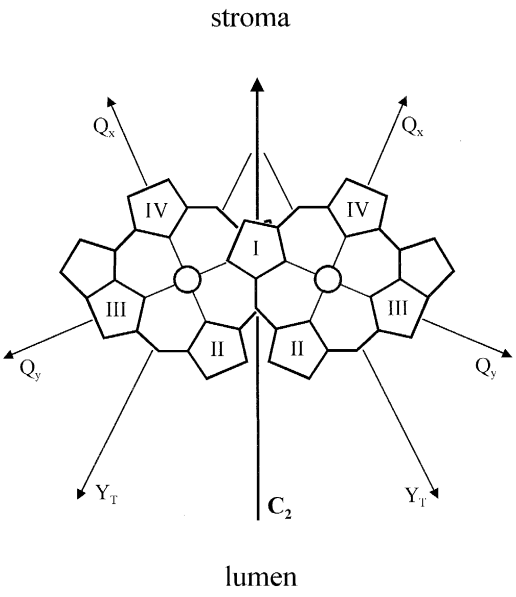

Fig. 4. Sketch of the proposed arrangement of the two chlorophylls constituting P700. The C_2 axis is perpendicular to the membrane. y_T denotes the magnetic *y*-axes of the triplet states localised on the individual chlorophylls. See text for further details and other possible orientations of the chlorophylls.

or around their Q_x-axes or around axes parallel to C_2 and through the centres of the chlorophylls (or any combination of these rotations); stromal and lumenal sides may also be exchanged. The arrangement shown in Fig. 4 is the one which most resembles the structure of the primary donors in purple bacteria. It is of note that similar arguments in Ref. [240] did not lead to a consistent picture because – based on Ref. [254] – the magnetic *y*-axis of the triplet state was assumed to be approx. parallel to the optical Q_y transition moment of Chl *a*. A structure similar to the one in Fig. 4 was recently suggested by Käß [124] based on an ENDOR study on PS I crystals.

For a pair of Chl *a* molecules arranged as in Fig. 4 (with a distance of 7.5 Å between the centres and 4.5 Å between the planes; see Section 3.1), exciton theory in its simplest form (e.g., Ref. [45]) predicts an exciton coupling of 186 cm^{-1}, corresponding to a separation of about 18 nm between the two exciton bands (calculated with a dipole strength of 16.7 D^2 for the $Q_y(0,0)$ transition of Chl *a* [234]). The low and high energy exciton bands should be polarised parallel and perpendicular to the membrane, respectively, and their intensity ratio should be about 6:1. While these polarisations and a dominance of the low energy band (at 695 nm) are compatible with experimental results (see above), the predicted exciton coupling is stronger than suggested in Ref. [213], but weaker than in the alternative suggestion [52,267] (see above). This may indicate that either the distance between the chlorophylls or their orientations in the above structural model (Fig. 4) are not correct (note that the orientations were derived with the unproved assumption of a C_2 symmetry for P700). It should also be mentioned that environmental shifts of the band positions (possibly different for the two chlorophylls) and coupling to other chlorophylls (e.g., A and A′ in Fig. 3) may affect the exciton splitting.

With respect to the coordination of P700 within the PS I protein complex, attempts to identify histidine ligands to the two chlorophylls constituting P700 have been reported. The suggestion [203] that histidines in the membrane span VIII of PsaA and PsaB may coordinate these chlorophylls was not supported by the analysis of site-directed mutations in *Chlamydomonas reinhardtii* [47]. As further candidates, histidine 656 in membrane span X of PsaB and the homologous histidine in PsaA were proposed [47,69]. Consistent with this proposal, Krabben et al. [137] found that the ^{1}H-ENDOR spectrum of $P700^+$ and the optical $P700^+/P700$ difference spectrum of the H656N mutant were significantly modified as compared to wild-type *Chlamydomonas reinhardtii*.

3.2.2. A_0

The primary electron acceptor A_0 is often considered to be a monomeric Chl *a* (see, e.g., Refs. [60,82,144] for reviews); this assignment could well account for the extremely low midpoint potential of A_0, but should still be regarded with caution because spectroscopic characterisation of A_0^- during forward electron transfer turned out to be rather difficult (see Section 4.1.1). Proposals that A_0 may be a derivative of Chl *a*, e.g., the C13^2-epimer (Chl *a*′) or a Chl *a* dimer are still under discussion [154,267]; see also Ref. [4] for a review on earlier work. A well resolved A_0^-/A_0 absorption difference spectrum was deduced from a study of charge recombination in the primary pair $P700^+A_0^-$ in a PS I preparation where the secondary acceptor A_1 (phylloquinone), carotenoids and approx. 90% of the antenna chlorophylls had been extracted by ethyl ether [167] (it should be

considered that such an extraction may have modified the interactions in between the remaining pigments and between the pigments and the protein). To obtain the A_0^-/A_0 difference spectrum, a $P700^+/P700$ difference spectrum was subtracted from the measured $P700^+A_0^-/P700A_0$ difference spectrum. The spectrum obtained showed bleachings around 690 and 430 nm and absorption increases around 760 and 460 nm, compatible with A_0 being a Chl *a* with its Q_y transition shifted to 690 nm. Similarly, a putative A_0^-/A_0 difference spectrum was obtained under strongly reducing conditions (electron transfer from A_0^- to A_1 presumably blocked) in PS I prepared with Triton X-100 [188]. This difference spectrum showed maximal bleaching at 693 nm and the most prominent absorption increase around 710 nm (instead of 760 nm in Ref. [167]). A bleaching around 690 nm observed by picosecond-spectroscopy during forward electron transfer was also attributed to transient reduction of A_0 (see Section 4.1.1). Earlier studies (reviewed in Ref. [82]) reported attempts to accumulate A_0^- by continuous illumination under strongly reducing conditions and an EPR spectrum indicative of Chl a^- and a main optical bleaching around 670 nm were observed. The shorter wavelength compared to the time-resolved studies was taken as indication that a chlorophyll different from A_0 may have been reduced in the photoaccumulation experiments [167]. As further possible explanations, I would like to suggest:

· a modification of the optical features of A_0 due to the harsh reduction treatment in the photoaccumulation experiments;

· a substantial deviation of the $P700^+A_0^-/P700A_0$ difference spectrum from the sum of the pure $P700^+/P700$ spectrum and the pure A_0^-/A_0 spectrum, for example due to electrochromic bandshifts exerted by $P700^+$ on A_0 (but not on A_0^-) or by A_0^- on P700 (but not, or differently, on $P700^+$). If this were the case, subtraction of the $P700^+/P700$ spectrum from the $P700^+A_0^-/P700A_0$ spectrum would not yield the pure A_0^-/A_0 spectrum.

With respect to the orientation of A_0, an angle of 46° between the Q_y transition moments of A_0 and P700 was estimated from dynamic linear dichroism measurements of $P700^+A_0^-$ in a PS I preparation lacking A_1 and most of the antenna chlorophylls [114].

3.2.3. A_1

The assignment of the secondary electron acceptor A_1 as one of the two phylloquinone molecules present in PS I was reviewed in detail in 1991 and 1992 [78,82]. I will therefore focus on more recent results and on some controversial points.

EPR detection of photoaccumulated A_1^-. The first evidence for the presence of two electron acceptors (A_0 and A_1) preceding the iron-sulphur clusters came from the observation by EPR of two radicals with different EPR properties after illumination of PS I under reducing conditions [22,72]. A high field (Q-band) EPR spectrum attributed to A_1^- showed considerable anisotropy of the g-values similar to those of reduced quinones [253], in line with the later assignment of A_1 as a phylloquinone. However, two observations raised doubts concerning the photoaccumulated radical being reduced phylloquinone: (1) destruction of phylloquinone by UV irradiation did not alter the EPR signal attributed to photoaccumulated A_1^- [282], and (2) the photoaccumulated spectrum did not show the expected line-narrowing when cyanobacteria containing specifically deuterated phylloquinone were studied [8]. Recently, Heathcote et al. [97] performed a detailed EPR study on photoaccumulation of radicals in PS I and established conditions (illumination at 205 K in the presence of dithionite at pH 8) which preferentially form a radical with an asymmetric EPR spectrum ($g = 2.0048$, $\Delta H = 0.95$ mT) similar to the one originally attributed to A_1^- [22,72] and compatible with reduced phylloquinone. After a pretreatment assumed to lead to double reduction of A_1, this EPR spectrum could no longer be induced, confirming its attribution to A_1 [97]. In the same study, it was shown that – depending on temperature and duration of the illumination, pH and type of sample – up to 4 radicals could be easily trapped by photoaccumulation. It appears to me that the experimental conditions of photoaccumulation need to be carefully established when this method is applied to study the acceptor A_1. In contrast to Ref. [8], Heathcote et al. [98,99] reported recently that deuteration of phylloquinone led to a narrowing of the EPR spectrum of photoaccumulated A_1^- when the experimental conditions established in Ref. [97] were used. With respect to the A_1^--like photoaccumulated EPR signal after destruction of phylloquinone by UV irradiation [282], Biggins et al. [17,18] pointed out

that the situation may be complicated by an extensive UV-induced modification of PS I.

EPR of spin-polarised P700$^+A_1^-$. A very large and unusual transient light-induced EPR signal has been attributed to the radical pair $P700^+A_1^-$. The X-band EPR spectrum shows a pattern of microwave emission, absorption, emission due to a non-Boltzmann population of the four electron spin states of the coupled spin pair in the static magnetic field of the EPR spectrometer (electron spin polarisation; see Refs. [108,246,249] for recent reviews and Ref. [104] for a review on the earlier literature). Rather similar transient spectra were observed at cryogenic temperatures (where $P700^+A_1^-$ decays mainly by charge recombination in approx. 150 μs) and at room temperature (where $P700^+A_1^-$ decays by electron transfer to the iron-sulphur clusters in approx. 200 ns). These spectra, and especially spectra measured with deuterated samples and also by high-field EPR (Q-band and K-band), provided strong evidence that a radical with g-values similar to those of semiquinones contributed (together with $P700^+$) to the spin-polarised signals. More recently, it was shown that replacement of protonated phylloquinone by deuterated phylloquinone led to a characteristic narrowing of the transient EPR spectrum measured at 10 K,

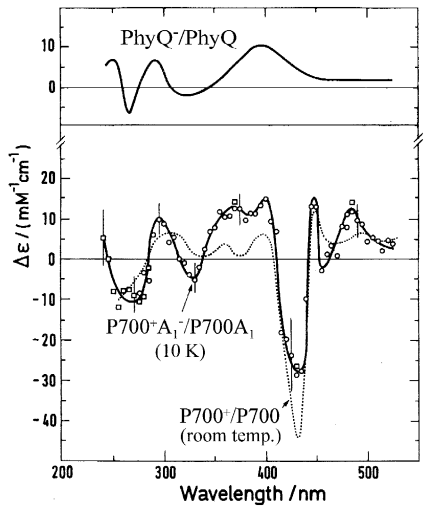

Fig. 5. Upper panel: absorbance difference spectrum for the reduction of phylloquinone to its semiquinone anion in methanol (measured by Dr E.J. Land). Lower panel: absorbance difference spectra attributed to $P700^+A_1^-/P700A_1$ at 10 K (150 μs charge recombination) and to $P700^+/P700$ at room temperature (dotted line; from Ref. [129]). See Ref. [32] for details. Adapted from Ref. [32].

indicating that phylloquinone contributes directly to the spin-polarised signal [208]. The signal could no longer be observed upon extraction of phylloquinone as well as upon a pretreatment assumed to doubly reduce A_1, confirming that A_1 is phylloquinone [208,245]. Also at room temperature, the spin-polarised signal attributed to $P700^+A_1^-$ could no longer be observed upon extraction of phylloquinone [240,241], but was still observable after extraction of the three iron-sulphur clusters [259].

Simulation of the spin-polarised spectra and of their time evolution (quantum beats and transient nutations) may provide structural information on the pair $P700^+A_1^-$. It was concluded from such simulations that the magnetic *x*-axis of A_1^- (oriented along the C = O bonds of phylloquinone) and the vector connecting P700 and A_1 are roughly parallel [70,74,248] or form an angle of 32° [136]. For comparison, the corresponding angle for the secondary pair $P^+Q_A^-$ in purple bacterial reaction centres is approx. 62° (Ref. [70] and refs. therein).

Transient optical spectroscopy of A_1^-. The characterisation of A_1 by optical spectroscopy was mostly based on flash-induced absorption changes attributed to formation of the pair $P700^+A_1^-$, i.e., the $P700^+A_1^-/P700A_1$ difference spectrum. Fig. 5 (from Ref. [32]) shows such a spectrum (measured in the presence of prereduced F_A and F_B at 10 K where $P700^+A_1^-$ decays by charge recombination with $t_{1/2} \approx 150$ μs), together with a $P700^+/P700$ difference spectrum (measured at room temperature) and an in vitro difference spectrum for the reduction of phylloquinone to its semiquinone anion ($PhyQ^-/PhyQ$). The deviations between the $P700^+A_1^-/P700A_1$ spectrum and the $P700^+/P700$ spectrum agree qualitatively with the $PhyQ^-/PhyQ$ spectrum in the range from 250 to 450 nm, and, most significantly, between 350 and 400 nm; this was taken as evidence that A_1 is a phylloquinone [32]. For the 450 to 500 nm region, superposition of electrochromic bandshifts induced by the charge of A_1^- was proposed [32]. A transient difference spectrum similar to the low temperature $P700^+A_1^-/P700A_1$ spectrum was later [27,171] observed at room temperature (measured in the range from 325 to 495 nm). It was formed within less than 5 ns and decayed with $t_{1/2} \approx 15$–200 ns (depending on the sample; see Section 4.1.2.) to a spectrum characteristic of the pair $P700^+F_X^-$ or

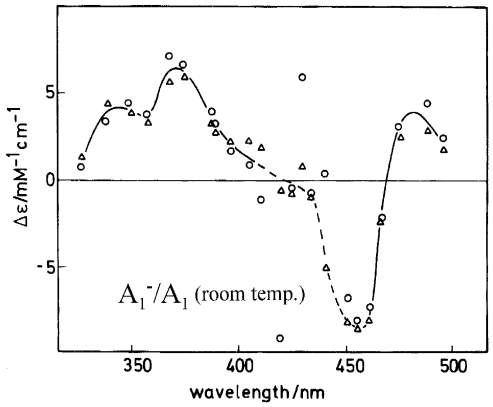

Fig. 6. A_1^-/A_1 difference spectrum constructed from transient absorbance changes in PS I from *Synechococcus* sp. at room temperature. The data between 410 and 440 nm (broken line) were not reliable. See Ref. [27] for details. Adapted from Ref. [27].

$P700^+(F_AF_B)^-$. This was taken as evidence that the acceptor A_1, characterised until then only at cryogenic temperatures, functions in physiological electron transfer between the primary acceptor A_0 and the iron-sulphur clusters [27,171]. The room temperature data permitted an A_1^-/A_1 difference spectrum to be extracted (Fig. 6; from Ref. [27]). Comparison with the $PhyQ^-/PhyQ$ spectrum in vitro (Fig. 5, top) reveals two major differences: the centre of the broad absorbance increase is shifted from around 390 nm ($PhyQ^-/PhyQ$) to around 375 nm in the A_1^-/A_1 spectrum, and there is a pronounced bleaching at around 450 nm exclusively in the A_1^-/A_1 spectrum. While shifts of absorption bands due to the protein environment are not unusual, the 450 nm bleaching can definitively not be assigned to the reduction of phylloquinone because oxidised phylloquinone absorbs only very weakly above 360 nm. It has been proposed that the 450 nm bleaching together with the absorption increase around 480 nm may reflect an electrochromic redshift of a carotenoid [27], but direct evidence for this is still lacking. Transient $P700^+A_1^-/P700A_1$ spectra were recently observed in several different PS I preparations [30,152,225]; they all showed the broad absorbance increase around 380 nm attributed to the contribution from A_1^-, but there were variations in the 450 to 460 nm range, indicating that in this region the spectra are sensitive to the preparation procedure and/or the origin of the samples. To my knowledge, there are two examples in the literature where the putative reduction of A_1 was not accompanied by an absorption increase around 380 nm. In a PS I preparation lacking all three iron-sulphur centres, absorbance changes attributed to $P700^+A_1^-$ were less positive between 380 and 400 nm than those attributed to $P700^+$ alone, indicating a bleaching due to the reduction of A_1 [271]. However, this effect could not be reproduced in a very recent study, where instead a $P700^+A_1^-/P700A_1$ spectrum similar to those cited above was observed [30]. The second example is a photoaccumulation experiment where, in the presence of a significant amount of A_1^- (detected by EPR), no significant absorption changes were observed between 350 and 750 nm [161]. I suppose that either the signal detected by EPR was not due to A_1^- or that the A_1^- concentration was too low to yield absorbance changes exceeding the noise level.

Phylloquinone extraction and reconstitution experiments contributed much to the discussion about the chemical nature of A_1. Essentially two different extraction procedures have been used: (A) extraction with hexane containing 0.3% methanol, which removes, in addition to the two phylloquinones, approx. 50% of the antenna chlorophylls and a considerable fraction of the carotenoids and lipids [15,227]; (B) extraction with mixtures of dry and water-saturated diethyl ether, which removes, in addition to the two phylloquinones, 60–95% (depending on the water content of the ether) of the antenna chlorophylls and all carotenoids [113]. With both procedures, charge separation at room temperature was essentially blocked at the level of A_0, i.e., in most of the centres only the primary pair $P700^+A_0^-$ was formed and decayed by charge recombination, supporting the assignment of A_1 as phylloquinone [15,113]. Data on electron transfer at cryogenic temperatures are less clear, however. The spin-polarised EPR signal attributed to the pair $P700^+A_1^-$ was absent after extraction of phylloquinone according to procedure A [208]. Further, it was reported that electron transfer to the terminal iron-sulphur acceptors at 18 K was inhibited after extraction according to procedure B [162]. Others, however, observed photoreduction of the iron-sulphur clusters after extraction of phylloquinone according to procedure A [227] and procedure B [113,227]. They suggested that there

may be direct electron transfer from A_0^- to F_X, at least at low temperature, or alternatively that A_1 is not a phylloquinone. As will be discussed in Section 7.2.5, it is plausible that electron transfer from A_0^- to F_X can compete with charge recombination in the pair $P700^+A_0^-$. The apparent contradiction between photoreduction of the iron-sulphur clusters at low temperature and primary pair recombination at room temperature may in part reflect the fact that reduction of F_A and F_B is quasi-irreversible at low temperatures, so that it is easily detected, although its quantum yield does not exceed 20% [227]. Some long-lived absorption changes at room temperature after extraction of phylloquinone may reflect charge separation beyond A_0 with a yield of 3 to 20%, depending on the preparation [15,113]. In addition, the ratio of the rates of electron transfer from A_0^- to F_X and from A_0^- back to $P700^+$ may increase with decreasing temperature.

Strong support for the assignment of A_1 as phylloquinone was provided by observations that incubation of extracted PS I with phylloquinone restored many features of native PS I at room temperature: long-lived (ms range) photooxidation of P700 [15,112,113], photoreduction of F_A or F_B [14,112], transient spin-polarised EPR signals attributed to formation of $P700^+A_1^-$ and electron transfer to an iron-sulphur cluster [239,241], ultrafast reoxidation of A_0^- ($\tau \approx 23$ ps) [142]. The spin-polarised EPR spectrum detected at 10 K and attributed to $P700^+A_1^-$ was also restored by addition of phylloquinone to extracted PS I [208]. As far as quoted by the authors, the reconstituted signals amounted to about 50–75% of what was expected for perfect reconstitution of all PS I complexes present (note that the procedures for extraction of phylloquinone extract also a large fraction of the antenna chlorophylls, so that extracted samples should contain more PS I per chlorophyll than unextracted controls).

There were several studies on reconstitution of electron transfer in phylloquinone depleted PS I by incubation with non-native quinones and even non-quinone carbonyl compounds. Such studies may help in exploring the A_1 binding site, and in understanding the energetics of the electron transfer chain (see Section 6) and the dependency of the electron transfer rates on the free energy gap (see Section 7). More than 30 compounds were tested for their capability to replace phylloquinone at the A_1 site. It is widely agreed that many benzoquinones, naphthoquinones, anthraquinones and even anthrones and fluorenones can accept electrons from A_0^- in phylloquinone depleted PS I (Refs. [116,207] and refs. therein). There is clear disagreement, however, as to which compounds restore electron transfer to the iron-sulphur clusters at room temperature: while Iwaki and Itoh (Ref. [116] and refs. therein) reported that a large variety of compounds could replace phylloquinone in this function and concluded that the appropriate reduction potential (in between that of A_0 and that of F_X) was the essential prerequisite for reconstitution, Biggins [14] was unable to restore electron transfer to the iron-sulphur clusters with several of the compounds which were successful in the studies by Iwaki and Itoh, and suggested structural constraints (the requirement of a hydrophobic side chain) in addition to the energetic constraints. The discrepancy may in part be related to the different procedures of phylloquinone extraction (procedure A (see above) in Ref. [14] and procedure B in Ref. [116] and earlier work by the same authors) which may have introduced different additional modifications at the A_1 site. As a criterion of successful reconstitution of samples extracted according to procedure A, Biggins and Mathis [15] checked whether long-lived photooxidation of P700 persisted after addition of dithionite (at pH 7.6), as in native PS I. This was the case in samples reconstituted with phylloquinone, but not with 2-methyl-naphthoquinone, indicating that the latter was reduced (presumably to the quinol form) by dithionite [15]. By contrast, in an early report using extraction procedure B, already the effect of incubation with phylloquinone was completely reversed by the addition of dithionite at pH 8 [111].

Unfortunately, only very few data are available on the kinetics of electron transfer through the compounds supposed to replace phylloquinone as acceptor A_1. Kumazaki et al. [142] showed by optical spectroscopy that addition of menaquinone-4 to phylloquinone-depleted PS I yielded the same ultrafast kinetics of A_0^- reoxidation ($\tau = 23$ ps) as addition of phylloquinone; with 2-methyl-1,4-naphthoquinone (vitamin K_3) the kinetics were slightly slower ($\tau = 34$ ps), but represented only 55% of the decay of A_0^-. Sieckmann et al. [241] studied the kinetics of the reduced quinones directly by transient EPR. After

addition of duroquinone or naphthoquinone to phylloquinone-depleted samples, the quinones were reduced within 50 ns (resolution limit); no electron transfer to the iron-sulphur clusters could be detected, in contrast to samples reconstituted with phylloquinone. Application of flash absorption spectroscopy in the near UV absorption band of the reduced quinones turned out to be difficult because absorption changes due to the recombination of the primary pair (in a fraction of the sample where reconstitution was not successful) and artefacts (probably from singlet and triplet excited states of antenna pigments which were disconnected during extraction of phylloquinone) were superimposed (Brettel, K., unpublished results).

Interestingly, the spin-polarised spectra of the secondary pair with duroquinone or naphthoquinone added to phylloquinone-depleted PS I indicated rather different orientations of these quinones compared to that of phylloquinone in native PS I [250,260,261]. A crucial question is, whether the native A_1 binding site allows non-native quinones to bind in deviating orientations or whether this is the result of structural modifications induced by the rather harsh treatment for extraction of phylloquinone. I feel that there is a need for milder procedures for the extraction of phylloquinone. A promising approach is the quinone exchange by incubation at elevated temperature in the presence of the replacement quinone which was shown to allow replacement of protonated phylloquinone by deuterated phylloquinone, and vice versa [7,207]. Unfortunately, the procedure was not yet successful with other quinones.

Summarising the data related to the chemical nature of A_1, a large body of independent evidence supports the assignment of A_1 as a phylloquinone, although some observations (inter alia, low temperature electron transfer to the iron-sulphur clusters in the absence of phylloquinone, and the bleaching around 450 nm accompanying the reduction of A_1) still await experimentally proven explanations. As a rather unambiguous proof for the direct participation of phylloquinone in forward electron transfer at room temperature, it may be useful to demonstrate by transient EPR that incubation of extracted PS I with deuterated phylloquinone restores electron transfer from A_1^- to the iron-sulphur centres at physiological temperature with kinetics as in native PS I, but with spectral characteristics of the spin-polarised signals as expected for deuterated A_1 (to my knowledge, this evident experiment has not yet been reported).

With respect to the environment of A_1, a recent ENDOR study of photoaccumulated A_1^- indicated that two protons are hydrogen-bonded to the quinone oxygens [99,201]. By contrast, a rather high g_x-value of A_1^- (higher than that of the semiquinone anion of phylloquinone in frozen alcohol [35] was obtained from simulations of the spin-polarised $P700^+A_1^-$ spectrum [248] and led to the suggestion that A_1 may be bound by $\pi-\pi^*$ interactions and not hydrogen bonds [261]; see also Ref. [260]. It is of note that reduction potentials of 2,3-substituted 1,4-naphthoquinones as low as what is required for an electron carrier between A_0 and F_X were, in vitro, only observed in aprotic solvents [38,197], and hence the environment of A_1 was assumed to be aprotic, as well [32,217]. However, there may well be other environmental factors which destabilise the semiquinone anion relative to the neutral quinone and hence lead to a low reduction potential, e.g., fixed negative charges or aromatic residues close to A_1 (see Ref. [115] for a discussion).

3.2.4. F_X

It is now widely accepted that F_X is a [4Fe-4S] cluster ligated by four cysteines; two of these cysteines are located in PsaA (C574 and C583 in maize) in a putative stromal-exposed extramembrane loop, and the other two in the homologous loop of PsaB (C582 and C591) (see Ref. [82] for a review and Ref. [204]). For PsaB, recent mutational analysis confirmed the implication of these two cysteines in the binding of F_X [244,263,273,274]. A similar study was performed for the first cysteine in the putative F_X binding region of PsaA, but the results were not yet conclusive [89,195]. EPR studies of F_X^- ($g_x \approx 1.76$, $g_y \approx 1.86$, $g_x \approx 2.06$ [62] in oriented thylakoid membranes demonstrated that the magnetic *x*-axis of F_X^- is oriented perpendicularly to the membrane [54,87,106]. This would be consistent with a cluster orientation as depicted in Fig. 3 if one assumes that the magnetic *x*-axis is parallel to a vector connecting two iron atoms; this was assumed for F_A^- in Ref. [33], but a different orientation of the magnetic *x*-axis in reduced [4Fe-4S] clusters appears to be possible (see Section 3.2.5). Furthermore, the somewhat unusual and not well understood EPR characteristics of F_X^-

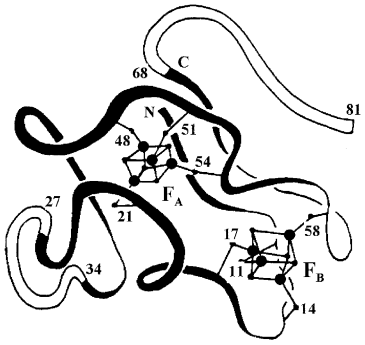

Fig. 7. Simulation of the three-dimensional structure of PsaC by Oh-oka et al. [191], combined with the cluster assignment by Zhao et al. [281]. The black ribbon shows the main chain folding of the *Peptococcus aerogenes* ferredoxin. The white ribbon shows the additional internal loop and the C-terminal extension of PsaC. Fat and thin dots represent iron and sulphur atoms, respectively. Adapted from Ref. [191]. The sequence numbering was adjusted to that in *Synechococcus* sp. PCC 7002.

(compared to other reduced [4Fe-4S] clusters, g_x and g_y are lower, the lines are broader and saturate at higher microwave power) may be related to an unusual orientation of the g-tensor axes.

3.2.5. F_A and F_B

The subunit PsaC, which binds the two terminal [4Fe-4S] clusters F_A and F_B, exhibits significant sequence homology to bacterial 2[4Fe-4S] ferredoxins; most of these proteins contain two distinct CxxCxxCxxxCP motifs providing the cysteine ligands to the iron-sulphur clusters. A structural model for PsaC has been developed in analogy to the crystal structure of the ferredoxin from *Peptococcus aerogenes* [55,191]; see also Fig. 7. F_A and F_B can be distinguished by low temperature EPR (see e.g. Ref. [82] for a review) because of their characteristic g-values ($g_x = 1.86$, $g_y = 1.94$, $g_z = 2.05$ for F_A^-, and $g_x = 1.89$, $g_y = 1.92$, $g_z = 2.07$ for F_B^-); reduction of both F_A and F_B in the same PS I complex ($F_A^- F_B^-$) yields a spectrum ($g = 1.89$, 1.92, 1.94 and 2.05) different from the superposition of F_A^- alone and F_B^- alone, indicating magnetic interaction and, hence, not a large distance between F_A and F_B. Recently, through site-directed mutations, cysteine ligands to F_A (C51) and F_B (C14), respectively, could be identified in PsaC from *Synechococcus* sp. strain PCC7002, allowing the assignment of the cluster ligated by cysteines 11, 14, 17, and 58 as F_B and the cluster ligated by cysteines 21, 48, 51, and 54 as F_A [281]; see Fig. 7. Until recently, models of the cofactor arrangement in PS I assumed that F_A and F_B are at approx. equal distances from F_X because of indications of parallel electron transfer pathways from F_X to F_A and to F_B (see Section 5). Independently from the crystal structure analysis, Guigliarelli et al. estimated from simulations of the EPR signals of F_A^-, F_B^-, and ($F_A^- F_B^-$) in oriented membranes, that the axis connecting F_A and F_B is tilted out of the membrane plane by 57°, suggesting a sequential electron transfer mechanism between the iron-sulphur clusters [87]. For comparison, the crystal structure analysis yielded an angle of 36° (assuming that the crystal c-axis is normal to the membrane) [218] (see also Fig. 3). The origin of the deviation remains to be elucidated.

EPR spectroscopy was also applied to single crystals of PS I in order to determine the orientation of F_A and F_B. As illumination of these crystals at 18 K preferentially formed the pair $P700^+F_A^-$, (and only a small amount of $P700^+F_B^-$; see also Section 5), a first study focused on the orientation of F_A [33]. Recording EPR spectra while turning the crystal with respect to the static magnetic field yielded a rotation pattern of the line positions (generally six lines, one for each of the six PS I complexes in the unit cell), which allowed the determination of the orientation of the three principal axes of the g-tensor of F_A^- with respect to the crystal axes for each of the six PS I complexes in the unit cell. To obtain the orientation of the F_A cluster, it was assumed that the g_z-axis is normal to a face of the [4Fe-4S] cluster (Fe and S atoms occupy alternating corners of a distorted cube; see Fig. 7), and that g_x and g_y are oriented parallel to the diagonals of the same face. In a recent study on single crystals of a [4Fe-4S] model compound, Gloux et al. [76] observed, in addition to reduced clusters with a g-tensor orientation close to the one just described (called species II_R), another reduced species (I_R) where all three principal g-tensor axes were close to normal to the faces of the cube. The principal g-values of the two species were significantly different, with those of species I_R being closer to the g-values of F_A^-. This result questions the F_A cluster orientation proposed in Ref. [33]. Very recently, the orientation of the g-tensor axes of F_B^- in PS I crystals was determined by using illumination at 200 K in order to increase the fraction of centres forming the

pair $P700^+F_B^-$ [123]. Taking into account the orientation of the axis connecting F_A and F_B (from the X-ray structure of PS I) and the structural analogy with the ferredoxin from *Peptococcus aerogenes*, Kamlowski et al. [123] suggest two possible orientations of PsaC (one with F_A closer to F_X and one with F_B closer to F_X; in both cases, the g-tensor orientation of F_A^- and of F_B^- is that of species II_R in [76]). These two orientations of PsaC agree with the result of adjusting the orientation of the ferredoxin of *Peptococcus aerogenes* as a PsaC substitute against the electron density map of PS I crystals [123,218]. It should be mentioned that the relative orientation of the g-tensor axes of F_A^- and F_B^- suggested in Ref. [123] disagrees with that estimated from a simulation of the EPR spectrum of interacting F_A^- and F_B^- [87]. Also the origin of the relatively low g_z-value of F_B^- (2.056) in the PS I crystals remains to be clarified.

The assignment of the two outer-most iron-sulphur clusters in the crystal structure (F_{AB1} and F_{AB2} in Fig. 3) to the species F_A and F_B as characterised by low temperature EPR is presently the subject of a controversial discussion. Assuming a sequential electron transfer pathway $F_X \rightarrow F_B \rightarrow F_A$ as apparently suggested by the reduction potentials (Fig. 2; see also Section 6), the proximal cluster F_{AB1} would be expected to be F_B, and the distal cluster F_{AB2} to be F_A. This electron transfer pathway, however, is far from being established (see also Section 5), and some data, although not unambiguous, indicate rather the opposite assignment of F_A and F_B (see also Ref. [79] for a discussion). Thus, based on observations that F_B is more susceptible to denaturation with exogenous chemicals, He and Malkin [95] speculate that F_{AB2} (which is closer to the surface of the PS I complex than F_{AB1} [69] and was suggested to be the immediate electron donor to ferredoxin [147]) may in fact be F_B. This assignment would be consistent with reports that selective denaturation of F_B does not impair electron transfer to F_A [67,71,86,95,120,211] (the opposite result, however, was reported in Ref. [156]). Electron transfer to the water-soluble acceptors ferredoxin and flavodoxin was inhibited by selective destruction of F_B [71,120]. The assignment of F_{AB2} as F_B was also deduced from studies on samples where F_B was assumed to be inactivated by mutation of a cysteine ligand (C14 of PsaC in *Synechococcus* sp. PCC 7002; see Fig. 7) to an aspartic acid, but photoreduction of F_A at low temperature was not impaired [81,281]. According to more recent results, however, the modified F_B cluster may have functioned as an electron acceptor ([278]; see also Section 4.1.3), so that the data on the C14D mutant cannot be considered as unambiguous evidence for direct electron transfer from F_X to F_A (but see Refs. [96,160] for a deviating conclusion from a study on *Anabaena variabilis*).

In a recent promising approach aimed at the assignment of F_A and F_B, possible binding sites between PsaC and the PS I core were analysed (inter alia by mutational analysis) in order to establish the orientation of the PsaC protein [16,182,183]. Preliminary results indicated that the aspartic acid at position 9 in PsaC interacts electrostatically with an arginine in PsaA or PsaB, supporting an orientation of PsaC where F_B is the proximal cluster F_{AB1} [16]. Naver et al. [182,183] concluded that the 'internal loop' of PsaC (which is lacking in the *Peptococcus aerogenes* ferredoxin; see Fig. 7) interacts with PsaA and PsaB, and that the C-terminal extension of PsaC (see Fig. 7) provides a binding site for PsaD. They proposed that the 'internal loop' of PsaC faces the thylokoid membrane and that the C terminus is oriented toward the stroma. No explicit conclusion for the assignment of F_A and F_B was drawn in Refs. [182,183], but comparison with the two orientations suggested by Kamlowski et al. [123] (see above) would favour the orientation where F_B is the proximal cluster F_{AB1}.

4. Recent data on the electron transfer reactions at physiological temperatures

4.1. Forward electron transfer

4.1.1. Formation of the primary pair, $P700^+A_0^-$, and subsequent reoxidation of A_0^-

The literature on forward electron transfer through A_0 has been reviewed in detail by Sétif in 1992 [220]. The kinetics appeared not yet well established, with estimates of approx. 30 ps or faster for the formation of $P700^+A_0^-$ and approx. 30 ps or 200 ps for the reoxidation of A_0^-. A major difficulty in studying these reactions by optical spectroscopy is that excitation energy transfer occurs on the same time scale and is accompanied by absorbance changes

in the same red spectral region as the most prominent absorbance changes due to oxidation of P700 and reduction of A_0 (discussed in Ref. [220]). According to recent data, it is virtually impossible to observe the transient state $P700^+A_0^-$ in the intact PS I complex when low excitation energies (less than 1 photon absorbed per P700) are used, because the rate constant of reoxidation of A_0^- is similar to or even faster than the trapping of the excitation energy (comprising energy transfer to P700 and formation of $P700^+A_0^-$) which takes approx. 20–40 ps [93,94,101,105]. The trapping kinetics could be accelerated, however, by using a higher excitation energy; thus, at 4–8 photons absorbed per P700, Hastings et al. [94] reported transient absorbance changes indicating formation of $P700^+A_0^-$ with a time constant $\tau \approx 4$ ps and reoxidation of A_0^- with $\tau \approx 21$ ps in intact PS I from a cyanobacterium. As the 4 ps for formation of $P700^+A_0^-$ include energy transfer to P700, the intrinsic time constant of primary charge separation (reaction $P700^*A_0 \rightarrow P700^+A_0^-$) should be shorter than 4 ps [94], in line with an estimate of 1.6 ps obtained from a study at low excitation energy using the same biological material [93]. The high excitation energy which had to be used in Ref. [94] had the disadvantage that the absorbance changes due to energy transfer processes were one order of magnitude larger than those due to electron transfer. To correct the data for the energy transfer processes, transients from samples with preoxidised P700 were subtracted, assuming that the energy transfer is independent of the oxidation state of P700. This assumption is supported by fluorescence measurements (see Ref. [220] for refs. and a discussion), but it seems unlikely to me that it is more than an approximation, because it would be difficult to understand how $P700^+$ should quench antenna excitations in exactly the same way as neutral P700 does, since the absorption spectra of both species are rather different. Slight deviations in excitation energy quenching by P700 and $P700^+$ would be sufficient to distort the spectra and the kinetics of electron transfer as obtained by the subtraction procedure considerably.

Kumazaki et al. [142,143] studied primary charge separation in PS I preparations from spinach where 85–90% of the antenna chlorophylls, all carotenoids and phylloquinone had been extracted (the water content of the extracting solvent diethyl ether was varied in order to vary the percentage of extracted chlorophyll). In these preparations, at moderate excitation energies (0.4 to 1.5 photons absorbed per P700), the absorbance changes due to electron transfer were rather large and comparable to those due to transfer and trapping of excitation energy, and the primary pair was relatively long-lived (approc. 50 ns) because of the absence of the secondary acceptor A_1 (see Section 4.2.1). Time constants between 6 and 11 ps were determined for the formation of $P700^+A_0^-$ [142,143], and the intrinsic time constant for the reaction $P700^*A_0 \rightarrow P700^+A_0^-$ was estimated to be 3.0 ps for one of the preparations (note that partition of the excitation between P700 and the antenna chlorophylls slows down the overall charge separation) [143]. The main bleaching feature attributed to the reduction of A_0 was centred at 683 to 686 nm [142,143]. Upon addition of menaquinone-4, phylloquinone or 2-methyl-1,4-naphthoquinone, rapid reoxidation of A_0^- was observed with time constants between 23 and 34 ps [142]. Compared to intact PS I, the risk of distortion of the kinetic and spectral data due to the subtraction of energy transfer processes appears less prominent in the extracted samples. However, one should be aware of the possibility that the rather harsh extraction procedure may have modified the native kinetics of electron transfer, the A_1 binding site, and the spectra of the pigments which are still present.

Hecks et al. [101] studied electron transfer in intact PS I from a cyanobacterium by picosecond photovoltage measurements. At an excitation energy corresponding to 2 absorbed photons per P700, their data analysis yielded, in addition to a very fast rising phase (attributed to formation of $P700^+A_0^-$; the rise time was not explicitly reported) a slower phase with $\tau \approx 50$ ps and approx. 25% of the electrogenicity of the very fast phase. The 50 ps phase was attributed to electron transfer from A_0^- to A_1. The photovoltage technique has the advantage that electron transfer kinetics can be measured without perturbation by excited state dynamics. Unfortunately, however, it does not provide direct information on the nature of the charge separated states, so that independent information is needed to assign the observed kinetics.

In summary, the newly available data from three different approaches are roughly consistent with respect to the intrinsic time constant of primary charge

separation (in the order of a few picoseconds; see also Ref. [257]) and with respect to the reoxidation kinetics of A_0^- (20–50 ps), although each of the approaches has its limitations. In none of these studies was kinetic evidence obtained that a further chlorophyll molecule (A or A′ in Fig. 3) functions as a real intermediate in electron transfer from P700 to A_0 (see also Section 7.2.1). However, it was suggested that the difference spectrum for the reduction of A_0 contains contributions from more than one single chlorophyll pigment [92]. It is of note that the real kinetics of $P700^+A_0^-$ formation apparently depends on the antenna size and the excitation energy, explaining in part the varying results in the earlier literature (reviewed in Ref. [220]). An A_0^- reoxidation time in the order of 30 ps had already been reported in some of the earlier work [65,238].

4.1.2. Electron transfer through A_1

Forward electron transfer through A_1 has been investigated systematically only since 1988. In flash absorption studies around 380 nm, the rise kinetics of the absorbance increase attributed to the reduction of A_1 was faster than 5 ns (instrumental time resolution) [27,171]. As A_0^- is reoxidised within approx. 30 ps (see Section 4.1.1), the existence of an intermediate between A_0 and A_1 cannot be ruled out yet. However, no positive indication for such an intermediate has been obtained by picosecond spectroscopy so far.

For the reoxidation of A_1^-, half times of 15 ns and 200 ns were reported for PS I preparations from spinach [171] and from the cyanobacterium *Synechococcus* sp. [27], respectively. More recently, comparison of different PS I preparations from spinach revealed a biphasic reoxidation of A_1^- with half times of approx. 25 and 150 ns at an amplitude ratio varying between approx. 2:1 and 1:2 for different preparations [225]. As harsh treatments during preparation of the PS I particles apparently increased the relative amplitude of the 25 ns phase, it was suggested that PS I in native spinach membranes could behave similarly to the cyanobacterial PS I particles, i.e., exhibit essentially monophasic reoxidation of A_1^- with $t_{1/2} \approx 200$ ns [225], but this has not yet been confirmed experimentally. It was observed, however, that in cyanobacteria a biphasic reoxidation of A_1^- similar to that in preparations from spinach could be induced by use of the detergent Triton X-100 for the isolation of PS I (Brettel, K. and Golbeck, J.H., unpublished results; see also Ref. [259]), supporting a similarity of electron transfer through A_1 in higher plants and cyanobacteria. The origin of the biphasic reoxidation kinetics of A_1^- in certain PS I preparations is not yet established. Sétif and Brettel [225] suggested either a heterogeneity of these samples with respect to the reoxidation kinetics of A_1^-, or a fast redox equilibrium between A_1 and F_X according to Scheme 1. In the latter case, the 25 ns phase would reflect the establishment of the equilibrium and the 150 ns phase its depopulation by electron transfer to F_A or F_B. Direct electron transfer from A_1^- to (F_AF_B) (k_2 in Scheme 1) was considered as a possibility in Ref. [225], but this was not confirmed by later work (see below). Assuming $k_2 = 0$ and a homogeneous sample, the experimental results for the reoxidation of A_1^- in the PS I-β preparation from spinach (65% of a 25 ns phase and 35% of a 150 ns phase) implied an equilibrium constant $K = k_1/k_{-1} \approx 3.2$ ($\Delta G^0 \approx -30$ meV at 298 K) [225].

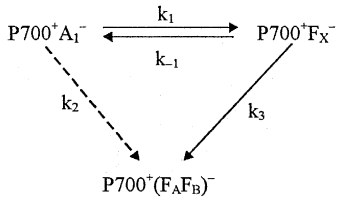

Scheme 1.

At variance with the references mentioned so far, Warden [269] reported that F_X was reduced within 5 ns after excitation, so that reoxidation of A_1^- should have occurred within 5 ns as well. The conclusion was based on a fast (≤ 5 ns) bleaching at 410 and 445 nm, two wavelengths assumed to be isosbestic points of the $P700^+$/P700 difference spectrum. These bleachings were attributed to the reduction of F_X. In the same report, a difference spectrum at 5 ns after excitation is presented which shows a pronounced absorbance increase between 350 and 400 nm, in line with spectra previously attributed to formation of the pair $P700^+A_1^-$ (see Section 3.2.3), but clearly different from a recent spectrum for the formation of the pair $P700^+F_X^-$ [152]. Hence, I consider it likely that $P700^+A_1^-$ was present at 5 ns after excitation in Ref. [269]; a slight deviation in effective wavelengths of the monitoring light from the isosbestic points of the

$P700^+/P700$ difference spectrum (which is very steep at the isosbestic points) may explain the bleachings observed at 410 and 445 nm as due to formation of $P700^+$; at 445 nm, reduction of A_1 may have contributed to the bleaching as well (see Fig. 6).

The reoxidation of A_1^- was also studied by transient EPR of the spin-polarised pair $P700^+A_1^-$, confirming a half-time in the order of 200 ns for different PS I preparations from spinach and from cyanobacteria [21,259]. A 25 ns phase was beyond the time resolution of these experiments, but indirect evidence for the presence of a phase with $t_{1/2} < 50$ ns in some of the samples was obtained from an analysis of the EPR spectra [259].

From recent photoelectric measurements in the ns-time range on PS I membranes from a cyanobacterium, a rising phase with a time constant τ of 220 ± 20 ns ($t_{1/2} \approx 150$ ns) was reported and attributed to electron transfer from A_1^- via F_X to F_A or F_B [146]; see also Section 4.1.3.

It is of note that evidence for a forward electron transfer step with $\tau \approx 170$ ns ($t_{1/2} \approx 120$ ns) was obtained already much earlier in electron spin echo experiments by Thurnauer et al. [255,256]. The signals were attributed to electron transfer from F_X^- to the $F_A - F_B$ complex because they disappeared upon chemical reduction of F_A and F_B [256]. It seems possible, however, that reduction of F_A and F_B had blocked forward electron transfer at the level of A_1 rather than F_X (suggested in Ref. [28]; see also below) or that A_1 had become doubly reduced (suggested in Ref. [176]), so that the 170 ns phase observed in Refs. [255,256] under moderate redox conditions could be attributed to the reoxidation of A_1^- during normal forward electron transfer. Recent electron spin echo experiments were interpreted to indicate reoxidation of A_1^- with a time constant between 130 and 190 ns in PS I from spinach and 300 ns in PS I from a cyanobacterium [176].

Until recently, it was not well established that electron transfer from A_1^- to the terminal iron-sulphur clusters F_A and F_B in intact PS I involves F_X as an intermediate acceptor (see also Section 5). This point had been addressed by studying the effect of chemical reduction of F_A and F_B. In PS I preparations from spinach, the fast phase of A_1^- reoxidation ($t_{1/2} \approx 25$ ns) persisted after chemical reduction of F_A and F_B and was hence attributed to electron transfer to F_X [171,225]. This is consistent with earlier work reporting that the pair $P700^+F_X^-$ was formed under these conditions and decayed by charge recombination with $t_{1/2} \approx 250$ μs (see Section 4.2.3). The approx. 200-ns phase of A_1^- reoxidation (which dominated in PS I from cyanobacteria but was only a minor phase in some PS I preparations from spinach), however, disappeared upon prereduction of F_A and F_B and was apparently replaced by a 250 μs charge recombination between A_1^- and $P700^+$ [20,28,225]. To explain the latter observations, it was suggested that either F_X was not involved in electron transfer from A_1^- to (F_AF_B), or that reduction of F_A and F_B blocked electron transfer from A_1^- to F_X, for example by an electrostatic interaction shifting the reduction potential of F_X to a value below that of A_1 [28].

The kinetics of A_1^- has now been studied after treatments which remove the terminal acceptors F_A and F_B (together with the stromal extrinsic subunits PsaC, PsaE, and eventually PsaD [84,152]. Data from flash absorption spectroscopy [152], electron spin echo spectroscopy [176], transient EPR [259] and photoelectric measurements [146] showed that the A_1^- reoxidation kinetics (half times in the range from 100 to 250 ns for the different PS I preparations from cyanobacteria and a preparation from spinach) was not modified by the removal of F_A and F_B. All these studies concluded that the sequence of forward electron transfer was $A_1 \rightarrow F_X \rightarrow (F_AF_B)$, i.e., rate constant k_2 in Scheme 1 is negligible. This is also consistent with the arrangement of these cofactors suggested from X-ray crystallography (Fig. 3) and with the sign of the photovoltage signal attributed to electron transfer from A_1^- to F_X which indicates that F_X is closer to the stromal side (and hence to F_A and F_B) than A_1 [146].

To explain the different effects of prereduction and removal of F_A and F_B which are most obvious in PS I from cyanobacteria, I suggest a shift of the redox equilibrium between A_1 and F_X, such that the pair $P700^+F_X^-$ is lower in free energy than the pair $P700^+A_1^-$ in the absence of F_A and F_B, but higher with F_A and F_B prereduced, as schematically shown in Fig. 8a,b. The equilibrium constants for these two cases may be estimated as follows. For removed F_A and F_B, the difference spectrum of the charge separated state after completion of forward electron transfer to F_X shows higher absorbance in the 350 to 390

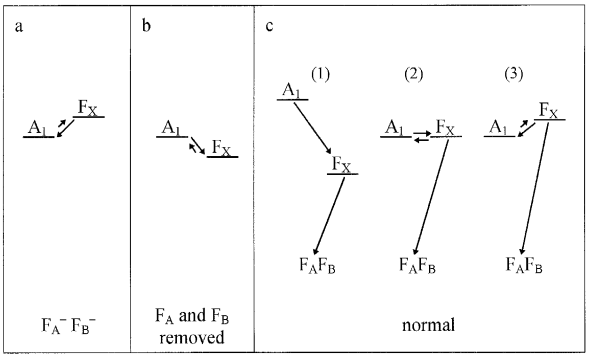

Fig. 8. Schematic representation of the redox equilibria between A_1 and F_X which might account for experimental results in PS I from cyanobacteria. A_1 and F_i (i = X, A, B) denote the states $P700^+A_1^-$ and $P700^+F_i^-$, respectively. Panel a: F_A and F_B prereduced. Panel b: F_A and F_B removed. Panel c (1), (2) and (3): typical examples for normal conditions (F_A and F_B oxidised). See text for details.

nm range than the state $P700^+(F_AF_B)^-$ in native PS I [152]. Lüneberg et al. [152] assumed that this reflects a difference in the optical features of F_X compared to F_A or F_B. Deviating from this view, I suggest that the presence of some A_1^- (in equilibrium with F_X^-) accounts for the higher absorbance between 350 and 390 nm. From the data ([152] and Brettel, K. and Golbeck, J.H., unpublished results), the equilibrium constant $K = k_1/k_{-1}$ can be estimated to be approx. 3, corresponding to $\Delta G^0 \approx -28$ meV (at 298 K). For prereduced F_A and F_B, the data presented in Ref. [28] demonstrated that forward electron transfer from A_1^- was largely blocked, but the signal-to-noise ratio was too poor to decide whether partial electron transfer from A_1^- to F_X still occurred. Improved measurements at 380 nm on PS I from *Synechocystis* sp. PCC 6803 in the presence of dithionite at pH 10 showed that about 25% of A_1^- was reoxidised on a nanosecond time scale ($t_{1/2} \approx 150$ ns) (Brettel, K., unpublished results). This indicates an equilibrium constant of approx. 0.33 corresponding to $\Delta G^0 \approx 28$ meV for the redox equilibrium between $P700^+A_1^-$ and $P700^+F_X^-$ in the presence of prereduced F_A and F_B. Thus, removal of F_A and F_B would decrease the free energy difference between $P700^+F_X^-$ and $P700^+A_1^-$ by approx. 56 meV compared to PS I with prereduced F_A and F_B. Interestingly, the reduction potential of F_X was reported to increase by 60 mV due to removal of F_A and F_B (compared to PS I with prereduced F_A and F_B) [193]. I would like to point out that the close correspondence between these two values may be fortuitous, because the equilibrium constants used above are only rough estimates and because the reduction potential of A_1 may also change upon removal of F_A and F_B; furthermore, redox titration of F_X is rather difficult, especially in the presence of F_A and F_B, where only partial reduction of F_X could be achieved in Ref. [193]. Possible reasons for the effect of reduction/removal of F_A and F_B on the energetics of the pair $P700^+F_X^-$ (and possibly $P700^+A_1^-$) include:

· an alteration of the electrostatic interaction energies between these pairs and the negative charges on F_A and F_B (cf. Ref. [193]) as well as the charged amino acids in the stromal extrinsic subunits which are removed together with F_A and F_B;

· a change in the dielectric environment because the aqueous phase is nearer to F_X upon removal of the stromal extrinsic subunits (cf. Ref. [193]), resulting most likely in an increased effective dielectric constant and a stabilisation of charged species (see, e.g., Ref. [75]); this might stabilise reduced F_X (three negative charges, including the cysteines ligating the cluster) more than oxidised F_X (two negative charges; note, however, that other charges in the vicinity of F_X may also have to be considered);

· conformational changes within the PS I core protein complex.

With respect to intact PS I with oxidised F_A and F_B, the reported monoexponential reoxidation of A_1^- with $t_{1/2} \approx 200$ ns in PS I from cyanobacteria (see above) could be explained most easily assuming $k_{-1} \ll k_1 \approx 3.5 \times 10^6$ s^{-1} (see Fig. 8c, example 1), as implicitly assumed in Refs. [146,152,176,259]. In view of the rather mediocre signal-to-noise ratio of all published measurements of the A_1^- reoxidation kinetics, one should admit that a second phase with a relative amplitude below approx. 15% may have escaped detection (see also Ref. [225]). If this were the case, one would not have to assume $k_{-1} \ll k_1$. For example, $k_1 = k_{-1} = 5 \times 10^6$ s^{-1} ($\Delta G^0 = 0$) and $k_3 = 1.4 \times 10^7$ s^{-1} (see Fig. 8c, example 2) would yield 9% of a phase with $t_{1/2} \approx 34$ ns, in addition to the dominating 200 ns phase. Even uphill electron transfer from A_1^- to F_X could be compatible with the experimental results, as, for example, $k_1 = 8 \times 10^6$

s^{-1}, $k_{-1} = 2 \times 10^7$ s^{-1} ($\Delta G^0 = 24$ meV at 298 K) and $k_3 = 2 \times 10^7$ s^{-1} (Fig. 8c, example 3) would yield approx. 11% of a phase with $t_{1/2} = 16$ ns, in addition to the dominating 200 ns phase. Assuming $k_1 \lesssim k_{-1}$ ($\Delta G^0 \gtrsim 0$) for intact PS I would imply that removal of F_A and F_B decreases the free energy of $P700^+F_X^-$ relative to $P700^+A_1^-$ (see Fig. 8). In summary, a dominating 200 ns phase of A_1^- reoxidation is compatible with a range of different equilibrium constants between the states $P700^+A_1^-$ and $P700^+F_X^-$.

Another not definitively resolved question is the potential role of the second phylloquinone molecule present in PS I. It has been reported that one phylloquinone is readily extracted with hexane, without considerable loss of activity in light-induced electron transfer to the terminal iron-sulphur centres and to extrinsic acceptors, demonstrating that one phylloquinone molecule (which is not extracted with hexane) is sufficient for charge separation [15,157]. This result does not rule out, however, that the second phylloquinone is in some way involved in electron transfer in intact PS I, for example as A'_1 (see Fig. 3) in a parallel electron transfer branch from P700 to F_X, or as a 'dead end' in redox equilibrium with the other phylloquinone (A_1). These possibilities might be addressed by studying whether extraction of the second phylloquinone affects the kinetics of electron transfer through A_1. Recently, Schwartz and Brettel [219] reported that extraction of PS I with hexane according to Ref. [15] did not change the reoxidation kinetics of A_1^-; surprisingly, however, thorough quantification of the phylloquinone content of the extracted samples yielded approx. two phylloquinones per P700, so that the unchanged kinetics does not provide evidence against a possible participation of the second phylloquinone.

4.1.3. Electron transfer between the iron-sulphur centres F_X, F_B and F_A

Spectroscopic distinction between F_A^-, F_B^- and F_X^- by EPR (see Sections 3.2.4 and 3.2.5) is unfortunately restricted to temperatures below approx. 30 K. For studies at higher temperatures, flash absorption spectroscopy might be applied, but the difference spectra for the reduction of the three iron-sulphur centres appear to be rather similar, showing a broad bleaching around 430 nm which is approx. four times weaker than the 430 nm bleaching due to oxidation of P700 [129,193]. F_A and F_B could not be distinguished so far, but there may be some deviations between the F_X^-/F_X spectrum and the $(F_AF_B)^-/(F_AF_B)$ spectrum [67,225]; note, however, that the reported deviations do not agree between these two references. Based on such a deviation at 453 nm, Franke et al. [67] resolved a kinetic component with $t_{1/2} \approx 800$ ns in PS I from *Synechococcus* sp. PCC6301 and attributed it to electron transfer from F_X^- to the proximal cluster F_{AB1} (see Fig. 3; it was suggested in Ref. [67] that F_{AB1} is F_A).

Electron transfer between the iron-sulphur centres was also studied by photovoltage measurements. Using spinach PS I particles which were partially oriented in a phospholipid layer and adsorbed to a Teflon film, Sigfridsson et al. [243] resolved rising phases with time constants of approx. 30 μs (approx. 30% of the total rise) and 200 μs (20%); the fast initial rise (50%) was limited by the 1 μs response time of the apparatus. More recently, using a time resolution of 50 ns, a fastest time constant of 500 ns was reported by the same authors [242]. Two alternative assignments were proposed for the three phases [242,243]:

(I) 500 ns phase, reduction of F_B; 30 μs phase, electron transfer from F_B^- to F_A; 200 μs phase, electron transfer from F_A^- to a soluble acceptor or proton transfer or conformational change

(II) 500 ns phase, reduction of F_X; 30 μs phase, electron transfer from F_X^- to F_B; 200 μs phase, electron transfer from F_B^- to F_A.

In both assignments it was assumed that the proximal cluster F_{AB1} is F_B.

Leibl et al. [146] studied oriented PS I membranes from *Synechocystis* PCC6803 which formed a multilayer on a platinum electrode. Approx. 60% of the total detected photovoltage rose within 35 ns (limited by the time resolution of the instrument; see Section 4.1.1 for measurements with a faster time resolution), and 40% rose with a time constant τ of 220 ns. The latter phase was attributed to electron transfer from A_1^- via F_X to (F_AF_B), assuming that the time constant of the first step (A_1 to F_X) is 220 ns, and that of the second step (F_X to (F_AF_B)) is faster than 50 ns. I would like to mention that a kinetic scheme with uphill electron transfer from A_1^- to F_X and depopulation of the redox equilibrium between A_1 and F_X by electron transfer to (F_AF_B) (see Section 4.1.2 and Fig.

8c, example 3) could yield similar photovoltage kinetics. The μs time range was not accessible in Ref. [146] because of fast ionic relaxations within the sample (see also below). With respect to the kinetics in the ns range, it is of note that Sigfridsson et al. [242] mentioned an artefact in the reverse direction which obscured components faster than 500 ns. Thus, one cannot yet exclude that the different photovoltage kinetics reported by the two laboratories reflect technical limitations and problems rather than real differences in the electron transfer rates between different samples.

Independent evidence for a submicrosecond electron transfer from F_X^- to F_A or F_B in *Synechocystis* sp. PCC6803 was derived from studies of electron transfer from PS I to ferredoxin. Sétif and Bottin [222,233] found that in about one-third of the PS I-ferredoxin complexes, the ferredoxin was reduced with $t_{1/2} \approx 500$ ns, so that F_A or F_B must have been reduced at least partly within less than 500 ns (F_X was excluded as a potential immediate electron donor to ferredoxin [222]). This is in line with the interpretation of the photovoltage measurements of Leibl et al. [146]. Considering the rather mediocre accuracy of the experimental data and accepting some variation of the kinetics between different PS I preparations, the fast ferredoxin reduction may be compatible with the interpretation of the optical data on electron transfer from F_X to F_{AB1} ($t_{1/2} \approx 800$ ns [67]; see above) and with assignment I, but not with assignment II (see above), of the photovoltage measurements of Sigfridsson et al. [242,243]. A difficulty with assignment I is, however, that electron transfer from P700 to F_{AB1} would correspond to only about 50% of the total electrogenicity of charge separation in PS I. Furthermore, an electron microscopy study suggests that the distal iron sulphur cluster (F_{AB2} in Fig. 3) is the immediate donor to ferredoxin [147] and should hence be reduced within less than 500 ns instead of 30 μs as assumed in assignment I.

I would also like to mention an interesting effect of glycerol on the photovoltage kinetics reported in Ref. [146]: the phase rising with $\tau \approx 220$ ns (in the absence of glycerol) slowed down to 350 to 600 ns (depending on the glycerol concentration) and decreased in amplitude, although the reoxidation kinetics of A_1^- as measured by flash absorption spectroscopy ($\tau = 200–230$ ns in the absence of glycerol) slowed down only slightly. Leibl et al. [146] point out that glycerol may slow down electron transfer from F_X^- to (F_AF_B) (see Sections 5 and 6 for further glycerol effects), but could not exclude a specific effect of glycerol on the electrical response of their measuring cell (e.g., 66% glycerol slowed the time constant of ionic relaxation from about 50 ns (no glycerol) to more than 5 μs). I feel that one should not yet completely rule out the opposite case, i.e., that the results obtained under conditions of slow ionic relaxation (high glycerol concentration) reflect the charge separation kinetics correctly, whereas the deconvolution procedure applied to resolve the kinetics of electrogenic events which are slower than the fast ionic relaxation in the absence of glycerol may have distorted the kinetics (e.g., a strictly monoexponential relaxation was assumed in the deconvolution procedure, but the real ionic relaxation may be more complex).

A promising approach for a better understanding of electron transfer between the iron-sulphur clusters in PS I is the selective modification of either F_A or F_B by site-directed mutagenesis of their cysteine ligands. Thus, it was reported that the PsaC mutant C51D of *Synechococcus* sp. PCC 7002 assembled a [3Fe-4S] cluster in the F_A site, while the mutant C14D assembled an altered cluster of unknown identity in the F_B site [281]. Surprisingly, flash absorption spectroscopy performed by the author of this review in collaboration with J.H. Golbeck (see Refs. [278,280]) demonstrated that both mutants could successively stabilise two electrons beyond F_X, as did unmodified PS I (see also Refs. [211,212]). It has now been shown that both mutants assemble [4Fe-4S] clusters in the modified sites (at least when PsaC is rebound to the PS I complex [174]); the magnetic properties of the reduced clusters were, however, modified such that they could not be detected under the EPR conditions used normally for the detection of F_A^- and F_B^-; the reduction midpoint potentials were modified as well, but not as much as to impair electron transfer from F_X^- to the modified clusters, or from the modified clusters to ferredoxin and flavodoxin [278,280]. A study on PsaC mutants of the cyanobacterium *Anabaena variabilis* yielded similar results, except that the mutant C13D (corresponding to C14D in *Synechococcus* sp. PCC 7002) appeared to contain no functional cluster in the F_B site [96,160].

In summary, it remains a challenge to establish the pathway and kinetics of electron transfer between the iron-sulphur clusters of PS I.

4.2. Charge recombination reactions

The high quantum yield of charge separation observed in natural photosynthetic systems can only be achieved because forward electron transfer outcompetes charge recombination in each step, e.g., electron transfer from the i-th acceptor A_i to A_{i+1} is much faster than charge recombination between A_i^- and the oxidised electron donor. Charge recombination can be observed when forward electron transfer from A_i^- to A_{i+1} is blocked, e.g., by removing or prereducing A_{i+1}. Such studies have contributed much to establish the electron transfer pathway and energetics of PS I and to characterise charge separated states which were difficult to detect during forward electron transfer because of their short lifetime. When studying charge recombination, one should keep in mind, however, that the procedures applied to block forward electron transfer may modify the energetic, kinetic and spectroscopic properties of the preceding acceptor(s).

4.2.1. $P700^+A_0^-$ recombination

When forward electron transfer from A_0^- to A_1 is blocked, the primary pair $P700^+A_0^-$ decays by charge recombination with a half time in the order of 30 ns, forming two products: the singlet ground state of P700 and the triplet state ^{3}P700, which decays to the singlet ground state on a μs time scale (see, e.g., Ref. [82] for a review). These observations were explained in the framework of the reaction scheme shown in Fig. 9 (P and A_0 denote the primary electron donor and acceptor, respectively) which was based on studies of primary pair recombination in purple bacterial reaction centres (see Ref. [264] for a recent review). In brief, the primary pair is created from its singlet precursor $^1P^*$ in a singlet spin configuration $^1(P^+A_0^-)$; due to hyperfine interactions, the two unpaired spins can evolve to a triplet configuration $^3(P^+A_0^-)$ and eventually back again (indicated by the ω-symbol in Fig. 9). The typical time scale of singlet-triplet spin evolution is 10^{-8} s. Charge recombination forms either the singlet ground state P or the triplet state ^{3}P, depending on the spin configuration of the primary pair in the moment of recombination. An external magnetic field can modulate the spin evolution in the primary pair and hence the triplet yield and, if $k_S \neq k_T$ (see Fig. 9), the overall recombination kinetics. Based inter alia on magnetic field effects, estimates of $k_S \approx 4 \times 10^7$ s^{-1} and $k_T = (0.4–2.5) \times 10^9$ s^{-1} were obtained in purple bacteria, and the energy splitting between singlet and triplet states of the primary pair (exchange interaction) was estimated to be around 15 G ($\approx 1.7 \times 10^{-8}$ eV) [264]. The magnetic field effect curve for the ^{3}P700 yield in PS I showed a resonance at approx. 60 G; this value should correspond to the exchange interaction in the primary pair and indicates a stronger magnetic coupling than in purple bacteria [31]. The rate constant k_S is most likely somewhat slower in PS I than in purple bacteria [31], and k_T could be in the order of 10^9 s^{-1} (see Section 4.2.2), i.e., comparable to purple bacteria; $k_T \approx 10^9$ s^{-1} would also be compatible with the assumption that the width of the resonance in the magnetic field effect curve is essentially due to lifetime broadening (Polm, M. and Brettel, K., manuscript in preparation; see Ref. [275] for simulations of this effect). It is of note that so-called CP1-SDS particles were used in Ref. [31] which had lost part of the antenna chlorophylls and functional A_1 during preparation with the detergent SDS. One should not exclude that the relatively harsh preparation procedure might have modified the native interactions in the primary pair. The magnetic field effect on the P700 triplet yield was also studied in PS I

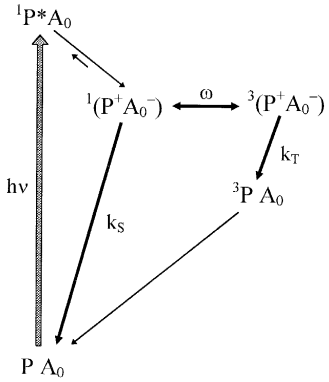

Fig. 9. Reaction scheme for charge recombination in the primary pair $P^+A_0^-$ in photosynthetic reaction centres when electron transfer to secondary acceptors is blocked. Adapted from Ref. [31].

treated with water-saturated diethyl ether which extracts phylloquinone, carotenoids and about 90% of the chlorophylls. The result was qualitatively similar to the SDS preparation, but the resonance at around 60 G was less pronounced [111]. Comparing data on the recombination kinetics of the primary pair in different PS I preparations with A_1 either extracted or doubly reduced, the reported half-times vary between 20 and 50 ns [15,23,31,110,167,221,223,271]; in one case, a biphasic description with $t_{1/2} = 26$ ns (59%) and 84 ns (41%) was provided [111]. Estimates of the yield of ^{3}P700 formation during the recombination vary between 15 and 62% [31,111,223,226]. The reasons for the variation of the reported recombination kinetics and yield of ^{3}P700 are not clear. The triplet yields should be regarded with some caution because of uncertainties in the exctinction coefficients used and because of possible contamination by antenna chlorophyll triplets.

The decay of the P700 triplet state shows some remarkable features. In CP1-SDS particles (see above), the decay half-time is approx. 6 μs at room temperature and is practically unaffected by the presence of oxygen in the medium, indicating that P700 is screened from oxygen [226]. The decay slows down upon cooling to $t_{1/2} \approx 800$ μs at 10 K [226]. The activation energy determined between 294 and 100 K is approx. 40 meV; below 60 K, the decay does not change any more with temperature ([169] in combination with [226]). A similar temperature dependency was observed for PS I particles prepared with Triton and poised at -625 mV [236], and for a preparation where A_1 was presumably doubly reduced by strong illumination in the presence of dithionite at pH 10 (Polm, M. and Brettel, K., manuscript in preparation). For comparison, the triplet state of Chl *a* in detergent micelles at room temperature is much longer lived ($t_{1/2} \approx 500$ μs) under anaerobic conditions, but can be quenched by oxygen ($t_{1/2} \approx 3$ μs in air-saturated medium at room temperature); the decay slows down upon cooling to $t_{1/2} \approx 1$ ms below 200 K [170,200]. The mechanism of the oxygen-independent activated decay of ^{3}P700 is not yet established. Interestingly, after treatment of PS I with diethyl ether, ^{3}P700 behaved more like ^{3}Chl *a* in vitro, showing a nearly temperature-independent decay under anaerobic conditions ($t_{1/2} \approx 560$ μs at 278 K and 1 ms at 10 K), and triplet quenching by oxygen ($t_{1/2} \approx 50$ μs in air-saturated medium at 278 K) [111]. Quenching of ^{3}P700 by oxygen at room temperature seems to occur also in PS I treated with hexane containing 0.3% methanol for extraction of phylloquinone (Schwartz, T. and Brettel, K., unpublished results; see also Ref. [15]). Ikegami et al. [111] pointed out that the difference between CP1-SDS particles and diethyl ether treated PS I may be due to the removal of carotenoid molecules in the latter preparation. They refer to a proposal by Schenck et al. [215] and suggest that the temperature dependency of the ^{3}P700 decay in CP1-SDS particles could be explained by a triplet energy transfer from an activated state ^{3}D (for example, a triplet state of a neighbour antenna chlorophyll) to a carotenoid molecule. To prove this model, one should check for the formation of carotenoid triplets at room temperature in CP1-SDS particles or in more native preparations after double reduction of A_1. With respect to alternative explanations for the activated decay of ^{3}P700, one may consider a decay pathway via an energetically higher radical pair state, as suggested for purple bacteria [41], or an unusually strong coupling between electronic states of P700 and phonon modes so that intersystem crossing may become an activated process [56]. I would also like to mention that ruffling distortions of the normally planar macrocycle skeleton of porphyrins can accelerate non-radiative transitions at room temperature (but not at 78 K) by several orders of magnitude [73].

4.2.2. $P700^+A_1^-$ recombination

Charge recombination in the secondary pair $P700^+A_1^-$ is expected to occur when the subsequent acceptors (F_X, F_B and F_A) are either prereduced or removed. It turned out that the kinetics of charge recombination and even its pathway are strikingly different for these two cases (see below). Charge recombination between $P700^+$ and A_1^- was also reported to occur when only F_A and F_B (but not F_X) were prereduced [28]; as it is likely that a fast redox equilibrium between A_1^- and F_X^- exists in this case, I will deal with this situation separately in Section 4.2.3.

Removal of F_A, F_B and F_X. When all three iron-sulphur clusters were removed, a transient decaying with $t_{1/2} \approx 10$ μs was observed in the flash-induced absorbance changes at 820 nm; it was originally

attributed to the P700 triplet state formed via charge recombination in the pair $P700^+A_1^-$ [272]. Analysis of the difference spectrum of the 10 μs phase revealed that (1) it is dominated by the P700 cation rather than the P700 triplet, indicating that the 10 μs transient represents a direct charge recombination which repopulates the ground state of P700 [271], and (2) that the partner of $P700^+$ in this recombination is definitively the secondary acceptor A_1^- [30], in agreement with a study by transient EPR [259]. A refined study of the recombination kinetics showed clear deviations from a monoexponential decay: at least two exponential phases ($t_{1/2} \approx 10$ μs and 110 μs at an amplitude ratio of approx. 2.5:1) were required for a satisfying fit, but a distribution of $P700^+A_1^-$ recombination rates may also account for the experimental results [30]. The origin of the non-monoexponential kinetics could not be established. The recombination slowed down only slightly upon cooling (at 10 K, $t_{1/2} \approx 15$ μs and 150 μs at an amplitude ratio of 1:1 yielded a satisfying fit) [30], in line with a direct recombination pathway (recombination via repopulation of an energetically higher state as the primary pair or the P700 triplet state should be a clearly activated reaction). In some 15% of the PS I complexes, charge recombination of the primary pair $P700^+A_0^-$ with $t_{1/2} \approx 50$ ns was observed at room temperature, indicating loss of A_1 in a fraction of the sample [272]; however, the percentage of primary pair recombination increased upon cooling, indicating that electron transfer from A_0^- to A_1 became blocked at low temperature in part of the centres [30]. Short incubation with dithionite at pH 8.3 of PS I devoid of the iron-sulphur clusters seemed to be capable of reducing a large fraction of A_1 (presumably to the quinol form), an event not occurring in intact PS I under these conditions [30]. These observations indicate that removal of all three iron-sulphur clusters (together with the stromal extrinsic proteins) modified the A_1 site considerably. It is hence not certain that the 10 μs recombination of $P700^+A_1^-$ dominating in this preparation represents the intrinsic recombination rate in intact PS I. I would like to add the following speculation: removal of the iron-sulphur clusters may have increased the redox potential of A_1 (for the one-electron reduction to the semiquinone-anion as well as for the double reduction to the quinol form) so that the free energy of the pair $P700^+A_1^-$ would be lower than in intact PS I. As the charge recombination to the P700 ground state almost certainly occurs in the Marcus inverted region (see Sections 7.1 and 7.2.3), a smaller free energy gap would imply a faster recombination rate. In addition, in PS I devoid of the three iron-sulphur clusters, A_1 is presumably less well shielded from the aqueous phase than it is in intact PS I so that the medium reorganisation energy (see Section 7.1) is presumably larger than it is in intact PS I. This would also imply a faster $P700^+A_1^-$ recombination (see Section 7.1). As a guess, the 150 μs recombination kinetics of $P700^+A_1^-$ observed in intact PS I below 180 K (see Section 5) may represent the intrinsic charge recombination rate also at room temperature. This could more easily be reconciled with the virtually 100% quantum yield of long-lived charge separation attainable in PS I [251] (a 10-μs recombination in competition with the 200-ns forward electron transfer from A_1^- to F_X would already cause 2% loss in the yield of charge separation).

Prereduction of F_A, F_B and F_X. When all three iron-sulphur clusters were prereduced by illumination of intact PS I in the presence of dithionite at pH 10, a transient decaying with $t_{1/2} \approx 3$ μs was observed at room temperature in the flash-induced absorbance changes at 820 nm [212,231]. Based on its difference spectrum in the near IR, the 3-μs phase was attributed to the decay of the triplet state of P700, formed with high efficiency ($> 90\%$) presumably via charge recombination in the secondary pair $P700^+A_1^-$ [221]. Extending the measurements to the blue and near UV regions, and improving the time resolution, led to the conclusion that the pair $P700^+A_1^-$ recombined with $t_{1/2} \approx 250$ ns to form the triplet state of P700 [224], consistent with data obtained by transient EPR at room temperature [240]. Obviously, this fast recombination is not operative under normal conditions because its competition with the 200 ns forward electron transfer from A_1^- to F_X would make long-lived charge separation in PS I rather inefficient. To account also for the high triplet yield, it was suggested that reduction of F_X (together with reduction of F_A and F_B) raises the free energy of the pair $P700^+A_1^-$ from its normal level (well below $^3P700$) to at least 30 meV above the free energy of $^3P700$, thus opening the fast triplet recombination channel [221,224]. From very recent results (Polm, M. and

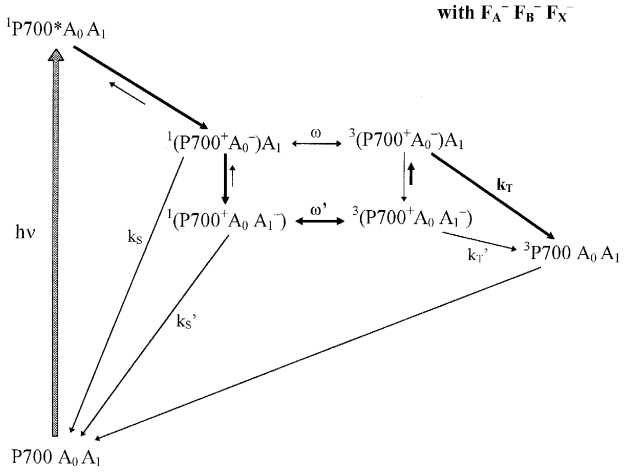

Fig. 10. Reaction scheme for charge recombination in the secondary pair ($P700^+A_0A_1^-$) when F_A, F_B and F_X are prereduced (by illumination in the presence of dithionite at pH 10). Bold arrows indicate the reaction route which is suggested to dominate at room temperature. Note that the free energy of $P700^+A_0A_1^-$ should be well below that of $^3P700$ under normal conditions, but is presumably above $^3P700$ due to the prereduction treatment.

Brettel, K., manuscript in preparation), an indirect recombination pathway via thermal repopulation of the primary pair (see Fig. 10) was suggested. This suggestion was based on the temperature dependency of the recombination kinetics which yielded an activation energy of approx. 150 meV (between 300 and 250 K; at lower temperatures, an only weakly activated direct recombination to the P700 ground state seemed to prevail, consistent with the 20 μs recombination observed previously at 10 K [230]); this activation energy may well correspond to the energy difference between the primary pair $P700^+A_0^-$ and the secondary pair $P700^+A_1^-$ which is raised to above the energy level of $^3P700$ due to prereduction of F_A, F_B and F_X (Polm, M. and Brettel, K., manuscript in preparation; see also Section 6.1.4). The suggested recombination pathway (Fig. 10) would also readily explain the high yield of $^3P700$, as k_T is expected to be faster than k_S (see Section 4.2.1) and as singlet-triplet spin evolution in the only very weakly coupled pair $P700^+A_1^-$ is expected to be rather efficient. Assuming that the activation energy of 150 meV corresponds approximately to the standard free energy difference between $P700^+A_0^-$ and $P700^+A_1^-$ (this assumption implies that the entropy difference is negligible), k_T should be in the order of $10^9\ s^{-1}$ to account for a decay of $P700^+A_1^-$ with $t_{1/2} \approx 250$ ns at room temperature. Some slowing of the $P700^+A_1^-$ recombination due to a weak external magnetic field may reflect a decreased efficiency of singlet-triplet spin evolution in the pair $P700^+A_1^-$ [29].

It should be mentioned that the treatment used in Refs. [221,224] and by Polm and Brettel (Polm, M. and Brettel, K., manuscript in preparation) to prereduce F_X (continuous illumination in the presence of dithionite at pH 10) could have induced additional modifications (e.g., reduction of other components, structural changes in the PS I complex, etc.) which may be necessary to enable the fast triplet recombination pathway of the secondary pair. This suspicion is supported by the observation, during the illumination treatment, of a 5 μs-transient at 820 nm, occurring apparently prior to the full development of the 250 ns recombination; this 5 μs-transient should not arise from $^3P700$ and might represent $P700^+A_1^-$ recombination in centres with a less modified acceptor site (Polm, M. and Brettel, K., manuscript in preparation). Previously, a 30-μs kinetics was tentatively attributed to $P700^+A_1^-$ recombination under conditions where F_B and F_X were presumably reduced by preflashes and F_A was inactivated [24].

4.2.3. Recombination in the redox equilibrium between $P700^+A_1^-$ and $P700^+F_X^-$

As outlined in Section 4.1.2, flash excitation of PS I with F_A and F_B prereduced or removed leads to a relatively long-lived charge-separated state which can be considered as a rapid redox equilibrium between $P700^+A_1^-$ and $P700^+F_X^-$, where the equilibrium constant $K = k_1/k_{-1}$ varies between differently prepared samples. Direct charge recombination within this equilibrium should be described by the kinetic Scheme 2.

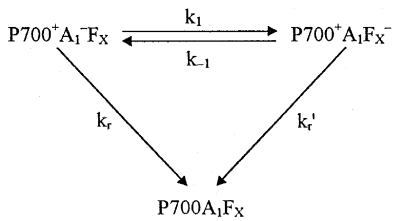

Scheme 2.

As the establishment of the equilibrium ($t_{1/2} \approx$ 20–200 ns) is more than three orders of magnitude faster than the recombination ($t_{1/2} \geq 250$ μs), Scheme 2 predicts a nearly monoexponential recombination with an effective rate

$$k_{eff} = (k_r + Kk'_r)/(K+1) \quad (1)$$

In principle, an activated recombination pathway via repopulation of the primary pair and recombination to the triplet state of P700 (as discussed in Section 4.2.2 for the case of prereduced F_A, F_B and F_X) might also be considered; as, however, the recombination of the pair $P700^+A_1^-$ seems to be essentially independent of temperature when only F_A and F_B are prereduced (see below), I neglect such an activated recombination pathway in the present section.

In earlier studies [85,135,212,252], a charge recombination with $t_{1/2} \approx 250$ μs in the presence of prereduced F_A and F_B was assigned to charge recombination in the pair $P700^+F_X^-$ (in the framework of Scheme 2, this assignment would imply $k_1 \gg k_{-1}$ ($K \gg 1$) and $k_{eff} \approx k'_r \approx 2.8 \times 10^3$ s^{-1}). However, these studies were performed prior to the discovery of the secondary acceptor A_1, and as the spectral data did not extend to the near UV, it is not clear whether and to what extent the pair $P700^+A_1^-$ contributed to the recombination. In a PS I preparation from *Synechococcus* sp. with prereduced F_A and F_B, it was demonstrated that the partner of $P700^+$ in the 250 μs recombination had spectral features characteristic of A_1^- rather than F_X^- [28]. Based on a refined measurement on PS I from *Synechocystis* sp. PCC 6803, a ratio of approx. 3:1 between $P700^+A_1^-$ and $P700^+F_X^-$ was estimated (i.e., $K \approx 0.33$; see Section 4.1.2). In the PS I-β preparation from spinach, however, a ratio of approx. 1:2 between $P700^+A_1^-$ and $P700^+F_X^-$ was observed for the state recombining with $t_{1/2} \approx 250$ μs in the presence of prereduced F_A and F_B [225]. After removal of F_A and F_B, a recombination with $t_{1/2} \approx 1.2$ ms to 750 μs (at room temperature) was assigned to the pair $P700^+F_X^-$ [83,84,152], although the spectral features of the recombination may indicate a contribution of approx. 25% $P700^+A_1^-$ (i.e., $K \approx 3$; see Section 4.1.2). Interestingly, the recombination in the absence of F_A and F_B and the recombination in the presence of prereduced F_A and F_B depended very differently on temperature. In the absence of F_A and F_B, the recombination slowed down upon cooling, following the Arrhenius law between 298 and 225 K with an activation energy of approx. 140 meV; between 225 and 77 K, the 85 ms half-time remained temperature-invariant [83]. With prereduced F_A and F_B, however, the recombination kinetics were virtually independent of temperature [231] or accelerated even slightly upon cooling to $t_{1/2} \approx 150$ μs at 10 K [32].

The observation that the recombination is slowest when $P700^+F_X^-$ dominates in the equilibrium (F_A and F_B removed) indicates that k'_r is slower than k_r (see Scheme 2), as expected with the reasonable assumption that F_X is farther away from P700 than A_1. In a first approximation, the contribution of k'_r to k_{eff} may be neglected for PS I from cyanobacteria with prereduced F_A and F_B ($K \approx 0.33$ at room temperature). The observed $k_{eff} \approx 2.8 \times 10^3$ s^{-1} ($t_{1/2} \approx 250$ μs) would then yield $k_r \approx 3.7 \times 10^3$ s^{-1}. Assuming the same k_r for PS I devoid of F_A and F_B and $K \approx 3$ (see above), the recombination of the equilibrium state via $P700^+A_1^-$ alone (k'_r neglected) would already yield $k_{eff} \approx 9.2 \times 10^2$ s^{-1}, corresponding to $t_{1/2} \approx 750$ μs (the observed half-time was 750 μs to 1.2 ms). According to this rough estimate, the recombination at room temperature may proceed virtually completely via $P700^+A_1^-$ and k_r even in PS I devoid of F_A and F_B where $P700^+F_X^-$ dominates in the equilibrium. The temperature dependency of the recombination kinetics in PS I devoid of F_A and F_B (see above) may be explained in the following simplified way. The 85 ms recombination below 225 K is essentially due to direct charge recombination in the pair $P700^+F_X^-$ ($k'_r \approx 10$ s^{-1}, independent of temperature). The population of $P700^+A_1^-$ in equilibrium with $P700^+F_X^-$ increases with increasing temperature, so that recombination via $P700^+A_1^-$ and k_r becomes competitive with k'_r at about 225 K and dominating at higher temperatures. The activation energy of the recombination should then correspond approximately to the energy difference between $P700^+A_1^-$ and $P700^+F_X^-$, i.e., $\Delta H^\circ \approx -140$ meV. The large deviation from $\Delta G^\circ \approx -28$ meV (equivalent to $K \approx 3$ at 298 K) may reflect an important entropic contribution and/or the fact that the activation energy was measured in a PS I preparation different from the preparation where the equilibrium constant was estimated.

I would like to mention that the very simplified view presented so far fails to explain the similar recombination kinetics ($t_{1/2} \approx 250$ μs) in PS I from cyanobacteria and in the PS I-β preparation from spinach (both with prereduced F_A and F_B): the rather different equilibrium constants between $P700^+A_1^-$ and $P700^+F_X^-$ (approx. 0.33 and 2 for the cyanobacterial and the spinach preparation, respectively) should lead to significantly different effective recombination rates, provided that k_r is the same for both samples and that k'_r is negligible (see Eq. (1)). Possibly, the not yet well understood influence of the preparation procedure, origin of the sample, etc., on the energetics and the equilibrium between the pairs $P700^+A_1^-$ and $P700^+F_X^-$ also affects the kinetics of charge recombination in these pairs.

4.2.4. Recombination in the pairs $P700^+F_A^-$ and $P700^+F_B^-$

A charge recombination with $t_{1/2} \approx 45$ ms (at room temperature) between $P700^+$ and the terminal membrane-bound electron acceptor (called P430 at that time; see Section 1) was discovered 25 years ago by Hiyama and Ke [103]. It is not yet established whether F_A^- or F_B^- is the partner of $P700^+$ in this recombination (see also Sections 3.2.5 and 6), or – assuming a fast redox equilibrium between the states $P700^+F_A^-$ and $P700^+F_B^-$ – which of these states dominates in the equilibrium. The observation that the recombination kinetics was not significantly modified by inactivation of F_B using $HgCl_2$ could indicate that F_A^- was the dominating recombination partner of $P700^+$ also in the untreated sample [71]. As further unresolved or controversial features of this charge recombination, I would like to mention:

(A) According to some reports, the recombination was not monoexponential and could be better decribed as a second order reaction with equivalent concentrations of the two reactants [103] or by two exponentials ($t_{1/2} \approx 15$ ms (30%) and 70 ms (70%) [265], or $t_{1/2} \approx 19$ ms (73%) and $t_{1/2} > 200$ ms (27%) [211]). It is of note that charge recombination between $P700^+$ and the electron in a fast redox equilibrium between $F_A^-F_B$ and $F_AF_B^-$ is expected to be virtually monoexponential in a homogeneous sample. One might suppose that the non-monoexponential kinetics were related to the following effect B.

(B) It was reported that only a fraction (in the order of 30–50%) of $P700^+$ was rereduced by charge recombination with $t_{1/2} \approx 50$ ms, while the remaining $P700^+$ was longer-lived [181,205,247]. According to Sonoike et al., the long-lived component was significantly diminished under anaerobic conditions and totally eliminated by the addition of dithionite, suggesting that a substantial fraction of $(F_AF_B)^-$ was reoxidised by oxygen [247]. Rousseau et al., however, excluded oxygen as electron acceptor because their experiments were done after severe degassing [205]. Hence, one should also consider other possibilities, as for example a not yet identified electron acceptor different from oxygen which became reduced by dithionite (see also Ref. [181]).

(C) The charge recombination between $P700^+$ and $(F_AF_B)^-$ slows down upon cooling so that the states $P700^+F_A^-$ and $P700^+F_B^-$ are virtually irreversible below approx. 100 K (see Section 5). Reported values for the activation energy E_A of the recombination at higher temperatures deviate substantially: $E_A \approx 240$ meV was determined from the decay of the EPR signal of $P700^+$ between 250 and 180 K [270]; $E_A \approx 200$ meV was determined from the decay kinetics between 320 and 285 K of a long-lived luminescence component assumed to reflect the pair $P700^+(F_AF_B)^-$ in equilibrium with the singlet excited state of P700 [237]; $E_A \approx 460$ meV was determined from electroluminescence measurements and from absorbance difference kinetics between 302 and 284 K, considering only the slower component of the apparently biphasic recombination [265]. Clarification of the activation energy should help to establish the pathway of charge recombination: a value in the order of 200 meV may be compatible with a recombination via thermal repopulation of the secondary pair $P700^+A_1^-$, while a value of approx. 460 meV would indicate repopulation of the primary pair $P700^+A_0^-$, as suggested in Ref. [265]. Obviously, the activation energy can only be determined reliably when the ambiguities with respect to the recombination kinetics (see points A and B) are relieved.

As it is possible to photoreduce F_A and F_B in the same PS I complex, a charge recombination in the state $P700^+F_A^-F_B^-$ may occur and show kinetics different from the state $P700^+$ $(F_AF_B)^-$. To my knowledge, the former recombination has not yet been characterised explicitly in the literature.

5. Electron transfer at cryogenic temperatures

Low temperature photochemistry in PS I was studied extensively in the seventies and early eighties, mainly by EPR spectroscopy at around 15 K which allows one to distinguish between the three iron-sulphur clusters. I will quote only the main results and refer the reader to earlier review articles [57,155,168,209,229] for more details and references.

Malkin and Bearden [159] discovered that illumination of PS I at 77 K led to virtually irreversible charge separation between P700 and an iron-sulphur cluster (now known as F_A). Later work established formation of $P700^+F_B^-$ in some fraction of the PS I complexes, in addition to $P700^+F_A^-$ in another fraction (note that low temperature illumination cannot reduce both F_A and F_B in the same PS I complex, because P700 can deliver only one electron). The ratio between $P700^+F_B^-$ and $P700^+F_A^-$ varied considerably according to certain experimental conditions and to the origin of the sample: while F_A^- clearly dominated in PS I from spinach, pea and lettuce [187] after illumination at around 20 K, an increased amount of F_B^- was detected under similar conditions in PS I from the cyanobacterium *Phormidium laminosum* [37] (but not, e.g., in *Anacystis nidulans* [187]) and in PS I from barley [187]. An increased $P700^+F_B^-$ to $P700^+F_A^-$ ratio could also be achieved in PS I from spinach by addition of glycerol (50% v/v) [39,59] or by H_2O to D_2O exchange [163] and in PS I lacking PsaD [44,79,148]. A relative increase in photoreduction of F_B was also observed after continuous illumination at 215 K and subsequent cooling to 25 K for EPR detection; this effect may in part reflect a faster recombination of the pair $P700^+F_A^-$ compared to $P700^+F_B^-$ at 215 K [39]; see also Ref. [102]. From the fact that it was possible to obtain stable samples with either F_A reduced (illumination at 25 K) or F_B reduced (illumination at 200 K in the presence of glycerol and cooling to 25 K), it was concluded that there was no electron transfer between these centres at 25 K [39] (see Section 8.1 for an alternative interpretation of this observation). It should be mentioned that an accurate determination of the ratio of F_A^- and F_B^- is not trivial because the EPR signal of F_B^- saturates at lower microwave power than the signal of F_A^- [206].

The electron transfer pathway from F_X to F_A and F_B at low temperature is a highly controversial issue (see also Section 3.2.5). The linear sequence $F_X \rightarrow F_B \rightarrow F_A$ as suggested by the midpoint potentials (see Fig. 2) was challenged by observations that F_A could be photoreduced at around 20 K in PS I complexes where F_B had been prereduced chemically [37,187], in agreement with photoreduction of F_A at 20 K after inactivation of F_B by treatment with $HgCl_2$ [211] and a similar trend during treatment with urea/ferricyanide [86]. Inactivation of F_B by treatment with diazonium benzene sulfonate, however, inhibited low temperature photoreduction of F_A, supporting the sequence $F_X \rightarrow F_B \rightarrow F_A$ [156]. The latter result should be regarded with caution because irreversible photooxidation of P700 still occurred at normal yield, indicating that an 'irreversible' electron acceptor was functioning, although it was not detected under the EPR conditions normally used to monitor F_A^- and F_B^-. A possible sequence $F_X \rightarrow F_A \rightarrow F_B$ may be supported by the almost negligible 18 K photoreduction of F_B in PS I complexes where F_A had been prereduced chemically [9]. In another report, however, significant photoreduction of F_B was observed in the presence of prereduced F_A [100]. Analysis of PS I mutated at either the F_A or the F_B site did not yet yield conclusive results with respect to the electron transfer pathway (see Sections 3.2.5 and 4.1.3). The difficulties in explaining the experimental results within either of these two linear electron transfer pathways led to the proposal of parallel electron transfer from F_X^- to F_A and F_B (e.g., [173,187]; see also the review articles cited at the beginning of this section). This point will be further discussed in Sections 7.2.7 and 8.1.

Time-resolved EPR and optical studies provided the surprising result that even after prolonged illumination at low temperature (supposed to induce the virtually irreversible charge separation between P700 and (F_AF_B)), there still occurred a reversible photooxidation of P700 in an important fraction of the PS I complexes [151,172,270]. This indicates a heterogeneity of PS I with respect to electron transfer at low temperature, possibly because PS I is frozen in different conformations only some of which are favourable for electron transfer to (F_AF_B) [37,232]. It is now established that the reversible reaction consists of a $P700^+F_X^-$ charge recombination with $t_{1/2} = 50–400$ ms in a minor fraction of the PS I com-

plexes [173,232] and a dominating $P700^+A_1^-$ recombination with $t_{1/2} \approx 150$ μs [166,216,232]; a similar $P700^+A_1^-$ recombination ($t_{1/2} \approx 220$ μs at 77 K) was also observed and characterised spectroscopically in PS I devoid of F_A and F_B [152].

Data about the fraction of PS I complexes which can be trapped irreversibly in the states $P700^+F_A^-$ and $P700^+F_B^-$ and the complementary fraction still performing reversible formation of $P700^+A_1^-$ and $P700^+F_X^-$ vary in the literature, with values ranging from 12% [37] to 100% [46] for the 'irreversible' fraction, and from 55–75% [216] to 20–30% [166] for the 'reversible' fraction. This variation may reflect different degrees of low temperature heterogeneity between different samples (different species and preparation procedures, presence or absence of cryoprotectants, etc.), and possibly also difficulties with the quantification of the EPR signals.

It is of note that a saturating single turnover laser flash given to dark-adapted PS I at around 20 K induced only 20–40% of the irreversible charge separation obtained by continuous illumination [46,232]. Based on a study of the yields of the different reactions induced by each flash in a series of laser flashes, Sétif et al. [232] suggested that, in the frozen state, there exists a very large distribution of rates of photoreduction of F_A (in competition with charge recombination between the preceding acceptor and $P700^+$), including a rate of zero in one-third of the PS I complexes (which underwent reversible charge separation even after prolonged illumination in this study).

In order to come to a better understanding of the apparent heterogeneity and inefficiency of low temperature photochemistry, Schlodder et al. [216] studied the kinetics of A_1^- and $P700^+$ in PS I from *Synechococcus elongatus* by flash absorption spectroscopy throughout the full range from 300 to 77 K (in the presence of 65% (v/v) glycerol as a glass-forming cryoprotectant). Between 300 and 200 K, the reoxidation of A_1^- could be described with a single exponential phase which slowed down from $t_{1/2} \approx$ 200 ns (300 K) to $t_{1/2} \approx 10$ μs (200 K), following Arrhenius behavior with an activation energy of approx. 220 meV. Between 200 and 150 K, a second kinetic phase with $t_{1/2} \approx 210$ μs appeared and grew at the expense of the faster phase. Below 150 K, the faster phase was hardly detectable, and the slower phase accelerated slightly to $t_{1/2} \approx 170$ μs at 77 K. From comparisons with the kinetics of $P700^+$ in the same temperature ranges, it was concluded that the reoxidation of A_1^- was due to electron transfer to the iron-sulphur centres above 200 K, but mainly due to charge recombination with $P700^+$ below 150 K (as the measurements of A_1^- reoxidation were performed under repetitive excitation, the PS I complexes capable of irreversible charge separation (25–45% in this sample) were trapped at low temperatures and could not contribute to the measured signals). The transition from dominating forward electron transfer to dominating recombination in the pair $P700^+A_1^-$ occurred around 170 K. It is of note that this transition could not simply be explained by competition between forward electron transfer from A_1^- to the iron sulphur centres (which slowed down upon cooling) and charge recombination between A_1^- and $P700^+$ (nearly temperature independent), because such a competition would yield a monophasic reoxidation of A_1^- rather than the observed biphasic kinetics. Schlodder et al. [216] attributed the slower phase ($t_{1/2} \approx 210$ μs) at around 170 K to $P700^+A_1^-$ recombination in a fraction of the PS I complexes in which electron transfer to F_X was blocked (this fraction would increase from 200 to 150 K), and the faster phase to competing electron transfer from A_1^- to F_X and from A_1^- to $P700^+$ in another fraction. Interestingly, the temperature of the transition from forward electron transfer beyond A_1 to charge recombination in the pair $P700^+A_1^-$ was close to the expected liquid to glass transition of the medium (165 K for 65% (v/v) glycerol in water [199]). Furthermore, the temperature of the transition between the two behaviors of PS I varied with the composition of the cryoprotecting medium in a similar way as the temperature of the liquid to glass transition. It was suggested that the inhibition of forward electron transfer to F_X was caused by the extreme increase of the viscosity to more than 10^{13} Poise due to the glass transition [216] (see also Section 8.2). It is of note that also in reaction centres from heliobacteria a transition from long-lived (12–15 ms) to a shorter-lived (2–4 ms) charge separation was observed upon cooling from 230 to 170 K in the presence of 67% glycerol [42].

With respect to electron transfer from excited P700 via A_0 to A_1, I am not aware of any time-resolved study at low temperature. However, the flash yield of

$P700^+A_1^-$ formation in PS I devoid of F_A, F_B and F_X was reported to decrease upon cooling, which may reflect blocked or drastically slowed electron transfer from A_0^- to A_1 in a fraction of the centres in this preparation (see Section 4.2.2). No such effect has been reported for intact PS I.

Finally, I would like to mention a kinetic problem of low temperature electron transfer in PS I. Crowder and Bearden [46] reported that irreversible reduction of F_A due to a single laser flash occurred within less than 1 ms at 25 K; under similar conditions, part of $P700^+$ decayed with $t_{1/2} \approx 200$ ms, indicative of charge recombination in the pair $P700^+F_X^-$ (see above). Obviously, if F_A received the electron from F_X^- within 1 ms, this electron transfer should outcompete the 200 ms recombination in the pair $P700^+F_X^-$. Because of this dilemma, it was suggested that F_X is not involved in forward photochemistry of PS I [46] and that F_A is directly reduced by A_1^- (in competition with the 120 μs recombination in the pair $P700^+A_1^-$) [232]. Such a bypass is, however, difficult to reconcile with other data (see Section 4.1.2). As a hypothetical explanation, I would like to suggest that the 200 ms recombination of $P700^+F_X^-$ occurs only in a fraction of the PS I complexes where electron transfer from F_X^- to F_A is extremely slow or impossible (see also Section 8.1), while in another fraction this recombination is in fact outcompeted by the faster electron transfer from F_X^- to F_A. One may also suggest that F_X^- formed by electron transfer from A_1^- relaxes on a time-scale shorter or approximately equal to 1 ms (at low temperature) to an energetically lower state which is no longer capable of reducing F_A at low temperature (see also Section 8.2); electron transfer from F_X^- to F_A would then compete with this relaxation rather than with the 200 ms recombination between relaxed F_X^- and $P700^+$.

6. Energetics of the charge separated states

6.1. Review of published data

A widely accepted energetic scheme of PS I has been presented in Fig. 2, using measured and estimated midpoint potentials of the redox cofactors. The standard free energy change ΔG° (per molecule) for the formation of a pair P^+A^- can be calculated approximately from the redox potentials by

$$\Delta G^\circ(PA \rightarrow P^+A^-) = q_e\left[E_m(P^+/P) - E_m(A/A^-)\right] \quad (2)$$

where q_e is the elementary charge. This relation neglects possible interactions between P^+ and A^- (see, e.g., Ref. [13]). Most obviously, the electrostatic interaction between P^+ and A^- tends to stabilise the state P^+A^-, i.e., its free energy may be smaller than expected according to Eq. (2) from the midpoint potentials. Calculation of the electrostatic interaction energy requires detailed (microscopic) knowledge of the surrounding protein which is not yet available for PS I. To get an impression of the possible magnitude of the effect, one may consider two elementary charges within a hypothetical homogeneous protein sphere (radius, 20 Å; dielectric constant $\epsilon = 2$) surrounded by water ($\epsilon = 78$) [75]. E.g., with one charge at 8 Å from the surface and the second charge in the centre of the sphere (i.e., 12 Å apart from the first charge), the electrostatic interaction energy would be approx. 250 meV; with the second charge at 8 Å from the surface at a position opposite to the first charge, one would obtain approx. 40 meV, and with the second charge at 2 Å from the surface only approx. 10 meV (these values were estimated using Fig. 7 in Ref. [75]; they constitute upper limits because dipolar reorientation of the protein was not incorporated in the calculation, i.e., $\epsilon = 2$ represents the electronic polarisability only).

6.1.1. $P700^+F_A^-$ and $P700^+F_B^-$

The midpoint potentials of F_A and F_B were determined by redox titration at room temperature and subsequent detection by low temperature EPR. For PS I from spinach, reduction potentials of about -540 and -590 mV were reported for F_A and F_B, respectively [61,100,131] (note that the lower potential corresponded to reduction of F_B when F_A was already reduced, i.e., to the couple $F_A^-F_B/F_A^-F_B^-$; see below). These values shifted to -510 mV (F_A) and -545 mV (F_B) in the presence of 50% (v/v) glycerol [59]. In PS I from barley and from *Phormidium laminosum*, however, F_B was more easy to reduce than F_A [37,187]. At first glance, this seems to indi-

cate a variation of the thermodynamically favourable electron transfer pathway between species ($F_X \rightarrow F_B \rightarrow F_A$ in spinach and $F_X \rightarrow F_A \rightarrow F_B$ in barley and *Phormidium laminosum*). However, it appears to me that the ratio of the singly reduced states $F_A^- F_B$ and $F_A F_B^-$ detected by EPR at low temperature is not necessarily the same as the ratio at room temperature where the potential was established. Provided that the midpoint potentials of the two clusters depend differently on temperature, it is, e.g., conceivable that at a certain ambient potential F_B is predominantly reduced at room temperature (i.e., F_B would have a higher potential than F_A), but the electron passes to F_A during cooling because the midpoint potential of F_B decreases more strongly than that of F_A (the opposite case is of course also conceivable). Possibly, the variation between species of the low temperature EPR results reflects a difference in some freezing effect (see also Section 8.1) rather than different electron transfer pathways at room temperature.

Another open question is whether reduction of one of the two iron-sulphur clusters on PsaC affects the potential of the other cluster. A decrease of this potential (negative cooperativity) could easily be explained by the electrostatic interaction between the negative charges, but the assumption of a positive cooperativity yielded a better fit to the redox titration curves in Ref. [61]. It should be mentioned that the shapes of the titration curves (plots of the amplitudes of certain peaks in the EPR spectra versus potential) in Refs. [61,131] appear different. This may in part reflect problems with the analysis of the EPR spectra because the principal g-values of the three contributing paramagnetic states ($F_A^- F_B$, $F_A F_B^-$ and $F_A^- F_B^-$) are partially overlapping. I feel that more reliable titration curves might be obtained by analysing the complete EPR spectra as superpositions of the spectra of the states $F_A^- F_B$, $F_A F_B^-$ and $F_A^- F_B^-$ and plotting their relative contributions versus potential. This may also help to establish a possible cooperativity between reduction of F_A and F_B.

In summary, transfer of one electron to the iron-sulphur clusters in PsaC occurs at a midpoint potential of about -540 mV (-510 mV in the presence of glycerol) at room temperature, but it is not sure whether F_A or F_B is reduced in this step (or whether this varies between species). A second electron is transferred at around -590 mV (-545 mV in the presence of glycerol) to form the state $F_A^- F_B^-$, but it is not sure whether this value would apply as well, if the cluster with the higher potential were still oxidised (as is normally the case during charge separation in PS I).

Redox titrations with EPR detection were also performed on isolated PsaC [91,174,190] and on several PsaC mutants [174,278–280]; the midpoint potentials varied in the range from -470 to -630 mV (as long as [4Fe-4S] cluster(s) were assembled), and in most cases the EPR spectra were modified compared to intact PS I. These effects are not yet well understood. After destruction of F_B by treatment with $HgCl_2$, F_A titrated at -530 mV, although there was some modification of the EPR spectrum of F_A^- [120].

The midpoint potential of the terminal acceptor(s) was also estimated more indirectly by monitoring photoreactions of P700 at low temperature as a function of the potential established previously at room temperature. Irreversible photooxidation of P700 (formation of $P700^+ F_A^-$ or $P700^+ F_B^-$; see Section 5) was lost upon reduction at a midpoint potential of -530 mV [51,150]. Reversible photooxidation of P700 (due to charge recombination in the pairs $P700^+ A_1^-$ and $P700^+ F_X^-$; see Section 5), however, grew with a midpoint potential of -585 mV [100]. Later it was suggested that both midpoint potentials reflected reduction of F_B when F_A was already reduced, and that the higher value reflected an effect of glycerol (see above) on the midpoint potentials [59]. However, the use of glycerol is not mentioned in Ref. [150], thus the interpretation of these titration experiments remains somewhat ambiguous.

Attempts were also made to determine the midpoint potential of the terminal iron-sulphur cluster by monitoring the photoreaction of P700 at room temperature during redox titrations. Long-lived (ms range) flash-induced $P700^+$ (attributed to $P700^+(F_A F_B)^-$; see Section 4.2.4) titrated with a midpoint potential of -470 mV [129] or -500 mV [77], i.e., at significantly higher potentials than those attributed to F_A and F_B in the titrations with detection at low temperature. Although the midpoint potentials of F_A and F_B may well decrease upon cooling, this is unlikely to be the origin of the discrepancy, because, as already pointed out by Lozier and Butler [150], the rate of cooling was usually much faster than the redox equilibration of the system. I consider it as

more likely that the loss of the long-lived $P700^+$ signal at room temperature was due to a faster rereduction of $P700^+$ by redox mediators which became reduced in the course of the titrations.

According to Eq. (2), a midpoint potential of -540 mV for the reduction of the terminal acceptor (F_A or F_B) together with the midpoint potential of 490 mV for the oxidation of P700 yields a free energy of 1.03 eV for the state $P700^+(F_AF_B)^-$, provided that the interaction between the two partners can be neglected. The latter assumption seems justified because of the large distance between the partners and because of their proximity to the aqueous phase. It is of note that the midpoint potential of P700 appears to vary between different PS I preparations. The value of 490 mV used above was reported for PS I isolated from spinach by relatively mild treatments; harsher treatments led to lower midpoint potentials (down to approx. 430 mV for a PS I complex isolated with SDS) [228]. Hence, in certain PS I preparations the free energy of the pair $P700^+(F_AF_B)^-$ may be lower than the above estimate of 1.03 eV.

A completely different way of estimating the energy of the state $P700^+(F_AF_B)^-$ is based on the luminescence emitted by excited antenna chlorophylls in equilibrium with this charge separated state. From the decrease of the intensity of the stationary luminescence with decreasing temperature, an activation energy of approx. 630 meV was estimated and attributed to the energy difference between the excited state (assumed to be approx. 1.7 eV above the ground state) and the charge separated state [237]. In view of the difficulties of the luminescence method (possible contamination by other luminescing processes; temperature dependence of the lifetime of the charge separated state) and some uncertainty about the energy of the excited state (1.7 eV corresponds to an optical transition at 730 nm), the resulting energy of 1.07 eV for $P700^+(F_AF_B)^-$ should be considered as only a rough estimate. It should also be pointed out that this is an energy (and not a free energy as the 1.03 eV estimated from the redox potentials), so that a possible entropic contribution might also account for a deviation between the two estimates.

6.1.2. $P700^+F_X^-$

The reduction potential of F_X was estimated by titration experiments similar to those described above for F_A and F_B. Monitoring F_X^- directly by low temperature EPR, Chamrovsky and Cammack [40] obtained a midpoint potential of -705 ± 15 mV. It is of note that the lowest potential attained in this study (-750 mV) was not sufficient to reduce F_X completely. The signal amplitude corresponding to complete reduction was estimated by illumination of the samples in the EPR cavity. Because of the heterogeneity of low temperature electron transfer in PS I (see Section 5), I consider it likely that the signal amplitude for complete reduction of F_X was underestimated in Ref. [40], and that the midpoint potential of F_X may be lower than -705 mV. Ke et al. [130] monitored the steady-state EPR signal of $P700^+$ during illumination at 15 K and observed a signal decrease for potentials below about -700 mV. This was attributed to reduction of F_X with an estimated midpoint potential of -730 mV (the titration extended down to -740 mV). Parrett et al. [193] followed the amplitude of flash-induced $P700^+$ decaying with $t_{1/2} \approx 250$ μs at room temperature; from the decrease of the signal with decreasing potential, a midpoint potential of -670 mV was estimated for the reduction of F_X. One may suspect that this value reflected electron donation to $P700^+$ by redox mediators and/or accumulation of F_X^- due to the actinic effect of the 698 nm measuring light and the repetitive flash excitation, or even double reduction of A_1 (cf. Ref. [23]). It should be pointed out that in all these titrations F_A and F_B were already reduced, which may have affected the midpoint potential of F_X, e.g., by electrostatic interaction. To clarify this point, Parrett et al. [193] performed an optical titration similar to the one described above for a PS I core devoid of F_A and F_B and the stromal extrinsic subunits. The midpoint potential attributed to the reduction of F_X was -610 mV. As pointed out in Ref. [193], this shift in potential might, in addition to the loss of electrostatic interaction with F_A^- and F_B^-, reflect a more hydrophilic environment of F_X after removal of the extrinsic subunits.

In summary, in the presence of prereduced F_A and F_B, the midpoint potential of F_X may be around -730 mV, and the free energy of the pair $P700^+F_X^-$ hence around 1.22 eV (assuming 490 mV for the oxidation of P700 and neglecting interactions between $P700^+$ and F_X^-). With F_A and F_B oxidised or extracted, F_X is presumably more easy to reduce and

the free energy of the pair $P700^+F_X^-$ hence somewhat lower (see also Section 4.1.2), but reliable quantitative data are not yet available.

6.1.3. $P700^+A_1^-$

The midpoint potential for reduction of A_1 is often assumed to be well below that of F_X in order to support efficient forward electron transfer (see also Fig. 2). It is likely that the environment of A_1 has a specific effect in lowering the potential compared to phylloquinone in vitro (see Section 3.2.3). To my knowledge, redox titrations of the A_1/A_1^- couple in PS I have not been reported (but see Ref. [23] for putative double reduction to the quinol form).

Vos and Van Gorkom [266] estimated a midpoint potential of -810 mV for the A_1/A_1^- couple, based on a model simulation of the luminescence kinetics induced by an external electric field pulse applied to PS I in the state $P700^+F_A^-$ (the electric field should affect the quasi-equilibrium between singlet excited chlorophylls, the charge separated states (including $P700^+A_1^-$) and the triplet states). It appears to me that this method of estimating the midpoint potential of A_1 is a very indirect one, depending on a number of model assumptions and (fixed) simulation parameters which are not unambiguously established. As another indirect approach, Sétif and Brettel [225] analysed the biphasic reoxidation kinetics of A_1^- in a PS I preparation from spinach, assuming a redox equilibrium between the states $P700^+A_1^-$ and $P700^+F_X^-$ (see Section 4.1.2). The equilibrium constant at room temperature was estimated to be in the range from 0.75 to 3.2, corresponding to a reaction free energy of $+7$ to -30 meV for electron transfer from A_1^- to F_X, i.e., the pair $P700^+A_1^-$ would be very close to or only slightly higher in free energy than the pair $P700^+F_X^-$. Evidently, this result depends on the validity of the kinetic model; furthermore, it was derived for a special PS I preparation, while other preparations show different kinetics (see Section 4.1.2). Iwaki and Itoh [116] also tried to estimate the free energy gap between $P700^+A_1^-$ and $P700^+F_X^-$ by kinetic modelling. They used a PS I preparation which had been depleted of phylloquinone and most antenna chlorophylls and subsequently had been reconstituted with different quinones, including phylloquinone (see also Section 3.2.3). With increasing in vitro midpoint potential of the quinones, long-lived ($t_{1/2} > 1$ ms) flash-induced charge separation was replaced by a 200-μs recombination between $P700^+$ and presumably the reduced quinone. E.g., after reconstitution with phylloquinone, the 200-μs phase represented approx. 15% of total flash-induced $P700^+$. The kinetic model in Ref. [116] assumes a rapid (in the order of 100 ns) redox equilibrium between reduced quinone and F_X, which decays by a much slower (approx. 150 μs) electron transfer from F_X^- to (F_AF_B), in competition with the 200 μs recombination between reduced quinone and $P700^+$. In the framework of this model, the 15% of a 200 μs phase observed with phylloquinone (PhyQ) implies that the pair $P700^+PhyQ^-$ lies 54 to 78 meV higher in free energy than the pair $P700^+F_X^-$ [116]. Unfortunately, the 200 μs phase appears to be a special feature of the PS I preparation used in Ref. [116] which has to my knowledge never been observed in intact PS I under conditions of normal forward electron transfer. Furthermore, an approx. 150 μs electron transfer from F_X^- to (F_AF_B) would be incompatible with the much faster reduction of ferredoxin by intact PS I (see Section 4.1.3). Hence, the estimate in Ref. [116] cannot be applied to intact PS I.

In summary, the literature does not provide reliably accurate data on the free energy of the pair $P700^+A_1^-$ during normal forward electron transfer in PS I.

6.1.4. $P700^+A_0^-$

The free energy of the primary pair $P700^+A_0^-$ was recently estimated by Kleinherenbrink et al. [134] from time-resolved fluorescence measurements after double reduction of A_1, i.e., when electron transfer beyond A_0 was blocked. The amplitude of the slowest component of the fluorescence decay ($\tau = 35$ ns, corresponding to the lifetime of the primary pair) was approx. 0.1% of the initial (prompt) fluorescence, indicating an equilibrium constant of approx. 1000 between excited state and primary pair state. Taking further into account the quasi-equilibrium between excited antenna chlorophylls and excited P700, a free energy gap of 250 meV between excited P700 and $P700^+A_0^-$ was obtained. Using 1.77 eV for the free energy of excited P700 (corresponding to the energy of a 700 nm photon), the free energy of the primary pair $P700^+A_0^-$ would be 1.52 eV. This value is compatible with an estimation using the activation

energy of 460 ± 30 meV observed for the charge recombination in the pair $P700^+F_A^-$ as an approximation for the free energy difference between $P700^+A_0^-$ and $P700^+F_A^-$ [265,266]; see however Section 4.2.4 for controversial results on the activation energy and the pathway of this recombination. Another estimation used the activation energy of about 150 meV observed for the charge recombination in the pair $P700^+A_1^-$ in the presence of prereduced F_A, F_B and F_X as approximation for the free energy difference between $P700^+A_0^-$ and $P700^+A_1^-$ (Polm, M. and Brettel, K., manuscript in preparation; see also Section 4.2.2). According to Ref. [224], the free energy of the pair $P700^+A_1^-$ in interaction with F_A^-, F_B^- and F_X^- lies at least 30 meV above the free energy of the triplet state of P700 (1.29 eV as estimated from the wavelength of phosphorescence [235]), so that the free energy of the pair $P700^+A_0^-$ should be larger than about 1.47 eV which is compatible with the estimations outlined above. I would like to point out that substitution of an activation energy for a free energy difference as done in the latter two approaches neglects the (unknown) entropic contributions; hence the first approach [134] appears to be more correct.

6.2. A hypothetical free energy scheme

The data and problems outlined so far lead me to suggest a hypothetical free energy scheme for PS I under conditions of normal forward electron transfer at room temperature (Fig. 11). It is based on the following considerations:

(1) the free energies of $P700^*$ (1.77 eV above the ground state), $^3P700$ (1.29 eV), $P700^+A_0^-$ (1.52 eV) and of the lowest lying charge separated state $P700^+(F_AF_B)^-$ (1.03 eV) were chosen as outlined in Sections 6.1.1 and 6.1.4.

(2) The $P700^+A_1^-$ state was placed at about 1.20 eV in order to be compatible with the following two restrictions: (a) A possible recombination of $P700^+(F_AF_B)^-$ via repopulation of the state $P700^+A_1^-$ should not be faster than the observed half-time of approx. 50 ms at room temperature. Assuming $t_{1/2} \approx 150$ μs for the direct charge recombination in the pair $P700^+A_1^-$ (k_r; see Section 4.2.3), the population of $P700^+A_1^-$ in equilibrium with the lowest lying charge separated state should not exceed

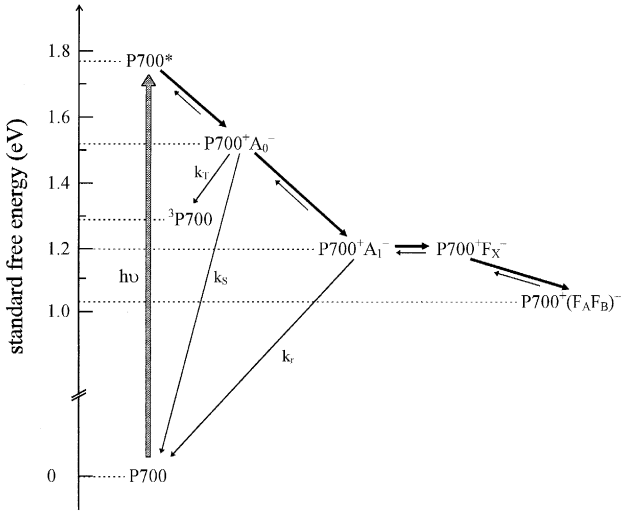

Fig. 11. Suggested free energy scheme of electron transfer in PS I at room temperature. The pathway of normal forward electron transfer is indicated by bold arrows. Thin arrows indicate real or hypothetical recombination pathways which were considered for the estimation of certain free energy levels (see text). Singlet triplet spin evolution in the radical pairs (see Sections 4.2.1 and 4.2.2) was omitted for clarity.

3×10^{-3}, corresponding to a free energy difference of at least 150 meV at 298 K, i.e., the free energy of $P700^+A_1^-$ should be higher than 1.18 eV. (b) A hypothetical activated charge recombination of the pair $P700^+A_1^-$ via repopulation of the primary pair $P700^+A_0^-$ and/or $^3P700$ should not be faster than approx. 150 μs, because otherwise the activated recombination would outcompete the assumed direct recombination (see Section 4.2.3). Supposing that triplet charge recombination (k_T) in the primary pair (forming $^3P700$ with $t_{1/2} \approx 1$ ns; note that $k_T \gg k_S$; see Section 4.2.2) would be the bottleneck of the activated recombination, the free energy difference between $P700^+A_0^-$ and $P700^+A_1^-$ should not be smaller than about 300 meV. Supposing that the approx. 5-μs decay of $^3P700$ (formed either via $^3(P700^+A_0^-)$ or directly from $^3(P700^+A_1^-)$) would be the bottleneck, the free energy difference between $^3P700$ and $P700^+A_1^-$ should not be smaller than about 90 meV.

(3) The free energy of the state $P700^+F_X^-$ was assumed to be close to that of $P700^+A_1^-$ because then relatively minor variations of the free energy levels could explain why in some cases $P700^+A_1^-$ and in other cases $P700^+F_X^-$ appears to dominate in

the redox equilibrium between these two states (see Sections 4.1.2 and 4.2.3). It is of note that the free energy of the state $P700^+F_X^-$ in the presence of prereduced F_A and F_B was estimated to 1.22 eV (based on redox titrations; see Section 6.1.2), i.e., slightly higher than the state $P700^+A_1^-$ in Fig. 11. This is in line with data indicating that $P700^+A_1^-$ dominated in the redox equilibrium with $P700^+F_X^-$ when F_A and F_B were prereduced (see Section 4.2.3).

It is not obvious whether the lowest lying charge separated state at room temperature (denoted as $P700^+(F_AF_B)^-$ in Fig. 11) represents $P700^+F_A^-$, $P700^+F_B^-$ or a redox equilibrium with similar contributions from these two pairs. The different major possibilities for the energetic order (a: $G°(P700^+F_A^-) < G°(P700^+F_B^-)$; b: $G°(P700^+F_A^-) \approx G°(P700^+F_B^-)$; c: $G°(P700^+F_A^-) > G°(P700^+F_B^-)$) are presented in Fig. 12 for the two possible spatial arrangements of F_A and F_B (row I: distal cluster $F_{AB2} \equiv F_A$; row II: $F_{AB2} \equiv F_B$).

Provided that the distal cluster is F_A, case Ia would explain most readily the redox titration results in PS I from spinach ($E_m(F_A/F_A^-) > E_m(F_B/F_B^-)$; see Section 6.1.1). The apparently opposite order of the midpoint potentials in barley and *Phormidium laminosum* could reflect a temperature effect on the potentials (see Section 6.1.1). With case Ib, the apparently different reduction potentials of F_A and F_B could be explained by an electrostatic interaction between F_A^- and F_B^- which would shift the potential for the second reduction step ($(F_AF_B)^- \rightarrow F_A^-F_B^-$) to below that of the first step ($F_AF_B \rightarrow (F_AF_B)^-$) (see also Section 6.1.1). With case Ic, freezing would need to invert the energetic order in PS I from spinach. Provided that the distal cluster is F_B, cases IIa, IIb and IIc could explain the redox titration results in the same way as cases Ia, Ib and Ic, respectively.

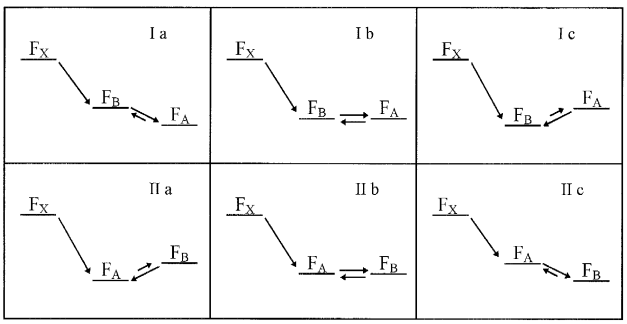

Fig. 12. Sketch of the different major possibilities for the energetics and spatial arrangement of the terminal iron-sulphur clusters in PS I. F_X, F_B and F_A symbolise the free energy levels of the pairs $P700^+F_X^-$, $P700^+F_B^-$ and $P700^+F_X^-$, respectively, at room temperature. The distal cluster F_{AB2} is assumed to be F_A (upper row) or F_B (lower row).

Summarising these considerations, none of the six cases presented in Fig. 12 can be safely excluded at present. Nevertheless, I would like to mention that the arguments favouring an assignment of the distal cluster as F_B (mainly based on effects of the destruction of F_B; see Section 3.2.5) appear to me at present more consistent than the arguments favouring the opposite assignment (see Section 3.2.5). In addition, it seems plausible to me to suppose that the two [4Fe − 4S] clusters in PsaC would have very similar reduction potentials if they were not shielded differently from the aqueous phase (e.g., in the ferredoxin from *Chlostridium pasteuranium*, the reduction potentials of the two [4Fe − 4S] clusters could not be distinguished [196]). Proximity of the aqueous phase with its high dielectric constant is expected to stabilise the reduced form of a [4Fe − 4S] cluster (three negative charges, including the sulphur atoms of the ligating cysteines) more than the oxidised form (two negative charges), and hence to increase the reduction potential (see, e.g., Refs. [128,145]). This effect should be more pronounced for the cluster which is most exposed to the stroma in intact PS I, i.e., F_{AB2} should be more easy to reduce than F_{AB1} (cases Ia and IIc). Upon freezing, the dielectric constant of water decreases dramatically, so that the different stabilisation of the two clusters could be lost. Hence, the reduction potential of F_{AB2} could approach that of F_{AB1} with decreasing temperature. The energetic order of the states $P700^+F_A^-$ and $P700^+F_B^-$ at very low temperatures may depend on the conformational substates in which the PS I complexes are frozen (see Section 8.1). Some variation in the distribution of the frozen conformational substates between different samples may then explain why F_A is found to be preferentially reduced at low temperature in some preparations and F_B in other preparations. In cases Ib and IIb, the variability between different PS I preparations could be explained similarly without invoking an important temperature effect on the reduction potentials. Because of the considerations outlined in this paragraph, cases IIb and IIc appear to me somewhat

more plausible than the other cases presented in Fig. 12.

Finally, I would like to mention an apparent contradiction between the free energy of the state $P700^+F_X^-$ suggested in Fig. 11 (close to that of $P700^+A_1^-$ or even slightly higher when F_A and F_B are prereduced) and the possibility to prepare a state of PS I where F_A, F_B and F_X are predominantly reduced while A_1 is still predominantly oxidised (see Section 4.2.2). A possible explanation could be that the electrostatic interaction with $P700^+$ is considerably stronger for A_1^- than for F_X^-, so that the two pairs could have similar free energies although the reduction potential of A_1 would be lower than that of F_X as long as P700 is reduced. Another explanation could be that the treatment applied to reduce F_A, F_B and F_X induced additional modifications of the PS I complex which might favour reduction of F_X relative to reduction of A_1 (see also Section 4.2.2).

7. Electron transfer rates and distances between the redox cofactors in photosystem I

7.1. General considerations

The purpose of Section 7 is to relate structural data, energetics and kinetics of electron transfer in PS I. According to electron transfer theory (see Refs. [53,164,194] for reviews), the rate k_{et} of electron transfer ($D^-A \rightarrow DA^-$) in weakly coupled pairs can be expressed in a non-adiabatic description based on Fermi's Golden Rule as

$$k_{et} = \frac{2\pi}{\hbar}|T_{DA}|^2(F.C.) \quad (3)$$

$|T_{DA}|^2$ is a measure of the electronic coupling between donor and acceptor and (F.C.) is the Franck-Condon factor (see below). The decrease of the electronic coupling with increasing distance, R, is often approximated as

$$|T_{DA}|^2 \propto e^{-\beta R} \quad (4)$$

where β depends on the medium between donor and acceptor. E.g., β is higher (i.e., $|T_{DA}|^2$ decreases more strongly) through vacuum ($\beta \approx 2.8$ Å^{-1}) than in a structure where donor and acceptor are covalently bridged ($\beta \approx 0.7$ Å^{-1}) [178]. To estimate $|T_{DA}|^2$ in proteins, Beratan et al. [10] introduced an approach which searches coupling pathways between donor and acceptor by combining segments along covalent bonds and hydrogen bonds with through space jumps in a way which maximises the coupling. Evidently, this approach requires detailed knowledge of the protein structure. In a simplified approach, Moser et al. [178] considered the protein as a glassy medium with a unique value of β. They showed that the rates of a number of electron transfer reactions in purple bacterial reaction centres over distances between 5 and 22 Å are compatible with $\beta = 1.4$ Å^{-1}, i.e., $|T_{DA}|^2$ would decrease by one order of magnitude every 1.7 Å.

The Franck-Condon factor (F.C.) in Eq. (3) reflects the overlap between the nuclear wave-functions of reactant (D^-A) and product (DA^-). From a classical treatment of nuclear motion, Marcus derived the expression

$$(F.C.) = \frac{1}{\sqrt{4\pi\lambda k_B T}} \exp\left[-\frac{(\Delta G^\circ + \lambda)^2}{4\lambda k_B T}\right] \quad (5)$$

where ΔG° is the standard reaction free energy ($\Delta G^\circ < 0$ for exergonic reactions) and λ the reorganisation energy (see Ref. [164] for details and original references). As illustrated in Fig. 13a, reactant and product are modelled as similar harmonic oscillator potentials. According to the classical treatment, electron

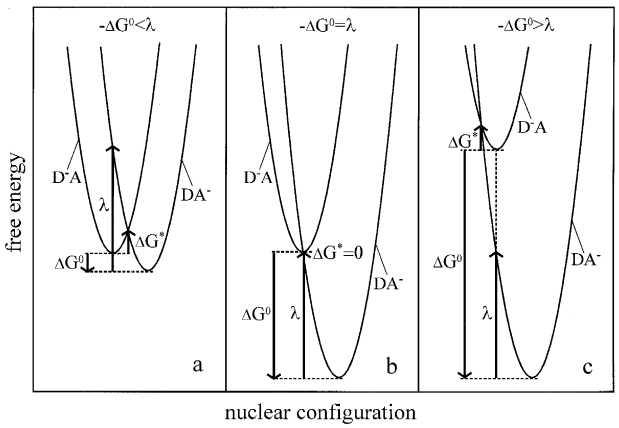

Fig. 13. Schematic presentation of the free-energy surfaces for reactant and product in a non-adiabatic electron transfer reaction $D^-A \rightarrow DA^-$. a: $-\Delta G^\circ < \lambda$ ('normal region'); b: $-\Delta G^\circ = \lambda$ ('optimal' case); c: $-\Delta G^\circ > \lambda$ ('Marcus inverted region'). See text for further details.

transfer can occur only at the intersection of the two potentials, which may be reached due to thermal fluctuations of the nuclear co-ordinates. The horizontal displacement of the potential minima reflects the adjustment of the equilibrium nuclear co-ordinates to the different electronic configurations of reactant (D^-A) and product (DA^-). The reorganisation energy λ is the energy which would be needed for the same displacement of the nuclei without, however, transferring the electron. Both 'inner' reorganisation of the nuclei of donor and acceptor (λ_i) and 'outer' reorganisation of the nuclei of the surrounding medium (λ_o) contribute to λ ($\lambda = \lambda_i + \lambda_o$), but λ_o is often dominating. For spherical reactants in a homogeneous medium, λ_o can be calculated as

$$\lambda_o = q_e^2 \left(\frac{1}{2a_D} + \frac{1}{2a_A} - \frac{1}{r} \right) \left(\frac{1}{\epsilon_{op}} - \frac{1}{\epsilon_s} \right) \qquad (6)$$

where q_e is the elementary charge, a_D and a_A are the radii of donor and acceptor, respectively, r is the centre-to-centre distance, and ϵ_{op} and ϵ_s are the optical and static dielectric constants of the medium, respectively. E.g., for donor and acceptor with $a_D = a_A = 5$ Å at a distance $r = 15$ Å, one obtains $\lambda_o = 1.05$ eV in water ($\epsilon_{op} = 1.78$ and $\epsilon_s = 80$), but only 0.37 eV in a hypothetical homogeneous protein with $\epsilon_{op} = 2.1$ and $\epsilon_s = 3.5$ [141]. The dielectric properties of the medium have hence a pronounced effect on the reorganisation energy. According to Eq. (5), the Franck-Condon factor (and hence the electron transfer rate) increases with increasing driving force ($-\Delta G^\circ$) of the reaction up to a maximum when $-\Delta G^\circ = \lambda$ (Fig. 13b), but decreases when $-\Delta G^\circ$ exceeds λ ('Marcus inverted region'; Fig. 13c). This is consistent with the view that the intersection between the potentials of reactants and products represents an activation barrier $\Delta G^* = (\Delta G^\circ + \lambda)^2/4\lambda$ for the electron transfer reaction (see Fig. 13).

Quantum mechanical treatment of the Franck-Condon factor is complicated by the fact that many different oscillations of nuclei in donor and acceptor, in the surrounding protein and even in the suspension medium may be coupled to the electron transfer and should hence be considered in the calculation of the overlap of the nuclear wave-functions of reactants and products. Manageable expressions were derived for simplified cases, e.g., for only one vibrational mode coupled to the electron transfer, or by treating low frequency environmental modes classically and one high frequency mode quantum mechanically. For a single vibrational mode with angular frequency ω, the following formula was derived [53,118,121]:

$$(\text{F.C.}) = (\hbar\omega)^{-1} \exp[-S(2n+1)] \times \left(\frac{n+1}{n} \right)^{\frac{p}{2}} I_p\left[2S\sqrt{n(n+1)}\right] \qquad (7)$$

where $S = \lambda/(\hbar\omega)$, $p = -\Delta G^0/(\hbar\omega)$, $n = \{\exp[\hbar\omega/(k_B T)] - 1\}^{-1}$; I_p is the modified Bessel function of order p (extended to non-integer values of p)

$$I_p(Z) = \sum_{k=0} \frac{(Z/2)^{p+2k}}{k!\Gamma(p+k+1)}.$$

A relatively simple semiclassical expression derived by Hopfield [107]

$$(\text{F.C.}) = \frac{1}{\sqrt{2\pi\lambda\hbar\omega\coth(\hbar\omega/2k_B T)}} \times \exp\left[-\frac{(\Delta G^\circ + \lambda)^2}{2\lambda\hbar\omega\coth(\hbar\omega/2k_B T)} \right] \qquad (8)$$

is sometimes used as an approximation of Eq. (7) (limitations of this approximation were discussed, e.g., in Ref. [164]).

In the high temperature (or low frequency) limit, $k_B T \gg \hbar\omega$, the quantum mechanical expressions converge to the classical expression (Eq. (5)). For low temperatures, however, the classical expression predicts a breakdown of electron transfer because of the activation barrier (except for the special case $-\Delta G^\circ = \lambda$), whereas quantum mechanics can explain virtually temperature-independent electron transfer at low temperatures for $-\Delta G^\circ \neq \lambda$ by a non-vanishing overlap between the lowest nuclear state wave-function of the reactants and some wave-function of the products ('nuclear tunnelling'; note that, e.g., Eq. (8) becomes virtually temperature-independent, but not zero, for $k_B T \ll \hbar\omega$ because the coth term approaches the value of 1).

Moser et al. [178] have shown that the ΔG° and temperature dependence of several electron transfer reactions in purple bacterial reaction centres could be

described assuming a common characteristic frequency ($\hbar\omega \approx 70$ meV), which was attributed to protein high frequency vibrational modes. Based on this observation and the empirical distance dependence of electron transfer (see above), Moser and Dutton [177] suggested the following simple approximation for intraprotein electron transfer:

$$\log k_{et} = 15 - 0.6R - 3.1(\Delta G^\circ + \lambda)^2/\lambda \qquad (9)$$

with k_{et} in s^{-1}, R in Å and ΔG° and λ in eV; R was defined as the shortest distance between centres of atoms at the edges of the donors and acceptors (including only atoms that are in conjugation and directly involved with the reaction [63]). The rate which would be expected if $-\Delta G^\circ$ were equal to λ (i.e., if the last term in Eq. (9) were zero), was called 'optimal rate'. I would like to point out that temperature does not appear explicitly in Eq. (9), and that the last term in Eq. (9) corresponds exactly to the low temperature limit of the second factor in the Hopfield expression (Eq. (8)) for $\hbar\omega = 70$ meV. In fact, the temperature dependence of the Franck-Condon factor according to Eq. (8) is rather weak for $\hbar\omega = 70$ meV and reasonable values of ΔG° and λ (even for the extreme case of $\Delta G^\circ = 0$ and $\lambda = 1.5$ eV, (F.C.) would increase only by a factor of 3.5 from 0 to 298 K).

7.2. Specific electron transfer steps

7.2.1. P700-A_0

Three different electron transfer reactions involving P700 and A_0 are known:

(1) primary charge separation $P700 * A_0 \rightarrow P700^+A_0^-$ has an intrinsic rate in the order of $5 \times 10^{11} s^{-1}$ at room temperature (see Section 4.1.1) and $\Delta G^\circ \approx -250$ meV (see Section 6);

(2) triplet charge recombination $^3(P700^+A_0^-) \rightarrow {}^3P700\ A_0$ may have a rate in the order of $10^9 s^{-1}$ at room temperature (see Section 4.2.2) and $\Delta G^\circ \approx -230$ meV (see Section 6);

(3) singlet charge recombination $^1(P700^+A_0^-) \rightarrow P700\ A_0$ may have a rate in the order of $10^7 s^{-1}$ at room temperature (see Section 4.2.1) and $\Delta G^\circ \approx -1.52$ eV (see Section 6).

According to the most recent X-ray structural model [218] (see Fig. 3), two other chlorophylls (marked A and A′ in Fig. 3) are located roughly between P700 and A_0 and A'_0, respectively. The centre-to-centre distances are approx. 12 Å between P700 and A/A′ and approx. 9 Å between A/A′ and A_0/A'_0 (see Fig. 3). The centre-to-centre distance between P700 and A_0 (A'_0) in the structural model shown in Fig. 3 is approx. 20.5 (19) Å (Schubert, W.D. and Krauß, N., personal communication). The edge-to-edge distances, which are relevant for the estimation of electron transfer rates, are still rather uncertain because the in-plane orientations of the chlorophylls are not unambiguously resolved in the X-ray structure analysis.

Nevertheless, taking into account the resolution of the structure shown in Fig. 3, one can estimate that the edge-to-edge distance between P700 and A_0/A'_0 can hardly be less than 10 Å. For electron transfer over this distance, Eq. (9) predicts an optimal rate of about $10^9 s^{-1}$, which is almost three orders of magnitude slower than the observed rate of primary charge separation. Hence, accepting the structural model in Fig. 3, it is very likely that the putative chlorophyll type acceptor A/A′ acts as an intermediate in electron transfer from excited P700 to A_0/A'_0, similarly to the situation in purple bacteria.

The rate of the triplet recombination (2) may be compatible with the rate predicted by Eq. (9) for direct electron transfer between A_0 and P700, provided that the chlorophylls are oriented such as to minimise the edge-to-edge distance, and that the reorganisation energy is comparable to the free energy gap. Verification of the first condition requires structural data with higher resolution. With respect to the second condition, the outer reorganisation energy may be estimated from Eq. (6): using the dielectric constants of a homogeneous protein given in Section 7.1, effective radii of 5.56 Å for A_0 as a monomeric Chl *a* [141] and 7 Å for P700 (taking into account some delocation of the positive charge in $P700^+$ over the two constituting chlorophylls) and a centre-to-centre distance of 19 Å, one obtains $\lambda_o = 300$ meV (assuming complete localisation of the positive charge on one chlorophyll, $\lambda_o = 350$ meV would be obtained). The inner reorganisation energy λ_i, is presumably considerably smaller for electron transfer between molecules such as chlorophyll which have an extended π-electron system [141]. The total reorganisa-

tion energy may therefore be in the order of 300–400 meV, i.e. not much larger than the free energy gap of 250 meV (e.g., for $\lambda = 350$ meV, the last term in Eq. (9) would be -0.09, which would decrease k_{et} by only 20% compared to the optimal rate).

The singlet recombination (3) appears to be about two orders of magnitude slower than the triplet recombination (2). A slower rate is qualitatively in line with the very large free energy gap (1.52 eV) which places reaction (3) far in the inverted region. However, quantitative estimation with Eq. (9) and $\lambda = 350$ meV (see above) predicts that reaction (3) should be 12 orders of magnitude slower than reaction (2). As possible reasons for this disagreement with the experimental result, one may consider that

· λ may have been underestimated; with $\lambda = 700$ meV, Eq. (9) would predict the observed rate ratio between reactions (2) and (3);

· the last term in Eq. (9) may be a very bad approximation for reaction (3) which is far in the inverted region. It is of note that, e.g., according to the fully quantum mechanical expression for a single vibrational mode coupled to electron transfer (Eq. (7)), reaction (3) should be 'only' 6 orders of magnitude slower than reaction (2) (calculated with $\hbar\omega = 70$ meV and $\lambda = 350$ meV). Furthermore, the Franck-Condon factor for electron transfer reactions far in the inverted region is predicted to increase dramatically when a high frequency mode is additionally coupled to the electron transfer [34].

I would also like to mention the possibility that part or all of reactions (1), (2) and (3) might proceed via the superexchange mechanism (see, e.g., Ref. [175] for a brief description) with A/A' as the virtual intermediate; this might increase the electronic coupling between P700 and A_0/A'_0 differently for the three reactions.

7.2.2. $A_0 - A_1$

The rate constant of forward electron transfer from A_0^- to A_1 is in the order of $(2–5) \times 10^{10} s^{-1}$ (see Section 4.1.1). Inserting their observed value of about $5 \times 10^{10} s^{-1}$ in Eq. (9) and assuming the optimal case ($-\Delta G° = \lambda$), Kumazaki et al. [142] estimated the edge-to-edge distance between A_0 and A_1 to be 7.3 Å. In a very recent report from the same group [117], kinetic data from PS I reconstituted with different quinones (corresponding to different free energy gaps for electron transfer from A_0^- to the modified A_1) were analysed with an expression for the Franck-Condon factor which treats low frequency modes classically and one high frequency mode quantum mechanically. The following parameters were reported: $\lambda_i = 0.18$ eV, $\lambda_o = 0.12$ eV and $T_{DA} = 14$ cm^{-1}. From the value of T_{DA}, the edge-to-edge distance was estimated to 7.8 Å. The free energy gap for samples reconstituted with native phylloquinone was estimated to 0.34 eV so that indeed $-\Delta G° \approx \lambda$. It was suggested that a very low dielectric constant of the protein aqueous environment may explain both the low value of λ_o and the low midpoint potential of phylloquinone in the A_1 site [117].

With respect to possible positions of A_1 in the PS I complex, the above estimates would favour the position marked (A_1) in Fig. 3 over the position (A'_1).

7.2.3. P700-A_1

Direct charge recombination in the pair $P700^+A_1^-$ in intact PS I appears to have an essentially temperature-independent rate of about $4 \times 10^3 s^{-1}$ (see Section 4.2.3) and a free energy gap of approx. 1.2 eV (see Section 6). As the environment of A_1 is likely to have a low static dielectric constant (see Section 7.2.2), the reorganisation energy of the charge recombination is presumably smaller than the free energy gap, placing this electron transfer reaction in the inverted region. An estimation using Eq. (6) with effective radii of 2.84 Å for A_1 [141,225] and 7 Å for P700 (see Section 7.2.1) and the dielectric constants of a homogeneous protein used in Section 6.1 yields λ_o values between 500 and 590 meV for centre-to-centre distances between 15 and 30 Å. Assuming $\lambda = 600$ meV, Eq. (9) yields an edge-to-edge distance of about 16 Å between P700 and A_1. Although this should be considered as only a rough estimate, it indicates that A_1 may be somewhat closer to P700 (or at least not farther apart) than the position marked (A_1) in Fig. 3. This would also be in line with a prediction from photoelectric measurements [146].

Faster recombination rates of up to about $10^5 s^{-1}$ were observed in a PS I core devoid of all iron-sulphur centres and stromal extrinsic subunits (see Section 4.2.2). As discussed in Section 4.2.2, this may reflect modifications of the environment of A_1, which possibly decrease the free energy of the pair $P700^+A_1^-$

and increase the reorganisation energy, so that the recombination could come closer to the optimal rate (for R = 16 Å and $-\Delta G^\circ = \lambda$, Eq. (9) predicts $k_{et} = 2.5 \times 10^5 s^{-1}$).

7.2.4. A_1-F_X

Based on an analysis of electron transfer from A_1^- to F_X in the PS I-β preparation from spinach ($k_{et} \approx 1.5 \times 10^7 s^{-1}$, $|\Delta G^\circ| \ll \lambda$; see Section 4.1.2) and using Eqs. (6) and (9), Sétif and Brettel [225] calculated a reorganisation energy $\lambda = 460$ meV and an edge-to-edge distance R = 10.7 Å. They pointed out that several simplifications in their approach (inter alia neglect of the inner reorganisation energy λ_i and the treatment of the environment of F_X as a hydrophobic protein) presumably led to some underestimation of λ and to an overestimation of R.

Schlodder et al. [216] analysed the temperature dependence of the reoxidation of A_1^- in PS I from *Synechococcus elongatus* (see Section 5) on the basis of the quantum mechanical expression for electron transfer coupled to a single vibrational mode (Eq. (7)). The experimental data were described with $\Delta G^\circ = -54$ meV, $\hbar\omega = 38$ meV, $\lambda = 1.2$ eV and $(2\pi/\hbar)|T_{DA}|^2 = 6 \times 10^{10}$ eV/s (or $T_{DA} = 20$ cm^{-1}), but the determination of these parameters was not unequivocal. Extrapolation to $-\Delta G^\circ = \lambda$ yielded an optimal electron transfer rate of $9 \times 10^{10} s^{-1}$, corresponding according to Eq. (9) to an edge-to-edge distance of approx. 7 Å. I would like to point out that it is not certain that the treatment with a single vibrational mode is adequate, and that a possible temperature dependence of ΔG° and λ may also have contributed to the temperature dependence of the electron transfer. Assuming a rapid redox equilibrium between A_1 and F_X (see Section 4.1.2), it is even conceivable that the temperature dependence of the reoxidation of A_1^- is in part due to an activated electron transfer from F_X^- to F_A or F_B. These uncertainties, however, do not affect the main conclusion, that the real rate of electron transfer from A_1^- to F_X is far below the optimal rate and that the edge-to-edge distance is most likely shorter than 11 Å. Both of the two tentative positions of phylloquinone molecules shown in Fig. 3 and also positions slightly closer to A_0/A'_0 and to P700 (as suggested in Section 7.2.3) would be compatible with this estimate.

7.2.5. A_0-F_X

The low temperature photoreduction of F_A and F_B in PS I devoid of phylloquinone (see Section 3.2.3) indicates a direct electron transfer from A_0^- to F_X in such samples. The rate of this electron transfer should be in the order of $2 \times 10^6 s^{-1}$, as its yield (in competition with charge recombination in the primary pair with $t_{1/2} \approx 80$ ns at cryogenic temperatures) appears to be in the order of 20% [227]. With $\Delta G^\circ \approx -320$ meV (see Section 6) and assuming $\lambda \approx 500$ meV (Eq. (6) yields $\lambda_o = 390$ meV assuming effective radii of 5.56 Å for A_0 (see Section 7.2.1) and 4.86 Å for F_X [225], $r = 19.8$ Å (see Fig. 3) and $\epsilon_{opt} = 2.1$ and $\epsilon_s = 3.5$ (see Section 6.1)), the edge-to-edge distance between A_0 and F_X according to Eq. (9) should be approx. 14 Å. This fits well with the structural model based on X-ray crystallography (Fig. 3). One should not exclude, however, the possibility that extraction of phylloquinone together with carotenoids and a large fraction of the antenna chlorophylls modified the distances between the cofactors as well as their dielectric environments.

I would like to point out that in intact PS I, electron transfer from A_0^- to A_1 should outcompete the 4 orders of magnitude slower direct electron transfer from A_0^- to F_X. However, A_1^- appears to be nearly a 'dead end' at low temperatures, presumably because of lacking driving force for electron transfer to F_X (see also Section 8.1). Removal of this 'dead end' by extraction of phylloquinone would enable direct downhill electron transfer from A_0^- to F_X. By coincidence electron transfer from A_1^- to F_X in intact PS I and electron transfer from A_0^- to F_X in the absence of A_1 may have similar (low) yields at cryogenic temperatures.

7.2.6. P700-F_X

The rate of direct charge recombination in the pair $P700^+F_X^-$ is presumably in the order of 10 s^{-1} (see Section 4.2.3). With $\Delta G^\circ \approx -1.20$ eV (see Section 6) and assuming $\lambda \approx 500$ meV (Eq. (6) yields $\lambda_o = 390$ meV assuming the same effective radii and dielectric constants as in Sections 7.2.1 and 7.2.5 and r = 31 Å (Schubert, W.D. and Krauß, N., personal communication)), Eq. (9) predicts an edge-to-edge distance of approx. 18 Å. The edge-to-edge distance in the structural model shown in Fig. 3 is, however,

significantly larger (between 21 and 26 Å, depending on the in plane orientation of the chlorophylls constituting P700 and on the orientation of F_X). This discrepancy might be due to an underestimation of the reorganisation energy λ (the environment of F_X may be more hydrophilic than assumed in the calculation of λ_o; see also Ref. [225]) or to an inadequacy of Eq. (9) (the optimal rate according to Eq. (9) (with $-\Delta G^\circ = \lambda$) would be between 250 and 0.25 s^{-1} for an edge-to-edge distance between 21 and 26 Å).

7.2.7. F_X-F_A-F_B

Electron transfer between the iron-sulphur clusters of PS I is only poorly characterised (see Section 4.1.3 and Section 5). However, the positions of these clusters were rather well resolved by X-ray crystallography (see Fig. 3), thus Eq. (9) may be used to predict approximate electron transfer rates.

Sétif and Brettel [225] assumed that all three iron-sulphur clusters in PS I have the same geometry as the [4Fe-4S] clusters in the ferredoxin of *Peptococcus aerogenes* [1,2], where the 4 sulphur atoms of the cluster are at an average distance of 2.15 Å from the centre, and the sulphur atoms of the 4 cysteines ligating the cluster are at an average distance of 3.87 Å from the centre (these values are relevant for the estimation of the edge-to-edge distances, because according to calculations for a model compound [185], each of these 8 sulphur atoms effectively receives approx. 0.1 electron charge upon reduction of the cluster). Considering the range of edge-to-edge distances compatible with this cluster geometry (note that the orientation of the clusters could not yet be resolved by X-ray crystallography) and the range of published midpoint potentials of F_A, F_B and F_X, and using dielectric constants of a hydrophobic protein for the estimation of λ (λ_i was neglected), Eq. (9) predicted an electron transfer rate between 5.1×10^7 and 3.6×10^{10} s^{-1} for electron transfer from F_X^- to the proximal cluster F_{AB1}, and between 2.3×10^3 and $1.9 \times 10^6 s^{-1}$ for electron transfer from F_X^- to the distal cluster F_{AB2} [225]. Although these rates are likely to be somewhat overestimated (inter alia because λ_i was neglected and ϵ_s presumably underestimated [225]), electron transfer from F_X^- to F_{AB1} may well be in the submicrosecond range, in line with some experimental results (see Section 4.1.3). Another consequence would be that direct electron transfer from F_X^- to F_{AB2} could hardly compete with electron transfer from F_X^- to F_{AB1} (see also Refs. [69,243]).

For electron transfer between F_A and F_B, Sigfridsson et al. [243] presented an estimation based on the coupling pathway approach (see Section 7.1 and Ref. [10]). They used the known structure of the *Peptococcus aerogenes* ferredoxin as a model for PsaC and stated that there are two symmetrical coupling pathways between the iron-sulphur clusters, each consisting of 18 covalent bonds; this yielded an optimal electron transfer rate of about $1.8 \times 10^6 s^{-1}$. Assuming $\Delta G^\circ = -60$ meV (attributed to electron transfer from F_B^- to F_A) and $\lambda = 260$ meV, and applying a classical treatment for the Franck-Condon factor, a real rate constant of $3.8 \times 10^4 s^{-1}$ was predicted for room temperature [243], in line with assignment I of the photovoltage measurements in the same publication (see Section 4.1.3). Interestingly, the following estimation based on Eq. (9) predicts a much faster electron transfer: the shortest distance between sulphur atoms associated with the two iron-sulphur clusters in the *Peptococcus aerogenes* ferredoxin [2] is 6.24 Å (between the sulphur atoms of cysteines 14 and 42 (numbering according to Ref. [6]), corresponding to cysteines 17 and 54, respectively, in Fig. 7). Inserting R = 6.24 Å in Eq. (9), one obtains an optimal rate of 1.3×10^{11} s^{-1}. The last term in Eq. (9) would decrease this value to 4×10^{10} s^{-1} for $\Delta G^\circ = -60$ meV and $\lambda = 260$ meV, or to 2×10^8 s^{-1} if λ were, e.g., 1000 meV (as F_A and F_B are rather close to the aqueous phase, λ might be rather large; using the dielectric constants of water (see Section 7.1), Eq. (6) would predict $\lambda_o = 990$ meV). The main origin of the discrepancy between these two approaches is the very long coupling pathway in Ref. [243] (18 covalent bonds correspond to approx. 25 Å) which seems to indicate that the protein structure in between the two iron-sulphur clusters functions as an insulator for the electronic coupling. Unfortunately, Sigfridsson et al. [243] did not specify the two coupling pathways, and did not explain by which method it was established that they are the pathways of maximal coupling. Without having performed a systematic pathway search, it appears to me that a hypothetical coupling pathway between the sulphur atoms of cysteines 14 and 42 via Cβ and Hβ_1 of Cys 14 and Hα, Cα and Cβ of Cys 42

would be much stronger than a pathway consisting of 18 covalent bonds, because the distance between Cys 14 Hβ_1 and Cys 42 Hα is only 2.7 Å [12].

Of particular interest are the electron transfer rates at very low temperatures, because many studies on the iron-sulphur clusters of PS I were performed by EPR at around 20 K (see Section 5). As already mentioned in Section 7.1, the empirical Eq. (9) is independent of temperature, and the Hopfield expression for the Franck-Condon factor (Eq. (8)) decreases only slightly with decreasing temperature, when $\hbar\omega = 70$ meV and reasonable values for $\Delta G°$ and λ are assumed. As F_A and F_B are rather close to the aqueous phase, electron transfer between F_X, F_A and F_B may be more strongly coupled to low frequency environmental modes than the other electron transfer reactions in PS I, and than the electron transfer reactions in purple bacterial reaction centres on which the estimate $\hbar\omega \approx 70$ meV [178] was based. In fact, Eq. (8) becomes more strongly temperature-dependent, when $\hbar\omega$ is lowered. It should also be mentioned that the semiclassical Eq. (8) overestimates the electron transfer rates at low temperature for reactions with small driving force and large reorganisation energy (compared to the quantum mechanical expression (Eq. (7)) for a single vibrational mode (see, e.g., Fig. 5 in Ref. [119]). Therefore, electron transfer between F_X, F_A and F_B may slow down considerably with decreasing temperature. As, however, F_A and F_B can still be photoreduced at around 20 K (although with lower yields than at room temperature; see Section 5), at least two of the three electron transfer steps $F_X^- \rightarrow F_A$, $F_X^- \rightarrow F_B$ and $F_A^- \rightarrow F_B$ (or $F_B^- \rightarrow F_A$) still function at low temperature. Prior to the crystallisation of PS I, it was generally believed that electron transfer between F_A and F_B is completely blocked at low temperature and that F_A and F_B are reduced through parallel pathways from F_X^- (see Section 5). As the edge-to-edge distance between F_X and the distal cluster F_{AB2} is now known to be nearly 3 times as large as the distance between F_{AB1} and F_{AB2}, it seems much more likely that F_{AB2} is reduced via F_{AB1}. A considerable electronic coupling between these two clusters would also be consistent with the magnetic coupling between F_A^- and F_B^- as detected by EPR (see Section 3.2.5).

Finally, I would like to mention that in several ferredoxins containing two [4Fe-4S] clusters, electron exchange between the two clusters as evidenced by the 'averaging' of NMR resonances in partially reduced samples appears to be fast on the NMR timescale (e.g., $> 10^5$ s^{-1} in the *Clostridium pasteurianum* ferredoxin at room temperature [11]), but in one case (*Chromatium vinosum* ferredoxin), the averaging of NMR resonances could not be observed, and there was also no magnetic interaction detected by EPR when both clusters were reduced [109]. Huber et al. [109] suggested that the different behavior of these ferredoxins might be related to a different distribution of the mixed valence pair (Fe^{2+}-Fe^{3+}) on one or both of the reduced clusters (reduced [4Fe-4S] clusters contain a Fe^{2+}-Fe^{3+} pair and a Fe^{2+}-Fe^{2+} pair; for each cluster, there exist a priori 6 different possibilities for the localisation of the Fe^{2+}-Fe^{3+} pair, but some of them may be energetically favoured over others). Future work on PS I may take into account the idea that the distribution of the mixed valence pair in each cluster might play a role for electron transfer between F_X, F_A and F_B.

7.3. Conclusions

In view of the relatively low resolution of the present structural data on PS I and the rather limited characterisation of most of the electron transfer steps, the analysis in Section 7.2 had to rely largely on the very simple empirical relation (Eq. (9)) for the rate of intraprotein electron transfer suggested by Moser and Dutton [177]. Future work may clarify whether this relation is a good approximation for all electron transfer reactions in PS I. At present, I would like to draw only a few tentative conclusions:

· It is very likely that the chlorophyll denoted as A (or A′) in Fig. 3 participates in the primary charge separation, either as a real intermediate or as a virtual intermediate in the superexchange mechanism.

· Between the two positions for phylloquinone suggested tentatively in Ref. [218], the position marked as (A_1) in Fig. 3 is more easy to reconcile with experimental electron transfer rates than the position (A'_1).

· Based on the structural data, it is likely that electron transfer between F_A and F_B proceeds in the sub-microsecond range, at least at room temperature.

· The last term in Eq. (9) may be a rather poor approximation for electron transfer reactions which

are far into the inverted region or have a very low driving force.

8. Hypothesis on the origin of the peculiar freezing effects on electron transfer in photosystem I [1]

8.1. Concomitant formation of stable $P700^+F_A^-$ and stable $P700^+F_B^-$ and heterogeneity of electron transfer at very low temperature

It is well established that illumination of PS I at around 20 K results in quasi-irreversible formation of the pair $P700^+F_A^-$ in a fraction of the PS I complexes and of the pair $P700^+F_B^-$ in another fraction (see Section 5; note that the ratio of $P700^+F_A^-$ and $P700^+F_B^-$ varied considerably, depending on the origin of the sample and certain treatments and preparation procedures). To account for this observation, it was suggested that F_A and F_B were reduced by competing parallel electron transfer pathways from F_X^-, and that there was no electron exchange between F_A and F_B (otherwise, at low temperature the electron should always end up on the acceptor with the highest reduction potential). The possibility of obtaining different ratios of stable $P700^+F_A^-$ and stable $P700^+F_B^-$ in the same sample at 25 K (by varying the temperature of illumination) was considered as further strong evidence against electron transfer between F_A and F_B at low temperature [39]; see also Section 5. In view of the distances between the iron-sulphur clusters, however, it seems unlikely that electron transfer between F_A and F_B should be blocked while transfer from F_X^- to the distal cluster F_{AB2} should still occur at low temperature (see Section 7.2.7). Therefore, I would like to put forward the following hypothesis which takes into account the concept of frozen conformational substates of proteins (see Ref. [68] for a review) and is consistent with a dominating linear electron transfer pathway as suggested by the spatial arrangement of the iron-sulphur clusters:

Hypothesis 1. At very low temperature, PS I may exist in a variety of frozen conformational substates which differ inter alia in the energy of the pairs $P700^+F_A^-$ and $P700^+F_B^-$. Electron transfer between F_A and F_B would be possible in the direction of decreasing energy, so that stable $P700^+F_A^-$ could be formed in those PS I complexes where $P700^+F_A^-$ is energetically below $P700^+F_B^-$, and vice versa for the formation of stable $P700^+F_B^-$. The frozen distribution of conformational substates may vary between different samples and treatments, giving rise to the observed variation of the ratio between light-induced $P700^+F_A^-$ and $P700^+F_B^-$.

The same concept could also account for the observation that an important fraction of the PS I complexes is unable to transfer electrons to F_A or F_B at low temperature and undergoes mainly charge recombination in the pair $P700^+A_1^-$ instead (see Section 5). Assuming a distribution of energies also for the states $P700^+A_1^-$ and $P700^+F_X^-$, a fraction of PS I may be frozen in substates where $P700^+F_X^-$ is energetically above $P700^+A_1^-$, so that only the latter pair could be formed and would decay by charge recombination. Among the conformational substates with $P700^+F_X^-$ energetically below $P700^+A_1^-$, there may be a fraction where $P700^+F_X^-$ is even below $P700^+F_A^-$ and $P700^+F_B^-$, explaining the $P700^+F_X^-$ charge recombination observed in a small fraction of PS I (see Section 5).

The four cases described so far are schematically presented in Fig. 14a–d (note that the assignment of F_A and F_B to the proximal (F_{AB1}) and distal cluster (F_{AB2}) is not yet clear; see Section 6.2). With respect to the possible width of the energetic spread of the individual charge separated states, I would like to mention a study on purple bacterial reaction centres where a Gaussian width of $2\sigma \approx 100$ meV was estimated for the distribution of the free energy of the primary pair [189]. The kinetic effects of this distribution are relatively weak because the free energy gaps for the electron transfer reactions involving the primary pair are larger than the energetic spread. For the energetically closely spaced secondary electron transfer reactions in PS I, however, a similar energetic spread should give rise to a pronounced heterogeneity at low temperature, as observed (note that the average energy levels of the states $P700^+F_X^-$, $P700^+F_A^-$ and $P700^+F_B^-$ may be even more closely spaced at low temperature than proposed in Figs. 11 and 12 for

[1] Presented, in preliminary form, at the Colloque Annuel de la Société Française de Photobiologie, Paris, 8–10 November 1993.

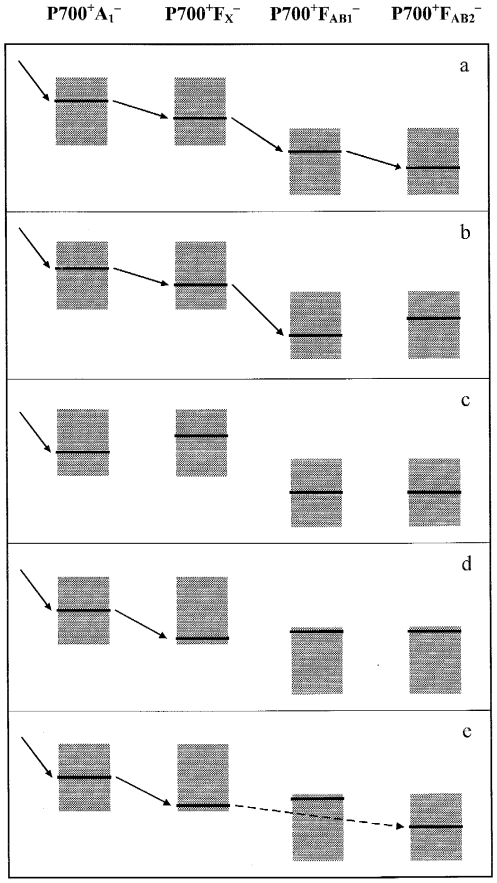

Fig. 14. Illustration of the suggested heterogeneity of secondary electron transfer in PS I at very low temperature. The energy levels and possible electron transfer steps are indicated for 5 selected conformational substates (a, b, c, d, e). The shaded areas represent the width of the distribution of the energy levels.

room temperature, because part of the stabilisation of the reduced terminal acceptors by reorienting water dipoles may be lost upon freezing; see Sections 6.2 and 8.2).

In addition to the 'all or nothing' effect described so far, it is likely that the rates of the downhill electron transfer reactions vary between different conformational substates, because of the $\Delta G°$ dependence of the Franck-Condon factor, and because some variation of the distances between the cofactors should affect the electronic couplings (see Section 7.1). As suggested by Sétif et al. [232], a distribution of forward electron transfer rates competing with charge recombination in the pairs $P700^+A_1^-$ and $P700^+F_X^-$ may explain the decrease of the efficiency of $P700^+F_A^-$ formation during a series of laser flashes at 20 K (see also Section 5).

Finally, I would like to point out that according to the rate predictions outlined in Sections 7.2.5 and 7.2.7, direct electron transfer from F_X^- to the distal cluster F_{AB2} should be faster than charge recombination in the pair $P700^+F_X^-$. Hence, in PS I complexes frozen in substates where $P700^+F_X^-$ is energetically below $P700^+F_{AB1}^-$, but above $P700^+F_{AB2}^-$, photoreduction of F_{AB2} may be possible (see Fig. 14e). This may also apply to PS I complexes where F_{AB1} was prereduced prior to freezing (see Section 5).

8.2. The transition from efficient photoreduction of the terminal acceptors to secondary pair recombination and heterogeneity

An optical study of the photochemistry throughout the temperature range from 300 to 77 K (in the presence of 65% (v/v) glycerol as a glass-forming cryoprotectant) revealed a relatively sharp transition around 170 K from long-lived charge separation in all PS I complexes to a heterogeneous behavior where about half of the complexes showed charge recombination in the pair $P700^+A_1^-$ with $t_{1/2} \approx 200$ μs; the temperature of this transition was found to vary with the composition of the suspension medium in a way which suggested a correlation with the liquid to glass transition of the medium [216]; see Section 5. I would like to propose the following mechanism by which the liquid to glass transition of the suspension medium might affect efficient forward electron transfer beyond A_1.

Hypothesis 2. For electron transfer to the terminal acceptors which are close to the surface of the PS I complex, reorientation of the electric dipoles in the aqueous medium (dielectric relaxation) in response to the change of the charge distribution in the protein may provide a considerable energetic stabilisation of the reduced acceptors. This stabilisation would be lost when the medium forms a glass (or ice), so that electron transfer to the terminal acceptors should become energetically less favourable or even unfavourable.

The basic idea is qualitatively illustrated in Fig. 15 for an intraprotein electron transfer reaction

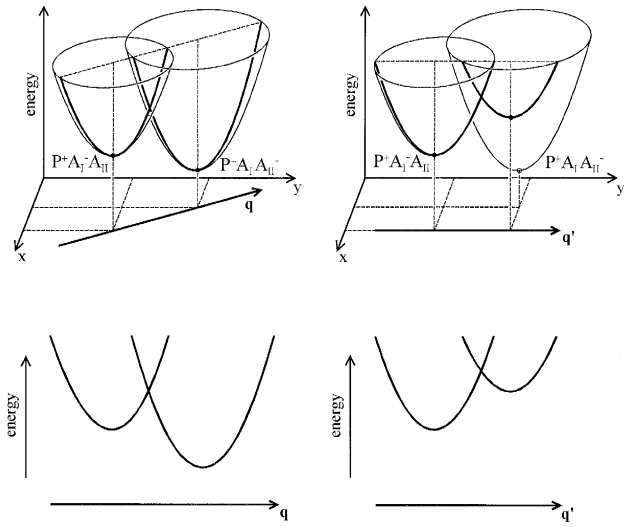

Fig. 15. Illustration of the suggested freezing effect on an intraprotein electron transfer reaction $P^+A_I^-A_{II} \rightarrow P^+A_IA_{II}^-$, where A_{II} (but not A_I and P) are located close to the surface of the protein complex. *x* represents the nuclear co-ordinates of the suspension medium which become fixed upon formation of a glass or ice. All other nuclear co-ordinates are represented by *y*. Left-hand panel: section along axis *q* (through the energy minima of the states $P^+A_I^-A_{II}$ and $P^+A_IA_{II}^-$), illustrating the energetics of the electron transfer when the suspension medium is liquid. Right-hand panel: section along axis *q′* (through the energy minimum of the state $P^+A_I^-A_{II}$ and keeping *x* constant), illustrating the energetics of the electron transfer when the suspension medium has formed a glass or ice.

$P^+A_I^-A_{II} \rightarrow P^+A_IA_{II}^-$, where A_{II} (but not A_I and P) is assumed to be located close to the surface of the protein complex. The energy hypersurfaces (entropy changes were neglected for the sake of simplicity) are drawn as functions of two generalised nuclear co-ordinates, *x* and *y*. *x* represents the co-ordinates which are fixed when the suspension medium forms a glass or ice (in addition to co-ordinates of the suspension medium itself, *x* may comprise co-ordinates of the protein surface which are stuck when the medium becomes rigid). At higher temperatures, when the medium is liquid (left-hand panel in Fig. 15), *x* and *y* can relax to the energy minimum of the state $P^+A_IA_{II}^-$, i.e., the nuclei can move along the axis *q*. In the glassy or frozen state of the suspension medium (right-hand panel of Fig. 15), however, *x* is fixed at the value of the energy minimum of the state $P^+A_I^-A_{II}$ and only *y* can relax; hence, the nuclei can only move along the axis *q′*, and the absolute energy minimum of the state $P^+A_IA_{II}^-$ cannot be reached. In the example of Fig. 15, electron transfer from A_I^- to A_{II} would therefore be energetically uphill at low temperature. A similar situation may exist in PS I for the electron transfer reactions beyond A_1. A_1 is presumably well-shielded from the aqueous phase (see Sections 3.2.3 and 7.2.2), but for F_X, F_A and F_B, the dielectric relaxation of the suspension medium might provide a significant stabilisation of the reduced form. Considering the location of the iron-sulphur clusters within the PS I complex (see Fig. 3), it is likely that the stabilisation increases in the order F_X, F_{AB1}, F_{AB2}. Therefore, an increase of ΔG° is expected for each of the electron transfer steps in the sequence $A_1 \rightarrow F_X \rightarrow F_{AB1} \rightarrow F_{AB2}$, when the relaxation of the suspension medium is frozen out. This effect, combined with some energetic spread between different conformational substates (see Section 8.1) may explain the inefficiency and heterogeneity of electron transfer beyond A_1 below the glass transition temperature of the suspension medium. The apparent absence of such effects for primary charge separation (up to A_1) may be due to a better shielding from the aqueous phase and to the larger free energy gaps, so that these electron transfer steps remain well exergonic when the relaxations of the suspension medium are frozen out.

The two situations illustrated in Fig. 15 should be considered as borderline cases where the dielectric relaxation of the suspension medium is either much faster (left-hand panel) or much slower (right-hand panel) than all other reactions which might compete with electron transfer from A_I^- to A_{II} (as for example charge recombination between P^+ and A_I^-). More complicated situations may arise when the relaxation rate is comparable to competing reactions. To give an idea of the relevant time scales, the dielectric relaxation time of pure glycerol (expected glass transition at about 190 K [199]), is about 500 ms at 200 K, 300 μs at 220 K and 3 μs at 240 K [48]. As a rough estimation for 65% (v/v) glycerol in water (glass transition at about 165 K [199]), these relaxation times may be valid at about 175, 195 and 215 K, respectively. One may speculate that the deviation from a monoexponential reoxidation of A_1^- which set in at about 200 K upon cooling in the presence of 65% glycerol (see Section 5) could be related to a competition between the dielectric relaxation of the

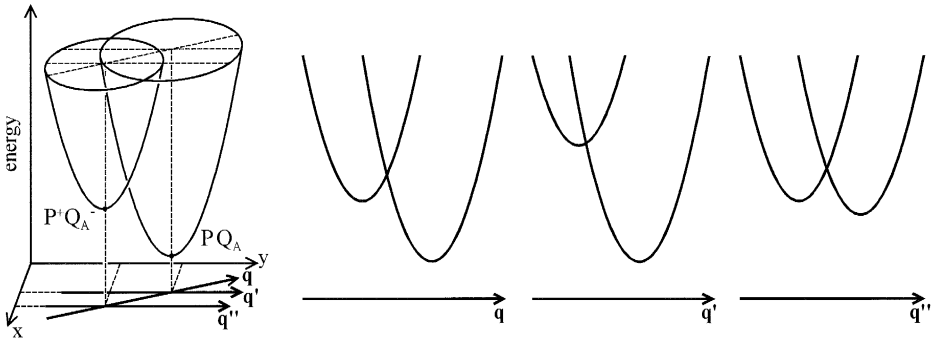

Fig. 16. Application of the principal underlying Fig. 15 to charge recombination in the secondary pair $P^+Q_A^-$ in purple bacterial reaction centres. Section along axis q: suspension medium liquid. Section along axis q': sample frozen in the equilibrium configuration of the state PQ_A. Section along axis q'': sample frozen in the equilibrium configuration of the state $P^+Q_A^-$. See text for further explanations.

medium and the 150 μs charge recombination in the pair $P700^+A_1^-$.

A presentation of energy hypersurfaces similar to Fig. 15 may provide a simple qualitative explanation of some features of the charge recombination in the secondary pair $P^+Q_A^-$ in purple bacterial reaction centres. In Fig. 16, it was assumed that the dielectric relaxation of the suspension medium contributes considerably to the stabilisation of the state $P^+Q_A^-$ (note that Q_A is presumably more exposed to the aqueous phase than the secondary acceptor A_1 in PS I). When the sample is frozen in the equilibrium conformation of the state PQ_A (section along axis q' in Fig. 16), the energy gap for the recombination should be larger and the reorganisation energy smaller than at room temperature (section along axis q), as suggested recently by Ortega et al. [192]. Interestingly, most of the decrease of the reorganisation energy occurred between 225 and 175 K, i.e., slightly above the glass transition of the suspension medium (60% (v/v) glycerol in water) [192]. Kleinfeld et al. [133] showed that the $P^+Q_A^-$ recombination at 77 K was slower and deviated from a monoexponential decay, when the reaction centres were cooled under illumination. They suggested that the distribution of distances between P and Q_A broadened and shifted to larger values (compared to reaction centres cooled in the dark). According to Fig. 16, one may alternatively suggest that the sample was frozen in the conformation corresponding to the energy minimum of the state $P^+Q_A^-$, and that x could not relax during the recombination (section along axis q'' in Fig. 16). This implies a lower free energy gap and hence a lower electron transfer rate than for the sample cooled in the dark. The non-monoexponential kinetics may reflect a distribution of free energy gaps related to the distribution of frozen conformational substates (see Section 8.1).

Finally, I would like to mention that the glass transition of the solvent appears to have a pronounced effect on the ligand rebinding kinetics of myoglobin, presumably because the strong increase of the viscosity of the solvent prohibits conformational relaxations of the protein [5,88]. If electron transfer to the terminal acceptors of PS I were accompanied by large-scale conformational relaxations of the protein complex, these could be prohibited in a similar way due to the glass transition of the suspension medium. Such a direct viscosity effect could add to the dielectric relaxation effect on electron transfer suggested above.

Acknowledgements

I am very grateful to Paul Mathis, Bill Rutherford, Pierre Sétif and particularily to Ursula Liebl and Tony Mattioli for critical reading of the manuscript and for helpful discussions and suggestions. This review greatly benefited from interchange of ideas on specific aspects with Petra Fromme, Andreas Kamlowski, Norbert Krauß, Winfried Leibl, Fraser MacMillan, Eberhard Schlodder, Wolf-Dieter Schubert and Art van der Est. I would also like to thank Drs. W.-Z. He, P. Heathcote, M. Hippler, S. Itoh, H.

Naver, K. Sigfridsson, M.C. Thurnauer, J.T. Warden, L.R. Vasiliev and H.T. Witt for providing preprints of manuscripts for inclusion in the review.

References

[1] Adman, E.T., Sieker, L.C. and Jensen, L.H. (1973) J. Biol. Chem. 248, 3987–3996.
[2] Adman, E.T., Sieker, L.C. and Jensen, L.H. (1976) J. Biol. Chem. 251, 3801–3806.
[3] Amesz, J. (1995) in Anoxygenic Photosynthetic Bacteria (Blankenship, R.E., Madigan, M.T. and Bauer, C.E., eds.), pp. 687–697, Kluwer Academic Publishers, Dordrecht.
[4] Andréasson, L.-E. and Vänngård, T. (1988) Ann. Rev. Plant Physiol. Plant Mol. Biol. 39, 379–411.
[5] Ansari, A., Jones, C. M., Henry, E.R., Hofrichter, J. and Eaton, W.A. (1992) Science 256, 1796–1798
[6] Backes, G., Mino, Y., Loehr, T.M., Meyer, T.E., Cusanovich, M.A., Sweeney, W.V., Adman, E.T. and Sandersloehr, J. (1991) J. Am. Chem. Soc. 113, 2055–2064.
[7] Barkoff, A., Brunkan, N., Snyder, S.W., Ostafin, A., Werst, M., Biggins, J. and Thurnauer, M.C (1995) in Photosynthesis: from Light to Biosphere (Mathis, M., ed.), Vol. 2, pp. 115–118, Kluwer Academic Publishers, Dordrecht.
[8] Barry, B.A., Bender, C.J., McIntosh, L., Ferguson-Miller, S. and Babcock, G.T. (1988) Isr. J. Chem. 28, 129–132.
[9] Bearden, A.J. and Malkin, R. (1976) Biochim. Biophys. Acta 430, 538–547.
[10] Beratan, D.N., Betts, J.N. and Onuchic, J.N. (1991) Science 252, 1285–1288.
[11] Bertini, I., Briganti, F., Luchinat, C., Messori, L., Monnanni, R., Scozzafava, A. and Vallini, G. (1992) Eur. J. Biochem. 204, 831–839.
[12] Bertini, I., Capozzi, F., Luchinat, C., Piccioli, M. and Vila, A.J. (1994) J. Am. Chem. Soc. 116, 651–660.
[13] Bertrand, P. (1991) Structure and Bonding 75, 1–47.
[14] Biggins, J. (1990) Biochemistry 29, 7259–7264.
[15] Biggins, J. and Mathis, P. (1988) Biochemistry 27, 1494–1500.
[16] Biggins, J., Rodday, S.M. and Do, L. (1995) in Photosynthesis: from Light to Biosphere (Mathis, M., ed.), Vol. 2, pp. 111–114, Kluwer Academic Publishers, Dordrecht.
[17] Biggins, J., Tanguay, N.A. and Frank, H. (1990) in Current Research in Photosynthesis (Baltscheffsky, M., ed.), Vol. 2, pp. 639–642, Kluwer Academic Publishers, Dordrecht.
[18] Biggins, J., Tanguay, N.A. and Frank, H.A. (1989) FEBS Lett. 250, 271–274.
[19] Blankenship, R.E., Madigan, M.T. and Bauer, C.E. (eds.) (1995) Anoxygenic Photosynthetic Bacteria, Kluwer Academic Publishers, Dordrecht.
[20] Bock, C.H., Brettel, K., Van der Est, A.J. Sieckmann, I. and Stehlik, D. (1990) in Current Research in Photosynthesis (Baltscheffsky, M., ed.), Vol. 2, pp. 623–626, Kluwer Academic Publishers, Dordrecht.
[21] Bock, C.H., Van der Est, A.J., Brettel, K. and Stehlik, D. (1989) FEBS Lett. 247, 91–96.
[22] Bonnerjea, J.R. and Evans, M.C.W. (1982) FEBS Lett. 148, 313–316.
[23] Bottin, H. and Sétif, P. (1991) Biochim. Biophys. Acta 1057, 331–336.
[24] Bottin, H., Sétif, P. and Mathis, P. (1987) Biochim. Biophys. Acta 894, 39–48.
[25] Breton, J. (1977) Biochim. Biophys. Acta 459, 66–75.
[26] Breton, J., Roux, N. and Whitmarsh, J. (1975) Biochem. Biophys. Res. Commun. 64, 1274–1277.
[27] Brettel, K. (1988) FEBS Lett. 239, 93–98.
[28] Brettel, K. (1989) Biochim. Biophys. Acta 976, 246–249.
[29] Brettel, K. (1990) in Current Research in Photosynthesis (Baltscheffsky, M., ed.), Vol. 2, pp. 627–630, Kluwer Academic Publishers, Dordrecht.
[30] Brettel, K. and Golbeck, J.H. (1995) Photosynth. Res. 45, 183–193.
[31] Brettel, K. and Sétif, P. (1987) Biochim. Biophys. Acta 893, 109–114.
[32] Brettel, K., Sétif, P. and Mathis, P. (1986) FEBS Lett. 203, 220–224.
[33] Brettel, K., Sieckmann, I., Fromme, P., Van der Est, A. and Stehlik, D. (1992) Biochim. Biophys. Acta 1098, 266–270.
[34] Brunschwig, B.S. and Sutin, N. (1987) Comments Inorg. Chem. 6, 209–235.
[35] Burghaus, O., Plato, M., Rohrer, M., Möbius, K., Macmillan, F. and Lubitz, W. (1993) J. Phys. Chem. 97, 7639–7647.
[36] Büttner, M., Xie, D.L., Nelson, H., Pinther, W., Hauska, G. and Nelson, N. (1992) Proc. Natl. Acad. Sci. USA 89, 8135–8139.
[37] Cammack, R., Ryan, M.D. and Stewart, A.C. (1979) FEBS Lett. 107, 422–426.
[38] Chambers, J.Q. (1974) in The Chemistry of the Quinoid Compounds Part 2 (Patai, S., ed.), Wiley, London.
[39] Chamorovsky, S.K. and Cammack, R. (1982) Biochim. Biophys. Acta 679, 146–155.
[40] Chamorovsky, S.K. and Cammack, R. (1982) Photobiochem. Photobiophys. 4, 195–200.
[41] Chidsey, C.E.D., Takiff, L., Goldstein, R.A. and Boxer, S.G. (1985) Proc. Natl. Acad. Sci. USA 82, 6850–6854.
[42] Chiou, H.C. and Blankenship, R.E. (1995) in Photosynthesis: from Light to Biosphere (Mathis, M., ed.), Vol. 2, pp. 167–170, Kluwer Academic Publishers, Dordrecht.
[43] Chitnis, P.R., Xu, Q., Chitnis, V.P. and Nechushtai, R. (1995) Photosynth. Res. 44, 23–40.
[44] Chitnis, V.P., Jung, Y.-S., Albee, L., Golbeck, J. and Chitnis, P.R. (1996) J. Biol. Chem. 271, 11772–11780.
[45] Clayton, R.K. (1980) Photosynthesis: Physical Mechanisms and Chemical Patterns, pp. 132–146, Cambridge University Press, Cambridge.
[46] Crowder, M.S. and Bearden, A.J. (1983) Biochim. Biophys. Acta 722, 23–35.

[47] Cui, L.Y., Bingham, S.E., Kuhn, M., Käss, H., Lubitz, W. and Webber, A.N. (1995) Biochemistry 34, 1549–1558.
[48] Davidson, D.W. and Cole, R.H. (1951) J. Chem. Phys. 19, 1484–1490.
[49] Davis, I.H., Heathcote, P., Maclachlan, D.J. and Evans, M.C.W. (1993) Biochim. Biophys. Acta 1143, 183–189.
[50] Deisenhofer, J., Epp, O., Huber, R. and Michel, H. (1984) J. Mol. Biol. 180, 385–398.
[51] Demeter, S. and Ke, B. (1977) Biochim. Biophys. Acta 462, 770–774.
[52] Den Blanken, H.J. and Hoff, A.J. (1983) Biochim. Biophys. Acta 724, 52–61.
[53] Devault, D. (1980) Q. Rev. Biophys. 13, 387–564.
[54] Dismukes, G.C. and Sauer, K. (1978) Biochim. Biophys. Acta 504, 431–445.
[55] Dunn, P.P.J. and Gray, J.C. (1988) Plant Mol. Biol. 11, 311–320.
[56] Englman, R. and Jortner, J. (1970) Mol. Phys. 18, 145–164.
[57] Evans, M.C.W. (1982) in Iron-Sulfur Proteins (Spiro, T.G., ed.), pp. 249–284, Wiley, New York.
[58] Evans, M.C.W., Bratt, P.J., Heathcote, P. and Moënne Loccoz, P. (1995) in Photosynthesis: from Light to Biosphere (Mathis, M., ed.), Vol. 2, pp. 183–186, Kluwer Academic Publishers, Dordrecht.
[59] Evans, M.C.W. and Heathcote, P. (1980) Biochim. Biophys. Acta 590, 89–96.
[60] Evans, M.C.W. and Nugent, J.H.A. (1993) in The Photosynthetic Reaction Center (Deisenhofer, J. and Norris, J.R., eds.), Vol. 1, pp. 391–415, Academic Press, San Diego.
[61] Evans, M.C.W., Reeves, S.G. and Cammack, R. (1974) FEBS Lett. 49, 111–114.
[62] Evans, M.C.W., Sihra, C.K., Bolton, J.R. and Cammack, R. (1975) Nature 256, 668–670.
[63] Farid, R.S., Moser, C. and Dutton, P.L. (1993) Curr. Op. Struct. Biol. 3, 225–233.
[64] Feiler, U. and Hauska, G. (1995) in Anoxygenic Photosynthetic Bacteria (Blankenship, R.E., Madigan, M.T. and Bauer, C.E., eds.), pp. 665–685, Kluwer Academic Publishers, Dordrecht.
[65] Fenton, J.M., Pellin, M.J., Govindjee and Kaufmann, K.J. (1979) FEBS Lett. 100, 1–4.
[66] Fish, L.E., Kück, U. and Bogorad, L. (1985) in Molecular Biology of the Photosynthetic Apparatus (Steinback, K.E., Bonitz, S., Arntzen, C.J. and Bogorad, L., eds), pp. 111–120, Cold Spring Harbor Laboratory, Cold Spring Harbor, New York.
[67] Franke, J.E., Ciesla, L. and Warden, J.T (1995) in Photosynthesis: from Light to Biosphere (Mathis, M., ed.), Vol. 2, pp. 75–78, Kluwer Academic Publishers, Dordrecht.
[68] Frauenfelder, H., Sligar, S.G. and Wolynes, P.G. (1991) Science 254, 1598–1603.
[69] Fromme, P., Schubert, W.D. and Krauß, N. (1994) Biochim. Biophys. Acta 1187, 99–105.
[70] Füchsle, G., Bittl, R., Van der Est, A., Lubitz, W. and Stehlik, D. (1993) Biochim. Biophys. Acta 1142, 23–35.
[71] Fujii T., Yokoyama E., Inoue K. and Sakurai H. (1990) Biochim. Biophys. Acta 1015, 41–48.
[72] Gast, P., Swarthoff, T., Ebskamp, F.C.R. and Hoff, A.J. (1983) Biochim. Biophys. Acta 722, 163–175.
[73] Gentemann, S., Medforth, C.J., Ema, T., Nelson, N.Y. Smith, K.M., Fajer, J. and Holten, D. (1995) Chem. Phys. Lett. 245, 441–447.
[74] Gierer, M., Van der Est, A. and Stehlik, D. (1991) Chem. Phys. Lett. 186, 238–247.
[75] Gilson, M.K., Rashin, A., Fine, R. and Honig, B. (1985) J. Mol. Biol. 184, 503–516.
[76] Gloux, J., Gloux, P., Lamotte, B., Mouesca, J.M. and Rius, G. (1994) J. Am. Chem. Soc. 116, 1953–1961.
[77] Golbeck, J.H. (1987) Biochim. Biophys. Acta 895, 167–204.
[78] Golbeck, J.H. (1992) Annu. Rev. Plant Physiol. Plant Mol. Biol. 43, 293–324.
[79] Golbeck, J.H. (1993) Curr. Opin. Struct. Biol. 3, 508–514.
[80] Golbeck, J.H. (1993) Proc. Natl. Acad. Sci. USA 90, 1642–1646.
[81] Golbeck, J.H. (1994) in The Molecular Biology of Cyanobacteria (Bryant, D.A., ed.), pp. 319–360, Kluwer Academic Publishers, Dordrecht.
[82] Golbeck, J.H. and Bryant, D.A. (1991) in Current Topics in Bioenergetics, Vol. 16 (Lee, C.P. ed.), pp. 83–177, Academic Press, Inc. San Diego, New York.
[83] Golbeck, J.H. and Cornelius, J.M. (1986) Biochim. Biophys. Acta 849, 16–24.
[84] Golbeck, J.H., Parrett, K.G., Mehari, T., Jones, K.L. and Brand, J.J. (1988) FEBS Lett. 228, 268–272.
[85] Golbeck, J.H., Velthuys, B.R. and Kok, B. (1978) Biochim. Biophys. Acta 504, 226–230.
[86] Golbeck, J.H. and Warden, J.T. (1982) Biochim. Biophys. Acta 681, 77–84.
[87] Guigliarelli, B., Guillaussier, J., More, C., Sétif, P., Bottin, H. and Bertrand, P. (1993) J. Biol. Chem. 268, 900–908.
[88] Hagen, S.J., Hofrichter, J. and Eaton, W.A. (1995) Science 269, 959–962.
[89] Hallahan, B.J., Purton, S., Ivison, A., Wright, D. and Evans, M.C.W. (1995) Photosynth. Res. 46, 257–264.
[90] Hamacher, E., Kruip, J., Rögner, M. and Mäntele, W (1995) in Photosynthesis: from Light to Biosphere (Mathis, M., ed.), Vol. 2, pp. 95–98, Kluwer Academic Publishers, Dordrecht.
[91] Hanley, J.A., Kear, J., Bredenkamp, G., Li, G., Heathcote, P. and Evans, M.C.W. (1992) Biochim. Biophys. Acta 1099, 152–156.
[92] Hastings, G., Hoshina, S., Webber, A.N. and Blankenship, R.E. (1995) Biochemistry 34, 15512–15522.
[93] Hastings, G., Kleinherenbrink, F.A.M., Lin, S. and Blankenship, R.E. (1994) Biochemistry 33, 3185–3192.

[94] Hastings, G., Kleinherenbrink, F.A.M., Lin, S., McHugh, T.J. and Blankenship, R.E. (1994) Biochemistry 33, 3193–3200.
[95] He, W.-Z. and Malkin, R. (1994) Photosynth. Res. 41, 381–388.
[96] He, W.-Z., Mannan, R.M., Metzger, S., Whitmarsh, J., Pakrasi, H.B. and Malkin, R (1995) in Photosynthesis: from Light to Biosphere (Mathis, M., ed.), Vol. 2, pp. 91–94, Kluwer Academic Publishers, Dordrecht.
[97] Heathcote, P., Hanley, J.A. and Evans, M.C.W. (1993) Biochim. Biophys. Acta 1144, 54–61.
[98] Heathcote, P., Moënne-Loccoz, P., Rigby, S.E.J. and Evans, M.C.W. (1996) Biochemistry 35, 6644–6650.
[99] Heathcote, P., Rigby, S.E.J. and Evans, M.C.W. (1995) in Photosynthesis: from Light to Biosphere (Mathis, M., ed.), Vol. 2, pp. 163–166, Kluwer Academic Publishers, Dordrecht.
[100] Heathcote, P., Williams-Smith, D.L., Sihra, C.K. and Evans, M.C.W. (1978) Biochim. Biophys. Acta 503, 333–342.
[101] Hecks, B., Breton, J., Leibl, W., Wulf, K. and Trissl, H.-W. (1994) Biochemistry 33, 8619–8624.
[102] Hippler, M., Riedel, A., Schröer, U., Nitschke, W. and Haehnel, W. (1996) Arch. Biochem. Biophys. 330, 414–418.
[103] Hiyama, T. and Ke, B. (1971) Arch. Biochem. Biophys. 147, 99–108.
[104] Hoff, A.J. (1984) Q. Rev. Biophys. 17, 153–282.
[105] Holzwarth, A.R., Schatz, G., Brock, H. and Bittersmann, E. (1993) Biophys. J. 64, 1813–1826.
[106] Hootkins, R. and Bearden, A. (1983) Biochim. Biophys. Acta 723, 16–29.
[107] Hopfield, J.J. (1974) Proc. Natl. Acad. Sci. USA 71, 3640–3644.
[108] Hore, P.J. (1989) in Advanced EPR. Applications in Biology and Biochemistry (Hoff, A.J., ed.), pp. 405–440, Elsevier, Amsterdam.
[109] Huber, J.G., Gaillard, J. and Moulis, J.M. (1995) Biochemistry 34, 194–205.
[110] Ikegami, I., Itoh, S., Warren, P.G. and Golbeck, J.H. (1993) Plant Cell Physiol. 34, 849–853.
[111] Ikegami, I., Sétif, P. and Mathis, P. (1987) Biochim. Biophys. Acta 894, 414–422.
[112] Itoh, S. and Iwaki, M. (1989) FEBS Lett. 243, 47–52.
[113] Itoh, S., Iwaki, M. and Ikegami, I. (1987) Biochim. Biophys. Acta 893, 508–516.
[114] Itoh, S., Mimuro, M. and Iwaki, M. (1992) in Research in Photosynthesis (Murata, N., ed.), Vol. 1, pp. 541–544, Kluwer Academic Publishers, Dordrecht.
[115] Iwaki, M. and Itoh, S. (1991) Biochemistry 30, 5347–5352.
[116] Iwaki, M. and Itoh, S. (1994) Plant Cell Physiol. 35, 983–993.
[117] Iwaki, M., Kumazaki, S., Yoshihara, K., Erabi, T. and Itoh, S. (1995) in Photosynthesis: from Light to Biosphere (Mathis, M., ed.), Vol. 2, pp. 147–150, Kluwer Academic Publishers, Dordrecht.
[118] Jortner, J. (1976) J.Chem.Phys. 64, 4860–4867.
[119] Jortner, J. (1980) Biochim. Biophys. Acta 594, 193–230.
[120] Jung, Y.S., Yu, L. and Golbeck, J.H. (1995) Photosynth. Res. 46, 249–255.
[121] Kakitani, T. and Kakitani, H. (1981) Biochim. Biophys. Acta 635, 498–514.
[122] Kallas, T. (1994) in The Molecular Biology of Cyanobacteria (Bryant, D.A., ed.), pp. 259–317, Kluwer Academic Publishers, Dordrecht.
[123] Kamlowski, A., Van der Est, A., Fromme, P. and Stehlik, D. (1995) in Photosynthesis: from Light to Biosphere (Mathis, M., ed.), Vol. 2, pp. 29–34, Kluwer Academic Publishers, Dordrecht.
[124] Käß, H. (1995) Ph.D. Thesis, Technische Universität Berlin, Germany.
[125] Käß, H., Bittersmann-Weidlich, E., Andreasson, L.-E., Boenigk, B. and Lubitz, W. (1995) Chem. Phys. 194, 419–432
[126] Käß, H., Fromme, P., Witt, H.T. and Lubitz, W. (1994) Biophys. J. 66, A228.
[127] Käß, H. and Lubitz, W. (1996), Chem. Phys. Lett. 251, 193–203.
[128] Kassner, R.J. and Yang, W. (1977) J. Am. Chem. Soc. 99, 4351–4355.
[129] Ke, B. (1972) Arch. Biochem. Biophys. 152, 70–77.
[130] Ke, B., Dolan, E., Sugahara, K., Hawkridge, F.M., Demeter, S. and Shaw, E. (1977) Photosynthetic Organelles, Special Issue of Plant and Cell Physiol. 187–199.
[131] Ke, B., Hansen, R.E. and Beinert, H. (1973) Proc. Natl. Acad. Sci. USA 70, 2941–2945.
[132] Kirsch, W., Seyer, P. and Herrmann, R.G. (1986) Curr. Genet. 10, 843–856.
[133] Kleinfeld, D., Okamura, M.Y. and Feher, G. (1984) Biochemistry 23, 5780–5786.
[134] Kleinherenbrink, F.A.M., Hastings, G., Wittmershaus, B.P. and Blankenship, R.E. (1994) Biochemistry 33, 3096–3105.
[135] Koike, H. and Katoh, S. (1982) Photochem. Photobiol. 35, 527–531.
[136] Kothe, G., Weber, S., Ohmes, E., Thurnauer, M.C. and Norris, J.R. (1994) J. Phys. Chem. 98, 2706–2712.
[137] Krabben, L, Käß, H., Schlodder, E., Kuhn, M., Lubitz, W., Xu, H., Bingham, S. and Webber, A. (1995) in Photosynthesis: from Light to Biosphere (Mathis, M., ed.), Vol. 2, pp. 123–126, Kluwer Academic Publishers, Dordrecht.
[138] Krauß, N., Hinrichs, W., Witt, I., Fromme, P., Pritzkow, W., Dauter, Z., Betzel, C., Wilson, K.S., Witt, H.T. and Saenger, W. (1993) Nature 361, 326–331.
[139] Krawczyk, S. and Ikegami, I. (1993) Biochim. Biophys. Acta 1143, 282–290.
[140] Krawczyk, S. and Maksymiec, W. (1991) FEBS Lett. 286, 110–112.
[141] Krishtalik, L.I. (1989) Biochim. Biophys. Acta 977, 200–206.
[142] Kumazaki, S., Iwaki, M., Ikegami, I., Kandori, H., Yoshihara, K. and Itoh, S. (1994) J. Phys. Chem. 98, 11220–11225.

[143] Kumazaki, S., Kandori, H., Petek, H., Yoshihara, K. and Ikegami, I. (1994) J. Phys. Chem. 98, 10335–10342.
[144] Lagoutte, B. and Mathis, P. (1989) Photochem. Photobiol. 49, 833–844.
[145] Langen, R., Jensen, G.M., Jacob, U., Stephens, P.J. and Warshel, A. (1992) J. Biol. Chem. 267, 25625–25627.
[146] Leibl, W., Toupance, B. and Breton, J. (1995) Biochemistry 34, 10237–10244.
[147] Lelong, C., Boekema, E.J., Kruip, J., Bottin, H., Rögner, M. and Sétif, P. (1996) EMBO J. 15, 2160–2168.
[148] Li, N., Zhao, J., Waren, P.V., Warden, J.T., Bryant, D.A. and Golbeck, J.H. (1991) Biochemistry 30, 7863–7872.
[149] Liebl, U., Mockensturmwilson, M., Trost, J.T., Brune, D.C., Blankenship, R.E. and Vermaas, W.F.J. (1993) Proc. Natl. Acad. Sci. USA 90, 7124–7128.
[150] Lozier, R.H. and Butler, W.L. (1974) Biochim. Biophys. Acta 460–464.
[151] Lozier, R.H. and Butler, W.L. (1974) Biochim. Biophys. Acta 465–480.
[152] Lüneberg, J., Fromme, P., Jekow, P. and Schlodder, E. (1994) FEBS Lett. 338, 197–202.
[153] Mac, M., McCracken, J. and Babcock, G.T (1995) in Photosynthesis: from Light to Biosphere (Mathis, M., ed.), Vol. 2, pp. 35–38, Kluwer Academic Publishers, Dordrecht.
[154] Maeda, H., Watanabe, T., Kobayashi, M. and Ikegami, I. (1992) Biochim. Biophys. Acta 1099, 74–80.
[155] Malkin, R. (1982) Ann. Rev. Plant Physiol. 33, 455–479.
[156] Malkin, R. (1984) Biochim. Biophys. Acta 764, 63–69.
[157] Malkin, R. (1986) FEBS Lett. 208, 343–346.
[158] Malkin, R. (1987) in The Light Reactions (Barber, J., ed.), pp. 495–525, Elsevier, Amsterdam.
[159] Malkin, R. and Bearden, A.J. (1971) Proc. Natl. Acad. Sci. USA 68, 16–19.
[160] Mannan, R.M., He, W.-Z., Metzger, S., Whitmarsh, J., Malkin, R. and Pakrasi, H.B. (1996) EMBO J. 15, 1826–1833.
[161] Mansfield, R.W. and Evans, M.C.W. (1985) FEBS Lett. 190, 237–241.
[162] Mansfield, R.W., Hubbard, J.A.M., Nugent, J.H.A. and Evans, M.C.W. (1987) FEBS Lett. 220, 74–78.
[163] Mansfield, R.W., Nugent, J.H.A. and Evans, M.C.W. (1987) Biochim. Biophys. Acta 894, 515–523.
[164] Marcus, R.A. and Sutin, N. (1985) Biochim. Biophys. Acta 811, 265–322.
[165] Mathis, P. (ed.) (1995) Photosynthesis: from Light to Biosphere, Vol. 1, Kluwer Academic Publishers, Dordrecht.
[166] Mathis, P. and Conjeaud, H. (1979) Photochem. Photobiol. 29, 833–837.
[167] Mathis, P., Ikegami, I. and Sétif, P. (1988) Photosynth. Res. 16, 203–210.
[168] Mathis, P. and Rutherford, A.W. (1987) in Photosynthesis; New Comprehensive Biochemistry Vol. 15 (Amesz, J. ed.), pp. 63–96, Elsevier, Amsterdam.
[169] Mathis, P., Sauer, K. and Remy, R. (1978) FEBS Lett. 88, 275–278.
[170] Mathis, P. and Sétif, P. (1981) Isr. J. Chem. 21, 316–320.
[171] Mathis, P. and Sétif, P. (1988) FEBS Lett. 237, 65–68.
[172] Mayne, B.C. and Rubinstein, D. (1966) Nature 210, 734–735.
[173] McIntosh, A.R., Chu, M. and Bolton, J.R. (1975) Biochim. Biophys. Acta 376, 308–314.
[174] Mehari, T., Qiao, F.Y., Scott, M.P., Nellis, D.F., Zhao, J.D., Bryant, D.A. and Golbeck, J.H. (1995) J. Biol. Chem. 270, 28108–28117.
[175] Michel-Beyerle, M.E., Plato, M., Deisenhofer, J., Michel, H., Bixon, M. and Jortner, J. (1988) Biochim. Biophys. Acta 932, 52–70.
[176] Moënne-Loccoz, P., Heathcote, P., Maclachlan, D.J., Berry, M.C., Davis, I.H. and Evans, M.C.W. (1994) Biochemistry 33, 10037–10042.
[177] Moser, C.C. and Dutton, P.L. (1992) Biochim. Biophys. Acta 1101, 171–176.
[178] Moser, C.C., Keske, J.M., Warncke, K., Farid, R.S. and Dutton, P.L. (1992) Nature 355, 796–802.
[179] Mühlenhoff, U. (1991) Ph.D. Thesis, Technische Universität Berlin, Germany.
[180] Mühlenhoff, U., Haehnel, W., Witt, H. and Herrmann, R.G. (1993) Gene 127, 71–78.
[181] Mühlenhoff, U., Kruip, J., Bryant, D.A., Rögner, M., Sétif, P. and Boekema, E. (1996) EMBO J. 15, 488–497.
[182] Naver, H., Scott, M.P., Golbeck, J.H., Møller, B.L. and Scheller, H.V. (1995) in Photosynthesis: from Light to Biosphere (Mathis, M., ed.), Vol. 2, pp. 155–158, Kluwer Academic Publishers, Dordrecht.
[183] Naver, H., Scott, M.P., Golbeck, J.H., Møller, B.L. and Scheller, H.V. (1996) J. Biol. Chem. 271, 8996–9001.
[184] Nitschke, W. and Rutherford, A.W. (1991) Trends Biochem. Sci. 16, 241–245.
[185] Noodleman, L., and Case, D.A., (1992) in Advances in Inorganic Chemistry 38. Iron-Sulfur Proteins (Cammack, R., ed.), pp. 423–470, Academic Press, San Diego.
[186] Nozawa, T., Kobayashi, M., Wang, Z.-Y., Itoh, S., Iwaki, M., Mimuro, M. and Satoh, K. (1995) Spectrochim. Acta 51A, 125–134.
[187] Nugent, J.H.A., Møller, B.L. and Evans, M.C.W. (1981) Biochim. Biophys. Acta 634, 249–255.
[188] Nuijs, A.M., Shuvalov, V.A., Van Gorkom, H.J., Plijter, J.J. and Duysens, L.N.M. (1986) Biochim. Biophys. Acta 850, 310–318.
[189] Ogrodnik, A., Keupp, W., Volk, M., Aumeier, G. and Michel-Beyerle, M.E. (1994) J. Phys. Chem. 98, 3432–3439.
[190] Oh-oka, H., Itoh, S., Saeki, K., Takahashi, Y. and Matsubara, H. (1991) Plant Cell Physiol. 32, 11–17.
[191] Oh-oka, H., Takahashi, Y., Kuriyama, K., Saeki, K. and Matsubara, H. (1988) J. Biochem. 103, 962–968.
[192] Ortega, J.M., Mathis, P., Williams, J.C. and Allen, J.P. (1996) Biochemistry 35, 3354–3361.
[193] Parrett, K.G., Mehari, T., Warren, P.G. and Golbeck, J.H. (1989) Biochim. Biophys. Acta 973, 324–332.
[194] Parson, W.W. and Warshel, A. (1995) in Anoxygenic Photosynthetic Bacteria (Blankenship, R.E., Madigan, M.T.

and Bauer, C.E., eds.), pp. 559–575, Kluwer Academic Publishers, Dordrecht.
[195] Patel, V., Wright, D.W., Hallahan, B.J., Purton, S. and Evans, M.C.W. (1995) in Photosynthesis: from Light to Biosphere (Mathis, M., ed.), Vol. 2, pp. 187–190, Kluwer Academic Publishers, Dordrecht.
[196] Prince, R.C. and Adams, M.W.W. (1987) J. Biol. Chem. 262, 5125–5128.
[197] Prince, R.C., Dutton, P.L. and Bruce, J.M. (1983) FEBS Lett. 160, 273–276.
[198] Prisner, T.F., McDermott, A.E., Un, S., Norris, J.R., Thurnauer, M.C. and Griffin, R.G. (1993) Proc. Natl. Acad. Sci. USA 90, 9485–9488.
[199] Rasmussen, D.H. and MacKenzie, A.P. (1971) J. Phys. Chem. 75, 967–973.
[200] Reinman, S. and Mathis, P. (1981) Biochim. Biophys. Acta 635, 249–258.
[201] Rigby, S.E.J., Evans, M.C.W. and Heathcote, P. (1996) Biochemistry 35, 6651–6656.
[202] Rigby, S.E.J., Nugent, J.H.A. and O'Malley, P.J. (1994) Biochemistry 33, 10043–10050.
[203] Robert, B. and Moënne-Loccoz, P. (1990) in Current Research in Photosynthesis (Baltscheffsky, M., ed.), Vol. 1, pp. 65–68, Kluwer Academic Publishers, Dordrecht.
[204] Rodday, S.M., Jun, S.S. and Biggins, J. (1993) Photosynth. Res. 36, 1–9.
[205] Rousseau, F., Setif, P. and Lagoutte, B. (1993) EMBO J. 12, 1755–1765.
[206] Rupp, H., de la Torre, A. and Hall, D.O. (1979) Biochim. Biophys. Acta 548, 552–564
[207] Rustandi, R.R., Snyder, S.W., Biggins, J., Norris, J.R. and Thurnauer, M.C. (1992) Biochim. Biophys. Acta 1101, 311–320.
[208] Rustandi, R.R., Snyder, S.W., Feezel, L.L., Michalski, T.J., Norris, J.R., Thurnauer, M.C. and Biggins, J. (1990) Biochemistry 29, 8030–8032.
[209] Rutherford, A.W. and Heathcote, P. (1985) Photosynth. Res. 6, 295–316.
[210] Rutherford, A.W. and Sétif, P. (1990) Biochim. Biophys. Acta 1019, 128–132.
[211] Sakurai, H., Inoue, K., Fujii, T. and Mathis, P. (1991) Photosynth. Res. 27, 65–71.
[212] Sauer, K., Mathis, P., Acker, S. and Van Best, J.A. (1978) Biochim. Biophys. Acta 503, 120–134.
[213] Schaffernicht, H. and Junge, W. (1981) Photochem. Photobiol. 34, 223–232.
[214] Schaffernicht, H. and Junge, W. (1982) Photochem. Photobiol. 36, 111–115.
[215] Schenck, C.C., Mathis, P. and Lutz, M. (1984) Photochem. Photobiol. 39, 407–417.
[216] Schlodder, E., Brettel, K., Falkenberg, K. and Gergeleit, M (1995) in Photosynthesis: from Light to Biosphere (Mathis, M., ed.), Vol. 2, pp. 107–110, Kluwer Academic Publishers, Dordrecht.
[217] Schoeder, H.-U. and Lockau, W. (1986) FEBS Lett. 199, 23–27.
[218] Schubert, W.D., Klukas, O., Krauß, N., Saenger, W., Fromme, P. and Witt, H.T. (1995) in Photosynthesis: from Light to Biosphere (Mathis, M., ed.), Vol. 2, pp. 3–10, Kluwer Academic Publishers, Dordrecht.
[219] Schwartz, T. and Brettel, K. (1995) in Photosynthesis: from Light to Biosphere (Mathis, M., ed.), Vol. 2, pp. 43–46, Kluwer Academic Publishers, Dordrecht.
[220] Sétif, P. (1992) in The Photosystems: Structure, Function and Molecular Biology (Barber, J. ed.), pp. 471–499, Elsevier Science Publishers, Amsterdam.
[221] Sétif, P. and Bottin, H. (1989) Biochemistry 28, 2689–2697.
[222] Sétif, P. and Bottin, H. (1994) Biochemistry 33, 8495–8504.
[223] Sétif, P., Bottin, H. and Mathis, P. (1985) Biochim. Biophys. Acta 808, 112–122.
[224] Sétif, P. and Brettel, K. (1990) Biochim. Biophys. Acta 1020, 232–238.
[225] Sétif, P. and Brettel, K. (1993) Biochemistry 32, 7846–7854.
[226] Sétif, P., Hervo, G. and Mathis, P. (1981) Biochim. Biophys. Acta 638, 257–267.
[227] Sétif, P., Ikegami, I. and Biggins, J. (1987) Biochim. Biophys. Acta 894, 146–156.
[228] Sétif, P. and Mathis, P. (1980) Arch. Biochem. Biophys. 204, 477–485.
[229] Sétif, P. and Mathis, P. (1986) in Encyclopedia of Plant Physiology; Photosynthesis III (Staehelin, L.A. and Arntzen, C.J. eds.), pp. 476–486, Springer, Berlin.
[230] Sétif, P. and Mathis, P. (1986) Photosynth. Res. 9, 47–54.
[231] Sétif, P., Mathis, P., Lagoutte, B. and Duranton J. (1984) in Advances in Photosynthesis Research (Sybesma, C., ed.), Vol. 1, pp. 589–592, Martinus Nijhoff/Dr W. Junk Publishers, The Hague.
[232] Sétif, P., Mathis, P. and Vänngård, T. (1984) Biochim. Biophys. Acta 767, 404–414.
[233] Sétif, P.Q.Y. and Bottin, H. (1995) Biochemistry 34, 9059–9070.
[234] Shipman, L.L. (1977) Photochem. Photobiol. 26, 287–292.
[235] Shuvalov, V.A. (1976) Biophys. Biochim. Acta 430, 113–121.
[236] Shuvalov, V.A., Dolan, E. and Ke, B. (1979) Proc. Natl. Acad. Sci. USA 76, 770–773.
[237] Shuvalov, V.A., Klimov, V.V. and Krasnovskii, A.A. (1976) Molek. Biol. 10, 326–339.
[238] Shuvalov, V.A., Nuijs, A.M., Van Gorkom, H.J., Smit, H.W.J. and Duysens, L.N.M. (1986) Biochim. Biophys. Acta 850, 319–323.
[239] Sieckmann, I. (1993) Ph.D. Thesis, Technische Universität Berlin, Germany.
[240] Sieckmann, I., Brettel, K., Bock, C., Van der Est, A. and Stehlik, D. (1993) Biochemistry 32, 4842–4847.
[241] Sieckmann, I., Van der Est, A., Bottin, H., Sétif, P. and Stehlik, D. (1991) FEBS Lett. 284, 98–102.
[242] Sigfridsson, K., Hansson, O. and Brzezinski, P (1995) in Photosynthesis: from Light to Biosphere (Mathis, M., ed.),

Vol. 2, pp. 79–82, Kluwer Academic Publishers, Dordrecht.
[243] Sigfridsson, K., Hansson, O. and Brzezinski, P. (1995) Proc. Natl. Acad. Sci. USA 92, 3458–3462.
[244] Smart, L.B., Warren, P.V., Golbeck, J.H. and McIntosh, L. (1993) Proc. Natl. Acad. Sci. USA 90, 1132–1136.
[245] Snyder, S.W., Rustandi, R.R., Biggins, J., Norris, J.R. and Thurnauer, M.C. (1991) Proc. Natl. Acad. Sci. USA 88, 9895–9896.
[246] Snyder, S.W. and Thurnauer, M.C. (1993) in The Photosynthetic Reaction Center (Deisenhofer, J. and Norris, J.R., ed.), Vol. II, Academic Press, San Diego.
[247] Sonoike, K., Hatanaka, H. and Katoh, S. (1993) Biochim. Biophys. Acta 1141, 52–57.
[248] Stehlik, D., Bock, C.H. and Peterson, J. (1989) J. Phys. Chem. 93, 1612–1619.
[249] Stehlik, D., Bock, C.H. and Thurnauer, M.C. (1989) in Advanced EPR. Applications in Biology and Biochemistry (Hoff, A.J., ed.), pp. 371–404, Elsevier, Amsterdam.
[250] Stehlik, D., Sieckman, I. and Van der Est, A. (1992) in Research in Photosynthesis (Murata, N., ed.), Vol. 1, pp. 533–536, Kluwer Academic Publishers, Dordrecht.
[251] Sun, A.S.K. and Sauer, K. (1971) Biochim. Biophys. Acta 234, 399–414.
[252] Takahashi, Y. and Katoh, S. (1982) Arch. Biochem. Biophys. 219, 219–227.
[253] Thurnauer, M.C. and Gast, P. (1985) Photobiochem. Photobiophys. 9, 29–38.
[254] Thurnauer, M.C. and Norris, J.R. (1977) Chem. Phys. Letters 47, 100–105.
[255] Thurnauer, M.C. and Norris, J.R. (1980) Chem. Phys. Lett. 76, 557–561.
[256] Thurnauer, M.C., Rutherford, A.W. and Norris, J.R. (1982) Biochim. Biophys. Acta 682, 332–338.
[257] Trissl, H.-W., Hecks, B. and Wulf, K. (1993) Photochem. Photobiol. 57, 552–568.
[258] Valkunas, L., Liuolia, V., Dekker, J.P. and Van Grondelle, R. (1995) Photosynth. Res. 43, 149–154.
[259] Van der Est, A., Bock, C., Golbeck, J., Brettel, K., Sétif, P. and Stehlik, D. (1994) Biochemistry 33, 11789–11797.
[260] Van der Est, A., Sieckmann, I., Lubitz, W. and Stehlik, D. (1995) Chem. Phys. 194, 349–359
[261] Van der Est, A., Sieckmann, I., Lubitz, W. and Stehlik, D (1995) in Photosynthesis: from Light to Biosphere (Mathis, M., ed.), Vol. 2, pp. 143–146, Kluwer Academic Publishers, Dordrecht.
[262] Van Grondelle, R., Dekker, J.P., Gillbro, T. and Sundstrom, V. (1994) Biochim. Biophys. Acta 1187, 1–65.
[263] Vassiliev, L.R., Jung, Y.-S., Smart, L.B., Schultz R., McIntosh L. and Golbeck, J.H. (1995) Biophys. J. 69, 1544–1553.
[264] Volk M., Ogrodnik, A. and Michel-Beyerle, M.-E. (1995) in Anoxygenic Photosynthetic Bacteria (Blankenship, R.E., Madigan, M.T. and Bauer, C.E., eds.), pp. 595–626, Kluwer Academic Publishers, Dordrecht.
[265] Vos, M.H. and Van Gorkom, H.J. (1988) Biochim. Biophys. Acta 934, 293–302.
[266] Vos, M.H. and Van Gorkom, H.J. (1990) Biophys. J. 58, 1547–1555.
[267] Vrieze, J., Gast, P. and Hoff, A.J. (1992) in Research in Photosynthesis (Murata, N., ed.), Vol. 1, pp. 553–556, Kluwer Academic Publishers, Dordrecht.
[268] Vrieze, J. and Hoff, A.J. (1995) Chem. Phys. Lett. 237, 493–501.
[269] Warden, J.T. (1990) in Current Research in Photosynthesis (Baltscheffsky, M., ed.), Vol. 2, pp. 635–638, Kluwer Academic Publishers, Dordrecht.
[270] Warden, J.T., Mohanty, P. and Bolton, J.R. (1974) Biochem. Biophys. Res. Commun. 59, 872–878.
[271] Warren, P.V., Golbeck, J.H. and Warden, J.T. (1993) Biochemistry 32, 849–857.
[272] Warren, P.V., Parrett, K.G., Warden, J.T. and Golbeck, J.H. (1990) Biochemistry 29, 6545–6550.
[273] Warren, P.V., Smart, L.B., McIntosh, L. and Golbeck, J.H. (1993) Biochemistry 32, 4411–4419.
[274] Webber, A.N., Gibbs, P.B., Ward, J.B. and Bingham, S.E. (1993) J. Biol. Chem. 268, 12990–12995.
[275] Werner, H.-J., Schulten, K. and Weller, A. (1978) Biochim. Biophys. Acta 502, 255–268.
[276] Witt, H.T., Krauß, N., Hinrichs, W., Witt, I., Fromme, P. and Saenger, W. (1992) in Research in Photosynthesis (Murata, N., ed.), Vol. 1, pp. 521–528, Kluwer Academic Publishers, Dordrecht.
[277] Witt, I., Witt, H.T., Di Fiore, D., Rögner, M., Hinrichs, W., Saenger, W., Granzin, J., Betzel, C. and Dauter, Z. (1988) Ber. Bunsenges. Phys. Chem. 92, 1503–1506.
[278] Yu, L., Bryant, D.A. and Golbeck, J.H. (1995) Biochemistry 34, 7861–7868.
[279] Yu, L., Zhao, J.D., Lu, W.P., Bryant, D.A. and Golbeck, J.H. (1993) Biochemistry 32, 8251–8258.
[280] Yu, L.A., Vassiliev, I.R., Jung, Y.S., Bryant, D.A. and Golbeck, J.H. (1995) J. Biol. Chem. 270, 28118–28125.
[281] Zhao, J.D., Li, N., Warren, P.V., Golbeck, J.H. and Bryant, D.A. (1992) Biochemistry 31, 5093–5099.
[282] Ziegler, K., Lockau, W. and Nitschke, W. (1987) FEBS Lett. 217, 16–20.